CHALMERS

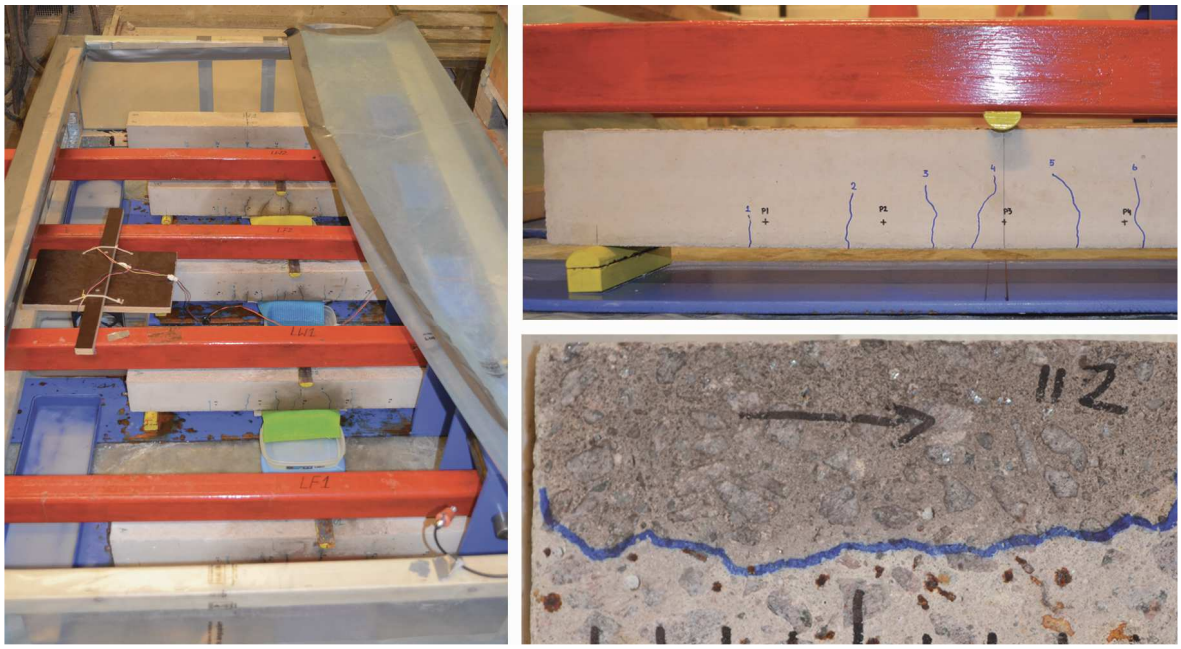

Effect of fibres on corrosion of steel reinforcement

Master of Science Thesis in the Master's Programme Structural Engineering and Building Performance Design 2012

MACIEJ ABRYCKI
ARKADIUSZ ZAJDZINSKI

Department of Civil and Environmental Engineering
Division of Structural Engineering
Concrete structures
CHALMERS UNIVERSITY OF TECHNOLOGY
Göteborg, Sweden 2012
Master's Thesis 2012:65

MASTER'S THESIS 2012:65

Effect of fibres on corrosion of steel reinforcement

Master of Science Thesis in the Master's Programme Structural Engineering and Building Performance Design 2012

MACIEJ ABRYCKI

ARKADIUSZ ZAJDZINSKI

Department of Civil and Environmental Engineering
Division of Structural Engineering
Concrete structures
CHALMERS UNIVERSITY OF TECHNOLOGY

Göteborg, Sweden 2012

Effect of fibres on corrosion of steel reinforcement

Master of Science Thesis in the Master's Programme Structural Engineering and Building Performance Design 2012

MACIEJ ABRYCKI
ARKADIUSZ ZAJDZINSKI

Examensarbete / Institutionen för bygg- och miljöteknik,
Chalmers tekniska högskola 2012:65

Department of Civil and Environmental Engineering
Division of Structural Engineering
Concrete structures
Chalmers University of Technology
SE-412 96 Göteborg
Sweden
Telephone: + 46 (0)31-772 1000

Cover:
Left side: exposure conditions for loaded beams (group L); Right side top: loading system; Right side bottom specimen after RCM test.

Chalmers Reproservice / Department of Civil and Environmental Engineering
Göteborg, Sweden 2012

Effect of fibres on corrosion of steel reinforcement

Master of Science Thesis in the Master's Programme Structural Engineering and Building Performance Design 2012

MACIEJ ABRYCKI
ARKADIUSZ ZAJDZINSKI
Department of Civil and Environmental Engineering
Division of Structural Engineering
Concrete structures
Chalmers University of Technology

ABSTRACT

Steel fibre reinforced concrete has found increased use as construction material, and could be beneficial for use in infrastructure and marine structures. Nevertheless using fibres combined with traditional steel reinforcement in chloride environment may cause other problems, as for example corrosion of fibres or galvanic corrosion. This study investigated the influence of steel fibres on corrosion of traditional reinforcement bars.

In order to investigate the influence of fibres on corrosion of reinforcing steel, three types of experiments were carried out: corrosion tests on beams to obtain time to corrosion initiation, rapid chloride migration and resistivity tests. Due to time limitation, the corrosion tests were done on beams with rather porous concrete mixtures (class C20/25, *w/c* 0.75) exposed to a high chloride concentration. The beams were divided in three groups: loaded, unloaded and beams that were never loaded, thus resulting in varying crack widths. In all groups, specimens both with and without steel fibres were tested.

The results show that the reinforcement bars in the beams with the widest cracks started to corrode first. Due to the scatter in the results, it was difficult to draw any clear conclusions about the effects of fibres on corrosion. However, it has been noticed that mechanical properties of fibres have beneficial impact on protecting of rebars. It was visually observed, that pitting areas were smaller for beams with fibres. The steel fibres decreased the resistivity, while the chloride diffusion coefficient appeared to be unaffected.

Key words: fibre reinforced concrete, crack width, galvanic corrosion, steel corrosion, chlorides, resistivity of concrete, chloride migration, half-cell potential.

Contents

Preface

In this study, accelerated corrosion test on beams, chloride migration tests and resistivity tests have been done. The thesis was conducted from January to May 2012 at Chalmers University of Technology, Department of Civil and Environmental Engineering, Division of Structural Engineering, Concrete structures. The experiments took place at Building Technology Division Laboratory, Chalmers and Central Laboratory of Thomas Concrete Group AB.

First of all, we would like to appreciate our supervisors' contribution to this study, Anders Lindvall, Ingemar Löfgren, Karin Lundgren (who also was examiner) and Tang Luping. We want to thank Marek Machowski and Lars Wahlström as well, for their support during laboratory work. The financial support from Färdig Betong AB and Brosamverkan Väst is gratefully acknowledged.

Göteborg May 2012

Maciej Abrycki

Arkadiusz Zajdzinski

1 Introduction

1.1 Background

Nowadays steel fibre reinforced concrete (SFRC) is more commonly used as a construction material. According to prior investigations it has been proved that it brings more effective crack control and improves its mechanical properties; see e.g. Mangat and Gurusamy (1987), Granju and Balouch (2005), and Löfgren (2005). Adding fibres to the mixture gives better post-cracking load bearing capacity due to the fibres capability to transfer stresses through cracks. Throughout the last decade fibre reinforcement has found many applications in civil engineering structures as floors or segmental linings in bored tunnels; see e.g. Bentur and Mindess (2007). As far as civil engineering structures are concerned, where their crack limiting effects is of interest, it could be beneficial to use fibres. This is particularly interesting for structures like bridges and harbours which usually have strict crack width limits due to the risk of reinforcement corrosion. Therefore it could be beneficial to apply fibres to reduce cracks as a supplement to the traditional reinforcement. Nevertheless using fibres combining with traditional steel reinforcement in chloride environment may cause other problems, as for example corrosion of fibres or galvanic corrosion.

1.2 Purpose and objectives

The main purpose of this thesis is to study the effect of fibres on corrosion of steel reinforcement in chloride environment. The main objectives of this study are:

- to investigate the fibres influence on resistivity and chloride migration coefficient;
- to examine the risk of galvanic corrosion due to using different steel types in fibres and traditional reinforcement;
- to analyse if the fibres ability to supress crack width can be beneficial when it comes to chloride ingress and corrosion initiation;
- to study if fibres corrode at surface which can give bad esthetical impression.

1.3 Scope and method

Due to time limitation, the corrosion tests were conducted on beams of rather porous concrete mixtures (class C20/25, water cement ratio - *w/c* 0.75) exposed to a high chloride concentration.

The thesis is divided into two parts: the first part is a literature study and the second part deals with experiments. The first part explains the reinforcement corrosion process, galvanic corrosion as well as influence of cracks on corrosion in reinforcement. Next part describes experiments which were conducted in order to examine influence of fibres on reinforcement corrosion. Three types of tests were carried out:

- corrosion tests on beams to obtain time to corrosion initiation;
- Rapid Chloride Migration tests (RCM tests) to determine chloride migration coefficient, according to NT Build (492);

- resistivity tests to determine the effect of fibres on resistivity, according to the procedure described in Tang and Nilsson (2002).

2 Corrosion in Concrete Structures

2.1 Introduction

Concrete structures are exposed to different degradation processes e.g. mechanical (abrasion) or physical (freeze-thaw). One of the most common is reinforcement corrosion initiated by chloride ingress. It deteriorates the concrete cover by inducing cracks reducing the protective characteristics of the cover. A schematic view of deterioration levels in concrete is presented in Figure 2.1.

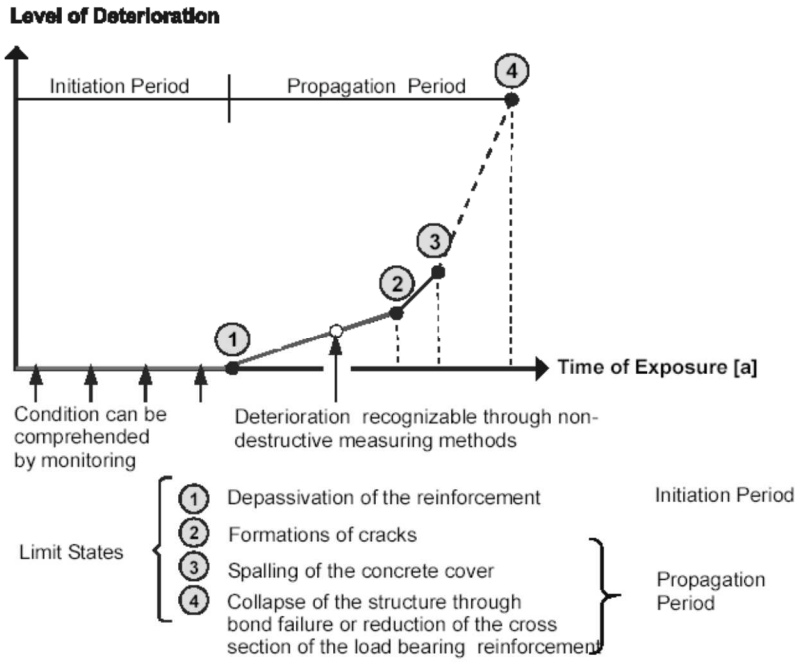

Figure 2.1 A schematic view of deterioration levels, FIB (2006).

Corrosion can develop on the reinforcing steel in full-length (general corrosion) as well as in cross section (pitting corrosion). Particular in the first case longitudinal cracks, caused by increase of expansive products produced by corrosion that generate tensile stresses in the concrete around reinforcing steel, can lead to reduction of bond strength between concrete and reinforcement. Moreover, corrosion decreases ductility of the structure, what is an effect of stress concentrations in the reinforcing steel.

Protection of reinforcement steel in concrete is based on sufficient concrete cover, maximum *w/c* and the process of forming thin protective layer (the passive film) on embedded reinforcing steel. The concrete surrounding reinforcing steel is highly alkaline (pH between 13 and 14). The passive film appears, by oxidation of the surface, and is a few nanometres thick. It is mostly made of insoluble iron oxides. The main function of passive film is to provide the corrosion resistance of steel. Unfortunately it is not enough protection against corrosion, and the passive film can be broken down by carbonation-induced corrosion and chloride-induced corrosion.

2.2 Carbonation

Carbonation is a process which is not damaging concrete itself, but influences the risk of corrosion of the reinforcing steel. Carbonation results in a lowering of the pH of the pore solution in concrete, from 13 - 14 to 9 As a result of loss the protective layer on the reinforcement is deteriorated and corrosion of the steel may commence.

The process of carbonation is caused by the reaction between carbon dioxide and calcium hydroxide, in the cement paste. Sodium and potassium hydroxides are present in the pore solution as well as calcium hydroxide. Calcium hydroxide becomes hydrated in the cement paste and reacts eagerly with aqueous carbon dioxide to form calcium carbonate and water. The reaction can be written as:

$$Ca(OH)_2 + CO_2 \rightarrow CaCO_3 + H_2O \quad (2.1)$$

As a result of this reaction, the pH value of the pore solution decreases and a neutralisation of the concrete occur. The neutralisation proceeds in steps, following several reactions, but the final product is always $CaCO_3$.

Carbonation rate decreases with time and depend on diffusion of carbon dioxide through the pores from the layer which is carbonated. To distinguish and measure the depth of carbonation, a solution of phenolphthalein can be sprayed on a surface of broken concrete. Parts of the surface which are not affected become pinkish in comparison to affected parts which are not changing colour.

Following factors influence the carbonation rate according to Bertolini et al. (2004):

- The humidity (moisture) is significant for the carbonation rate; when concrete is fully saturated, carbon dioxide cannot penetrate it. Thus, carbonation does not occur in fully saturated concrete. However, carbonation process cannot start without water. The optimum moisture is between 60% and 80%.
- The CO_2 concentration; mostly, the higher the concentration of carbon dioxide in the air, the higher the carbonation rate.
- The concrete composition; *w/c* is one of the most important factors that influence the penetration rate of carbonation. The higher the water-cement ratio, the larger penetration rate of the carbonation.
- The temperature; when temperature increases the carbonation rate raise.

2.3 Chloride ingress

In practice, durability of concrete is more endangered by chloride ingress than carbonation. Chloride contamination could be really destructive for prestressed and reinforced concrete structures. In order to avoid corrosion caused by chlorides in the concrete, there are limitations on chloride contents in materials used for prestressed and reinforced concrete structures. In the past (deliberately, but unaware of detrimental effects) chlorides were used in concrete mix as admixtures (calcium chloride), which is prohibited now.

There are some other sources of chlorides causing corrosion in concrete. Two of them are really important: de-icing salts on roads used in winters and seawater in marine environments.

Chloride ions are transported into the concrete and when the chloride content at the reinforcement exceeds the so-called threshold lever corrosion may be initiated.

The threshold level mostly depends on electrochemical potential of the reinforcing steel. Rather small amount of chlorides is needed to initiate corrosion in concrete structures exposed to the atmosphere, where sufficient amount oxygen is available. However, in structures immersed in water, the amount of chlorides needed to initiate corrosion is higher, because the access of oxygen to the reinforcement is limited. In the case of water saturated concrete, chloride agents penetrate through concrete cover by diffusion. When it comes to partially water saturated concrete, chloride substances can be transported by convection.

2.4 Active corrosion

It can be distinguished between general corrosion, which usually is initiated by carbonation, and pitting corrosion, which usually is initiated by chloride ingress.

Afterwards, reinforcing steel may start to corrode if sufficient moisture and oxygen is present, the volume of the corrosion product is 2~4 times greater than pristine steel. This causes splitting stresses around reinforcement bars, which can cause splitting cracks in the concrete cover.

Pitting corrosion may start when the amount of chlorides at the surface of a reinforcing steel exceed a threshold level. Then chlorides break down the protective layer of the reinforcement (the passive film). The areas that are no longer protected start acting as anodes (active zones) while the surrounding protected areas act as cathodes. If the ratio of cathodic area to anodic area is high, the pitting corrosion can occur. Schematically presented, pitting corrosion is shown in Figure 2.2. There it is shown that the corrosion started and the aggressive environment is produced inside pits. The chloride content is increasing due to the current flowing between anodic and cathodic regions. Chlorides that are negative ions move to the anodic areas and decrease the alkalinity. However, when it comes to current, it is strengthening the protective layer since it can reject chlorides, while cathodes increase alkalinity. It means that both processes are stabilised and corrosion is accelerated.

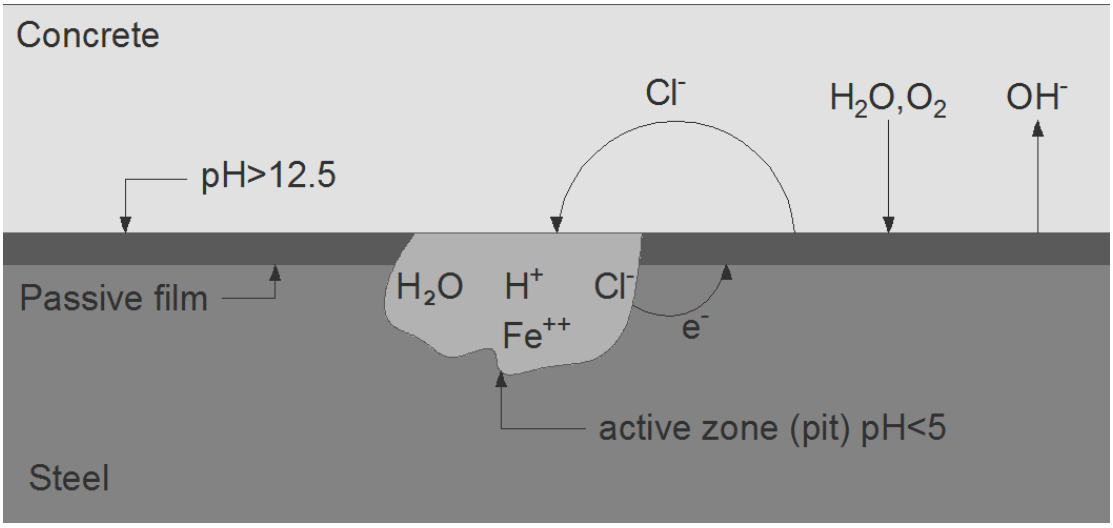

Figure 2.2 Scheme of pitting corrosion of reinforcing steel in concrete, based on Bertolini et al. (2004)

2.5 Galvanic corrosion

Galvanic corrosion appears between different kinds of metal. It occurs when alloy or metal is electrically coupled to the other metal or when non-metal is conducted in the same electrolyte. There are three following components that have to be fulfilled:

- The common electrolyte
- The common electrical path
- Materials that possess various surface potential

During galvanic corrosion process, the surface of the less protected metal becomes anodic and corrosion increases. However, the surface of the better protected metal becomes cathode and corrosion decreases. Disparities in potential between different alloys or metals cause electron flow while they are coupled electrically in a conductive solution. The corrosion rate is affected by the following factors:

- The potential disparity between alloys or metals
- The characteristics of the environment
- The polarization behaviour of alloys or metals

When it comes to flow direction, the more active alloy or metal will corrode. Hence, the metal which is more active becomes anode in contrary to the corrosion-resistant metal which becomes cathode.

2.6 Service life of concrete and corrosion (initiation and propagation)

The service lifetime and corrosion is often described in connection with initiation and propagation time. Those two different phases were firstly described and presented by Tuutti (1982), see Figure 2.3.

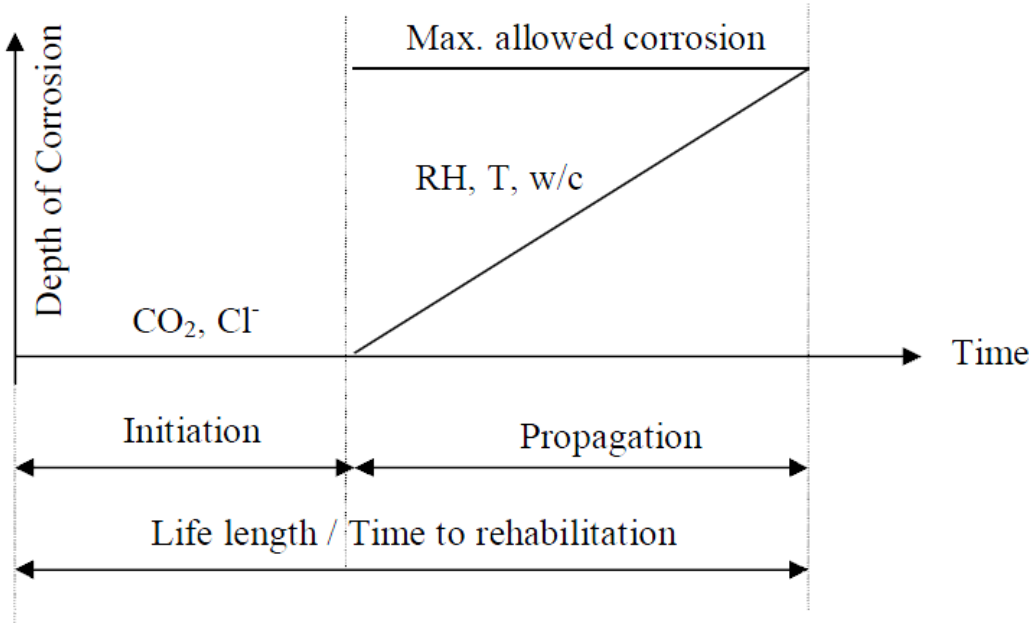

Figure 2.3 Initiation and propagation periods for corrosion in concrete, Tuutti (1982).

In the first phase, where reinforcing steel is passive, carbonation and/or chloride ingress into the concrete occurs and the cover deteriorates and finally the reinforcement is de-passivated when the thin protective layer of reinforcement is broken down. Initiation period is limited by the penetration depth of aggressive substances and cover depth as well as concentration difference needed to depassivate the reinforcement. Initiation period is strongly influenced by the presence and width of cracks; see e.g. Tammo (2006). Influence of cracks on corrosion is presented in Chapter 3.

However, the second phase is the stage where the protective layer has been broken down. The corrosion process can start if oxygen and water are present at the reinforcing steel. The propagation period is between the beginning of the corrosion process and final failure of the structure. It mainly depends on the following factors:

- The cover depth
- The porosity of the concrete
- The relative humidity in the pores the chemical composition of the pore fluid
- The temperature

3 Influence of cracks on corrosion

Concrete is a material which is characterised by a rather low tensile strength. Thus, it is very common that concrete structures are cracking due to tensile stresses or restraint forces. This is why cracks are taken into consideration while designing concrete structures almost since the beginning of the design process. The cracks are creating openings in the concrete surface which helps chloride ions to be transported into the concrete, and as a result corrosion initiation may occur earlier in the reinforcement bars.

3.1 Types of cracks

During the whole life cycle of concrete structures different types of cracks can be distinguished. The most common ones are presented in Figure 3.1.

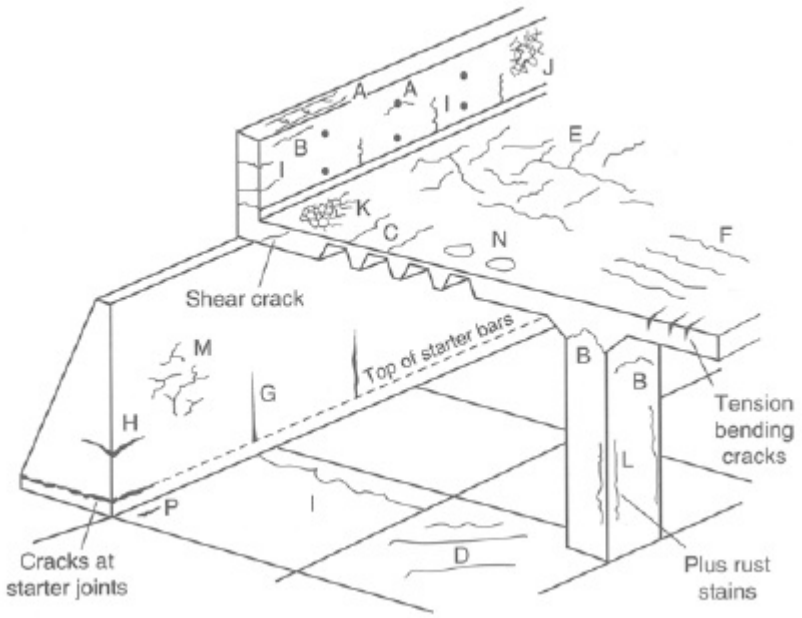

Figure 3.1 The most common crack types, CEB-rilem (1983).

According to CEB-rilem (1983), the cracks can be divided into three groups, regarding to the cause (capital letters refer to Figure 3.1):

- early cracks, due to:
  - plastic settlement – A, B, C;
  - plastic shrinkage – D, E, F;
  - thermal shrinkage – G, H;
  - long-term drying shrinkage - I
- corrosion and swelling aggregates – L, M;
- cracks caused by loads, due to:
  - bending,
  - shear
  - torsion

3.2 Summary of previous experiments

3.2.1 Tests by Schießl and Raupach

Experiments were conducted by Schießl and Raupach (1997). The purpose of their study was to clarify corrosion mechanism and factors which are influencing it, such as crack width, concrete cover and water/cement ratio. Cell current measurements were used to determine corrosion rate of reinforcement.

They used reinforced concrete beams of dimensions70 x 15 x 9.5 cm^3. In order to get unambiguous results, only one, centrally located, crack was obtained. This was achieved by inserting a 0.5 mm thick and 7 mm deep plastic strip. The experiment setup is shown in Figure 3.2.

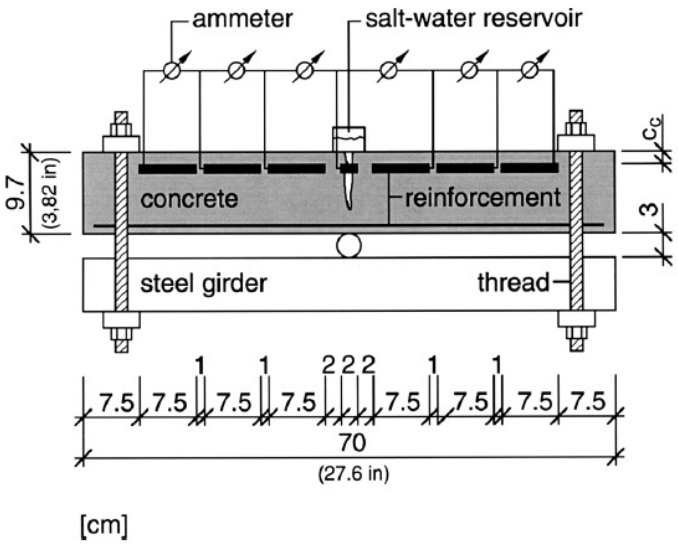

Figure 3.2 Test setup, from Schießl, Raupach (1997).

The concrete used for these tests had strength class B35 (C30/37) and *w*/*c* ratio 0.6. It was composed of 300 kg/m^3 OPC 35 F. The concrete cover varied as well; 15 and 35 mm. After casting, specimens were kept in a climate chamber with temperature of 20 ± 1 ^oC and relative humidity 80 ± 5 %.

After 28 days of curing, a salt-water reservoir was put on the top of the beam above the crack, to induce chloride corrosion. The 1% chloride solution was poured into reservoir once a week for a period of 24 hours for 12 weeks, followed with two periods of ponding with only tap water without chlorides. After that, the specimens were kept for one year at 80% of relative humidity. After one year 12 wetting cycles were repeated.

The results showed that increasing concrete cover from 15 mm to 35 mm gave lower mass loss of steel due to corrosion. A higher corrosion rate was observed also when the water/cement ratio increased from 0.5 to 0.6. The third influencing factor, which was investigated, was crack width. Crack width influenced the corrosion rate rather at the beginning of the corrosion propagation time; later the difference was not so significant. To sum up, the influence of crack width was not as significant as was the concrete cover and water / cement ratio.

3.2.2 Tests by Yoon et al.

Yoon et al. (2000) carried out tests studying interaction between loading level, corrosion rate, deflection and residual strength of reinforced concrete beams. Half-cell potential and galvanized current measurements were used to determine corrosion initiation time.

Two types of experiments were conducted; one to examine the influence of pre-cracking and previous loading on corrosion of reinforcement, and the second to examine influence of sustained loading on corrosion. The beams from the first group were loaded in four-point bending up to 45 or 75 % of the ultimate load and thereafter unloaded for the corrosion tests. Whereas the second ones were loaded up to 20, 45, 60 or 75% of the ultimate load respectively and the load was applied during the whole tests. Both groups were loaded after 28 days of curing. The dimensions of the beams were 100 x 150 x 1170 mm^3. The beams were reinforced with single bars. The concrete cover was 30 mm and the diameter of the reinforcing bar was 19 mm. The weight proportions of the mix used were 1:2:2:0.5 (cement-gravel-sand-water). Before loading the beams were exposed for 28 days to 95 % relative humidity at 22 ^oC. The loading system is presented in Figure 3.3.

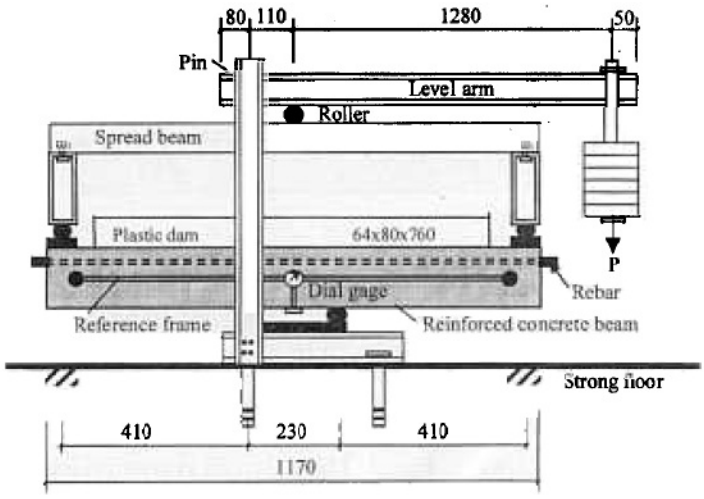

Figure 3.3 Sustained loading system, units in [mm], from Yoon et al. (2000).

After loading, the beams were kept in laboratory environment at room temperature with or without 3% NaCl solution. One cycle consisted of 4 days of wetting and 3 days of drying the specimens. The corrosion test was divided into two parts: Stage I and Stage II, which corresponded to initiation and propagation time of corrosion.

The experiment carried out by Yoon indicated that the loading level influenced the corrosion rate of the reinforcement bars. First of all, corrosion started earlier for the beams on which had been loaded, than for the unloaded beams. Increased load level decreased the corrosion initiation time. Moreover, in beams subjected to sustained load, the corrosion rate increased as well. Regarding failure mechanism, the corrosion level is important. With increasing corrosion level rate, the failure mode changed from shear to bond splitting failure.

3.2.3 Tests by Mohammed et al.

A study, conducted Mohammed et al. (2001), was aimed at investigating the influence of crack widths and type of bars (plain and ribbed) on corrosion of reinforcement in concrete. Macro- and microcell current measurements were used in this study.

Experiments were carried out on two groups of beams: the first one had only one centrally located crack while the second had several cracks. The dimensions of the beams in the first group were 10 x 10 x 40 cm^3. The proportions ratios of the mix were 1:2.5:0.3/0.5/0.7 (cement-sand-water). Three different crack widths were obtained: 0.1, 0.3 and 0.7 mm.

In the second group, the beams were 15 x 15 x 125 cm^3 with varying crack widths: 0.3, 0.5 and 0.7 mm. The concrete mixes used for this group, were characterised with two proportion mixes: 1:2.4:3:0.5 and 1:2.5:3.1:0.7 (cement-sand-gravel-water). The load used to crack the beams was 5 500 and 4 500 kg for plain and deformed bars respectively. The experimental setups are shown in Figure 3.4 - Figure 3.5.

After cracking, the beams with single cracks were subjected to an automatic wetting and drying cycle. A 3.5% NaCl solution of saltwater was sprayed for 24 h in a 60 ºC temperature, during the drying cycle the beams were kept in environment of temperature of 60 ºC and relative humidity 80% for 24 h. Before measurements, the beams were moved to environment of 20 ºC and 80% RH for 24 h. The experiment was continued for 13 weeks.

Regarding the multi-cracked beams, they were kept in open air and sprayed once a week with a 3.5% NaCl solution for 16 months.

The conclusion from this study was that crack width influenced only the initiation time. The presence of cracks were found to be more significant rather than crack width. During design it is more important to design a concrete mix with a low water / cement ratio than limiting crack width. Another conclusion of this study was that plain reinforcement bars had longer corrosion initiation time than ribbed bars.

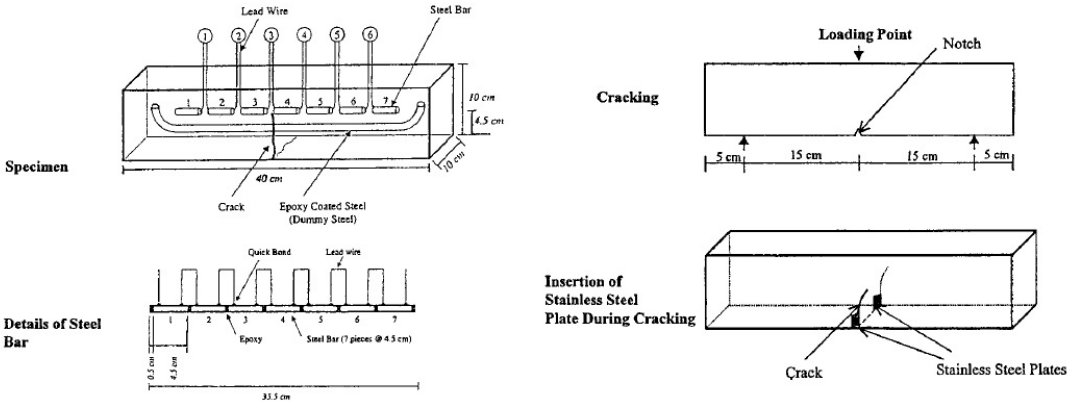

Figure 3.4 Test setup for single-cracked beams, from Mohammed et al. (2001).

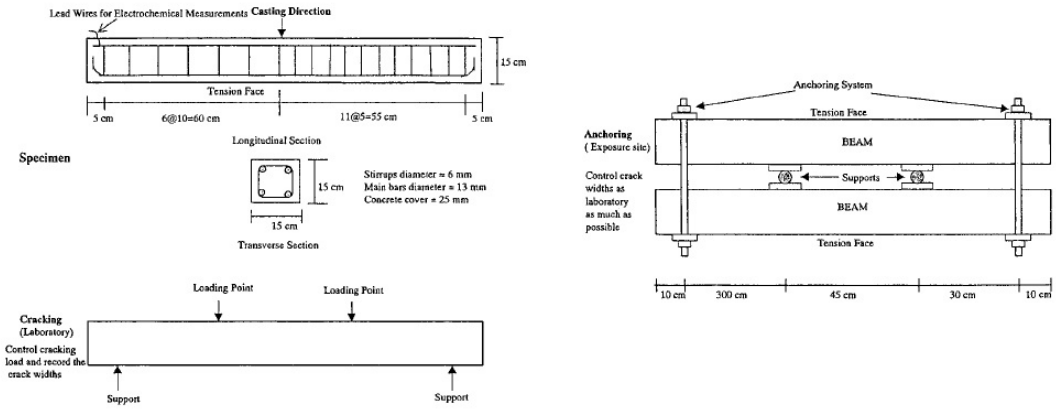

Figure 3.5 Test setup for multi-cracked beams, from Mohammed et al. (2001).

3.2.4 Tests by Tran and Huang

A Master's Thesis conducted by Tran and Huang (2006) was aimed at investigating the effect of cracks on steel reinforcement in chloride environment. Corrosion tests were conducted and the corrosion initiation time was recorded by half-cell potential measurements.

Beams with dimensions of 100 x 150 x 800 mm^3 were used with 20 mm of concrete cover. As reinforcement, 2 bars ϕ8 mm were used in every beam. In total 7 beams were produced. The specimens were divided into three groups: permanently loaded, loaded to crack and then unloaded and third group as a reference without cracks. The concrete used was C20/25 class with the mix proportions ratio 1:5:2.5:0.77 (cement-sand-aggregate-water). The beams were cured for 28 days in water. In order to crack beams, 12 kN load was applied by a loading lever, as shown in Figure 3.6.

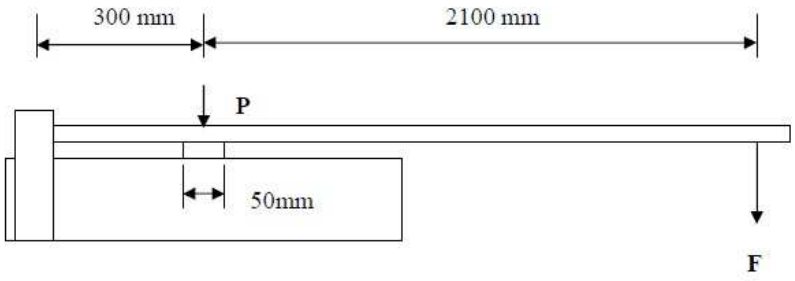

Figure 3.6 Loading system, from Tang and Huang (2006).

To initiate the corrosion process in reinforcement a 10 % NaCl solution was used. A Wettex® sponge was attached to the bottom of the beam to let the chloride ions migrate into the concrete. All of the specimens were exposed to the same conditions. The environment during testing was 30 % relative humidity and a temperature of 23 ^{o}C.

The main conclusion drawn from this study was that the crack width influenced corrosion initiation time. Moreover, the beams subjected to permanent load started to corrode first while for the beams without cracks (never loaded) no corrosion was detected during the exposure period (49 days).

3.2.5 Tests by Tammo

Tammo (2009) carried out experiments to investigate the influence of concrete cover and crack width on corrosion in concrete structures. The study focused on crack widths close to the reinforcement bar instead of crack widths at the surface. Time to initiation corrosion was determined by accelerated tests and measured by half-cell potential method.

The beams investigated were 980 mm long, 156 mm wide and had an effective depth of 76 mm. In total 26 beams were tested. Three different concrete covers were studied: 20, 40 and 60 mm. The beams were reinforced in two ways: the first one with two bars of ϕ8 mm diameter and the second with one bar of ϕ12 mm diameter. The concrete was of C20/25 strength class and the mix proportions ratio was 1:5:2.5:0.77 (cement-sand-aggregate-water). The specimens were cured for 28 days in water with a temperature of 20 ^{o}C. The beams were loaded twice to a steel stress of 380MPa, which corresponded to bending moment of 2.611 kNm (beams with ϕ8 mm rebars) and 2.923 kNm (beams with ϕ12 mm rebars), as presented in Figure 3.7. After two series of loading, the beams were loaded to final stress levels – 0, 250 and 350 MPa. The steel stress 250MPa corresponded to a bending moment of 1.718 kNm (beams with ϕ8 mm rebars) and 1.923 kNm (beams with ϕ12 mm rebars).

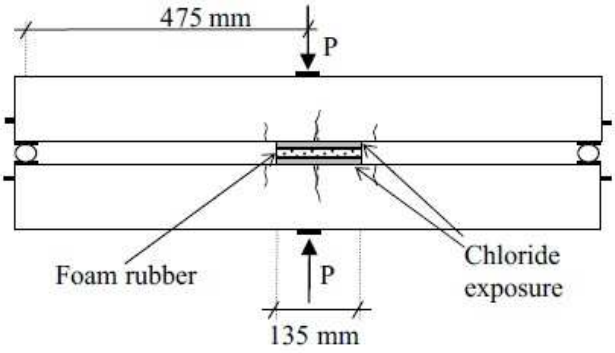

Figure 3.7 Test setup, Tammo (2009).

After the final loading the cracks widths were measured. The obtained crack widths were varying between 0.08 and 0.2 mm with spacing between 30 and 100 mm.

After cracking the specimens were kept in an environment with a temperature of 20 ^{o}C and 60 % relative humidity. After one week the beams were submitted to chloride exposure, which was a 10 % solution of NaCl.

The results of the study showed that large concrete covers protected the reinforcement from corrosion more efficiently than the smaller ones, even with wider crack at the surface. Moreover, the corrosion initiation time reduced with an increase of steel stress and crack widths close to the reinforcement.

3.3 Summary

To sum up the described research (Schießl and Raupach (1997), Yoon et al. (2000), Mohammed et al. (2001), Tran and Huang (2006), and Tammo (2009)), all of them stated that cracks have an influence on corrosion of reinforcement bars in concrete

structures. However, the influence is much more significant for the corrosion initiation time than in the corrosion propagation phase. Furthermore, concrete cover and water to cement ratio have a larger influence on corrosion than crack width. Cover is important also in that sense that when the cover is large, the crack width close to the reinforcement bar is smaller than when the cover is small. The higher the *w/c*, the faster the chloride transport in the concrete is, and thus, both corrosion initiation and corrosion propagation is affected negatively. It was also found that the loading history influences the corrosion as well; the higher the load level the earlier the corrosion initiation. Finally, plain reinforcement bars are more resistant to corrosion than ribbed bars.

4 Experimental programme

Three different experiments were conducted during this study. There were prepared specimens with fibres (F), without fibres (W), with different fibre volume: (1.3%), (1.0%), (0.6%), (0.3%), (0.0%) and with macro-synthetic fibres (0.6PP). The type of experiments and the number of specimens used are presented in Table 4.1.

Table 4.1 Overview of executed experiments.

Test method	**Test purpose**	**Number of specimens**							
		F	**W**	**1.3**	**1.0**	**0.6**	**0.3**	**0.0**	**0.6PP**
Corrosion tests on beams (Chapter 5)	Time to corrosion initiation	6	6	-	-	-	-	-	-
RCM tests (Chapter 7)	To determine the influence of fibres on the chloride migration coefficient	4	4	6	6	6	6	6	6
Resistivity tests (Chapter 0)	To determine the effect of fibres on the resistivity of concrete	4	4	6	6	6	6	6	6

Concerning the investigation of how fibres may influence reinforcement corrosion two concrete mixes were prepared. Both of them had a water cement ratio of 0.75. Of the two mixes, one contained 0.5 vol-% of steel fibres (40 kg/m^3) while the other mix was a control, without fibres. In order to conduct corrosion tests the beams had three different exposure conditions, as presented in Table 4.2:

- Group L were Loaded in three-point bending (permanently);
- Group U were cracked by loading in three-point bending and then Unloaded;
- Group W were not loaded and thus un-cracked.

Table 4.2 Arrangement of beams

Group name	L	U	W
With fibres	LF1, LF2	UF1, UF2	WF1, WF2
Without fibres	LW1, LW2	UW1, UW2	WW1, WW2

To study the corrosion process, half-cell potential measurements were made. To investigate the fibres effect on chloride migration coefficient, Rapid Chloride Migration (RCM) tests were performed according to NT BUILD 492 (1999). Resistivity tests were also conducted to determine the resistivity of the tested concrete.

4.1 Specimens preparation and treatment

4.1.1 Details of mixes

4.1.1.1 Concrete C 20/25

Two concrete mixes were prepared in the investigation of corrosion tests on beams. Details of mix designs are presented in Table 4.3. Both were produced by mixing cement, limestone filler, aggregate, sand, water and superplasticizer to achieve a self-consolidating concrete (SCC). The only difference between the two mixes was that the second mix contained cold drawn steel wire fibres with hooked ends (Dramix RC-65/35-BN). For each mix, 6 beams (100 x 100 x 800 mm) were cast for the corrosion tests, and 4 cylinders (ϕ100x 200 mm) for the chloride migration tests. Furthermore, 12 cubes (100 x 100 x 100 mm) and 4 cubes (150 x 150 x 150 mm) were cast for determination of the compressive strength.

With respect to the compressive strength, the concrete compressive strength class was determined according to EN 206-1. There are two criteria that were checked:

$$f_{cm} \geq f_{ck} + 1{,}48\sigma \quad (4.1)$$

$$f_{ci} \geq f_{ck} - 4MPa \quad (4.2)$$

For criteria (4.1), the standard deviation was assumed to be 10%*f_{cm}. Thus, the average compressive strength f_{cm} should be 28.7MPa. For criteria (4.2), any individual test result f_{ci} should be greater than f_{ck} - 4 MPa. Thus, the concrete can be classified as a C20/25 according to EN 206-1.

Table 4.3 Concrete mixtures for specimens used for corrosion tests.

Material	**Type**	**w/o fibres**		**w/ fibres**	
		mix 1	**mix 2**	**mix 1**	**mix 2**
		Weight (dry)	**Weight (dry)**	**Weight (dry)**	**Weight (dry)**
		[kg/m^3]	**[kg/m^3]**	**[kg/m^3]**	**[kg/m^3]**
Cement	CEM II/A-LL 42.5R Bygg, Skövde	280	280	280	280
Water	-	210	210	210	210
Sand 0-4	Sea sand	235	235	233	2323
Sand 0-8	Hol (natural)	631	631	625	625
Gravel 4-8	Tagene (crushed)	699	699	693	693
Limestone filler	Limus 40	220	220	220	220
Fibre	Dramix RC 65/35-BN	-	-	40	40
SP	Sikament 56/50	3.54	3.40	3.54	3.55
Slump flow [mm]		620	620	480	510
w/c		0.75	0.75	0.75	0.75
Density [kg/m^3]		2 330	2 331	2 305	2 310
Average compressive strength at 28 days [MPa]		31.5	30.5	29.3	29.3

4.1.1.2 Concrete C45/55

In order to check the influence of different amount of fibres on chloride migration coefficient and resistivity of concrete, 6 mixes of class C45/55 were prepared. Macro-synthetic fibers ENDURO HPP45 were used as an alternative to steel fibres. Details of mixes are presented in Table 4.4. The compressive strengths have been determined and the evaluation of the results shows that the concrete can be classified as a C45/55 according to EN 206-1.

Table 4.4 Concrete mixes for specimens with different fibre content.

Material	**Type**	**1.3**	**1.0**	**0.6**	**0.3**	**0.0**	**0.6PP**
		Weight (dry)	**Weight (dry)**	**Weight (dry)**	**Weight (dry)**	**Weight (dry)**	**Weight (dry)**
		[kg/m^3]	**[kg/m^3]**	**[kg/m^3]**	**[kg/m^3]**	**[kg/m^3]**	**[kg/m^3]**
Cement	CEM I 42.5 N (MH/SR/LA) Anläggnings -cement Degerhamn	425	425	425	425	425	425
Water	-	187	187	187	187	187	187
Sand 0-4	Sea sand	447	450	452	455	458	453
Sand 0-8	Hol (natural)	450	453	456	459	461	456
Gravel 4-8	Tagene (crushed)	592	595	598	602	606	599
Limestone filler	Limus 40	200	200	200	200	200	200
Fibre	Dramix RC 65/35-BN	100	75	50	25	0	5,733 Enduro HPP45
SP	Sikament 56/50	7.00	6.50	6.50	7.50	6.50	5.90

	1.3	**1.0**	**0.6**	**0.3**	**0.0**	**0.6PP**
Slump flow [mm]	640	635	750	650	770	710
w/c	0.44	0.44	0.44	0.44	0.44	0.44
Average compressive strength at 28 days [MPa]	74.4	65.1	69.4	71.3	63.9	68.7

4.1.2 Specimen details

As shown in Figure 4.1, each beam is 800 mm long with a cross section of 100 x 100 mm. The beams had two reinforcement bars with a diameter of 8 mm of quality B500B placed with a concrete cover of 20 mm. Prior to exposure to chlorides, the reinforcement bars were mechanically cleaned according to ASTM-G1-03 and weighed before casting. To be able to register the half-cell potential measurements, the rebars were longer than the concrete beams with a total length of 850 mm.

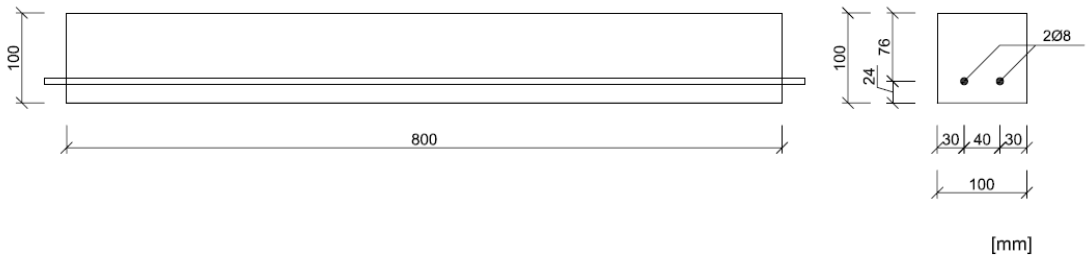

Figure 4.1 Measurements of beams

4.1.3 Casting and curing

All the specimens were cast with concrete from four mixes, where 3 beams (100 x 100 x 800 mm^3), 6 cubes (100 x 100 x 100 mm^3), 2 cubes (150 x 150 x 150 mm^3) and 2 cylinders (ϕ100 mm x 200 mm) were cast from each mix. The beams were cast in steel forms, thereafter covered with plastic sheets and demolded after 24 hours. Thereafter, the beams were cured in water for 14 days and further 14 days in a laboratory air where the temperature was approximately 18 ^oC and relative humidity around 35%. The smaller cubes and cylinders were cast in steel form while the larger cubes were cast in plastic forms and all cubes and cylinders were cured in water until testing.

4.1.4 Compressive strength tests

The cube strength tests were conducted to determine the compressive strength and to see if there were any significant differences between the different batches. Two types of cube specimens were cast, namely 100 x 100 x 100 mm and 150 x 150 x 150 mm. The 150 x 150 x 150 mm cubes were used to determine the standard strength (28 day compressive strength) while the smaller ones were used to determine the strength development.

The results showed that the concrete used in the beams, had roughly the same compressive strength regardless the inclusion of fibres or not, see Figure 4.2.

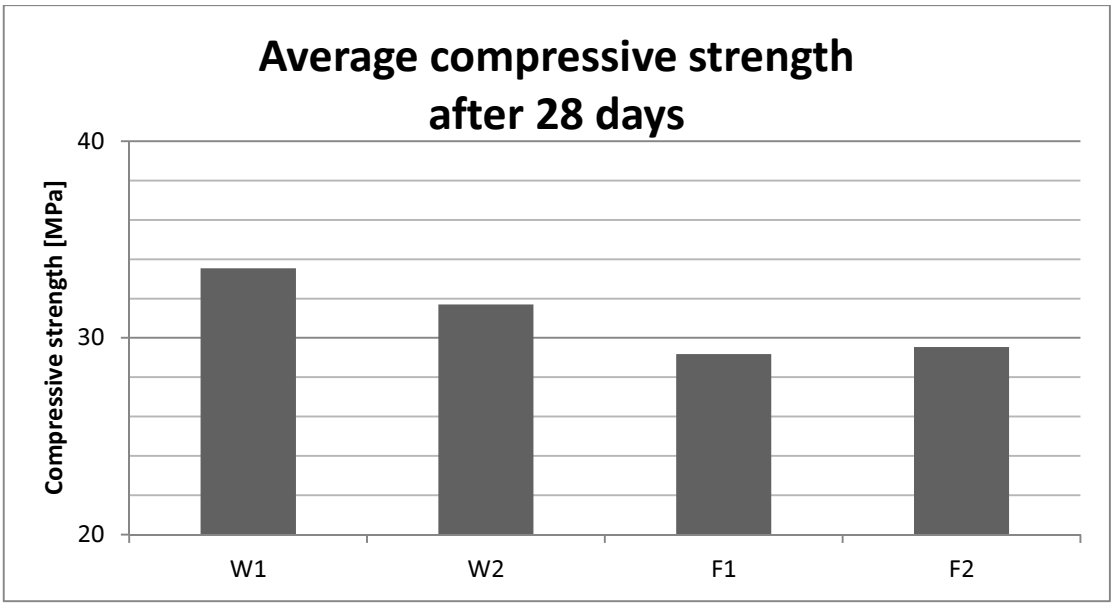

Figure 4.2 *Average compressive strength for concrete used for corrosion tests. "W" stands for specimens w/o fibres, "F" – w/ fibres. Concrete C 20/25.*

As can be seen from the results in Figure 4.2, addition of steel fibres did not influence the compressive strength significantly. This is contradictory to previous tests: see e.g. Mangat and Gurusamy (1987). Probably the results from this study are affected by using rather weak concrete with *w*/*c* 0.75. There were small increase for testing 100 x 100 x 100 mm cubes after 28, 56 and 98 days; see Figure 4.3.

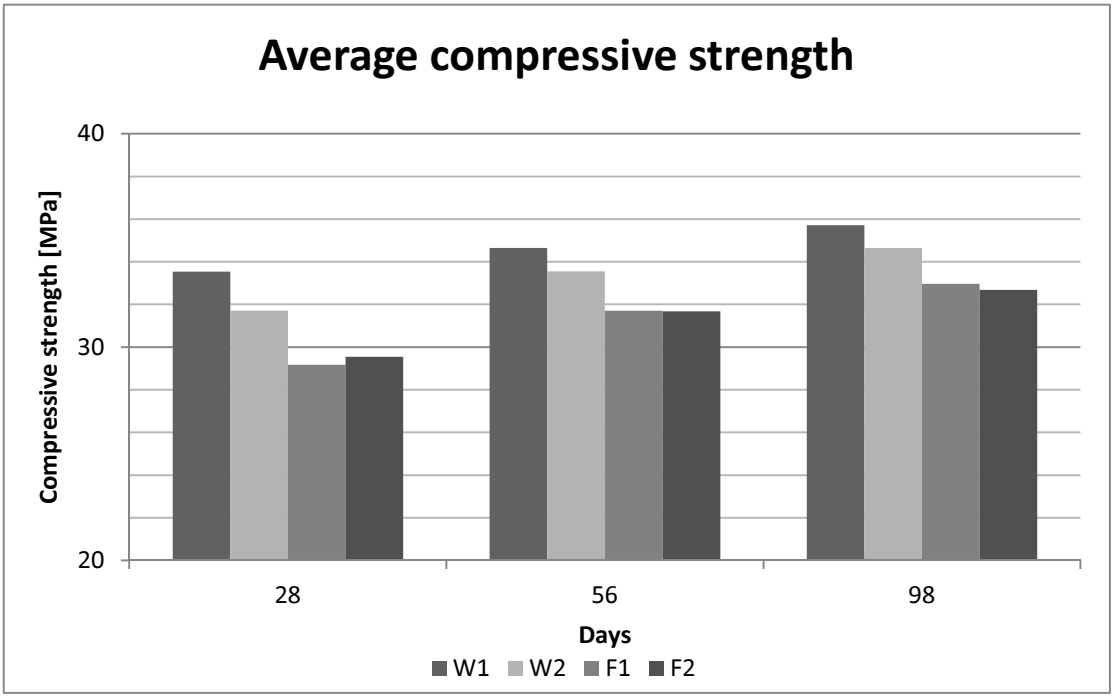

Figure 4.3 *Average compressive strength after 28, 56 and 98 days for concrete used for corrosion tests. "W" stands for specimens w/o fibres, "F" – w/ fibres. Concrete C 20/25.*

For specimens with lower *w/c* 0.44, which is more realistic for civil structures, a small increase (not significant) in compressive strength for specimens with fibres were noticed in comparison to the samples without fibres. Moreover, the results for the two types of fibres used were comparable, see Figure 4.4.

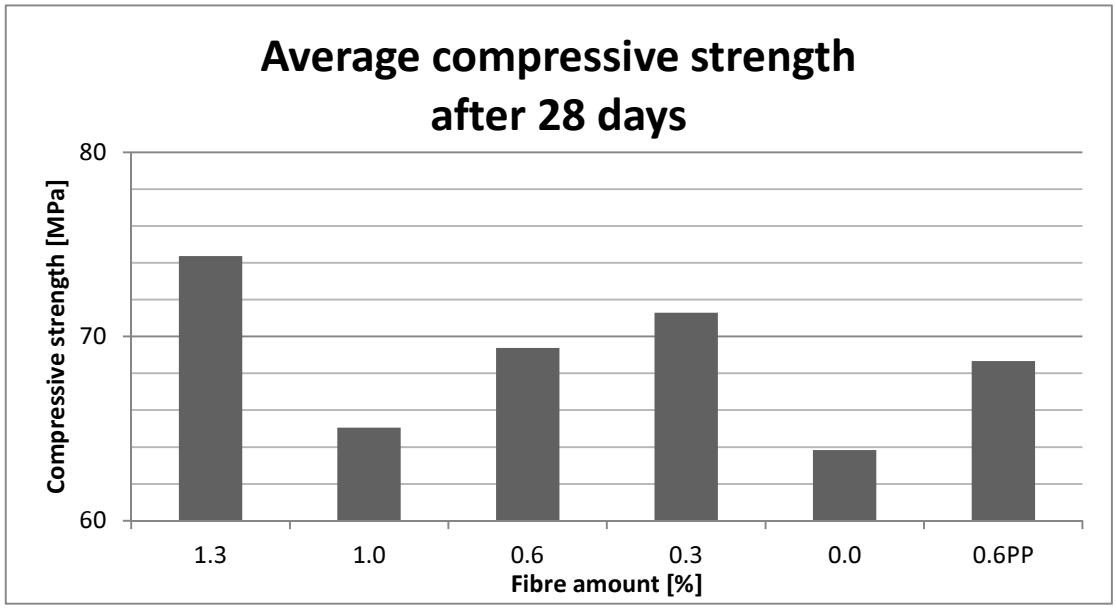

Figure 4.4 Average compressive strength for concrete with varying fibres amount. Concrete C 45/55.

5 Corrosion tests

5.1 Test setup

To investigate the time to corrosion initiation 12 beams were cast and divided into three groups as shown in Table 4.1 and Table 4.2. The beams from groups L (sustained load) and U (un-loaded) were subjected to three-point bending load after 28 days of curing with the load of 12 kN, which corresponds to 2.1 kNm of bending moment. The total bending moment including self-weight was 2.118 kNm. The calculated cracking moment was 0.367 kNm and mean crack width for beams without fibres was 0.10 mm. The boundary conditions are presented in Figure 5.1.

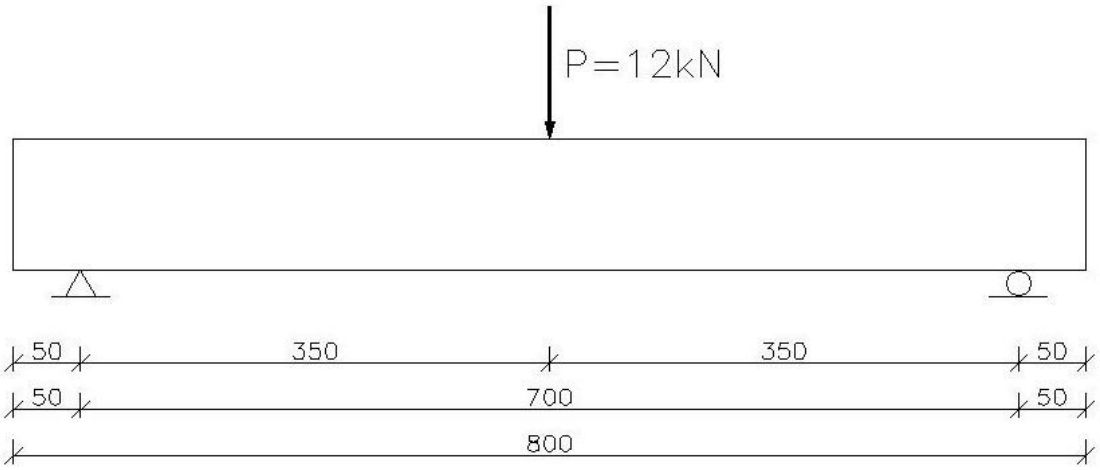

Figure 5.1 The boundary conditions

The load application method is schematically shown in Figure 5.2. Steel frames were prepared for each beam that were subjected to sustained loading; thus in total four frames. In each frame, a beam was placed inside on two supports with a distance of 700 mm between them. The frame was prevented from falling by use of 2000 kg counter weight which was put at the back side of frame. The beams were subjected to the load by a lever arm system. The lever arm was used to multiply a hung weight (*F*) 7 times to the midpoint of the beam. To reach those exact values, a load cell was used during pre-cracking beams from group U and during loading beams from group L, placed under the middle of the beam. The distance between hung load (*F*) and created load (*P*) was 1800 mm and from (*P*) to the end of the lever was 300 mm.

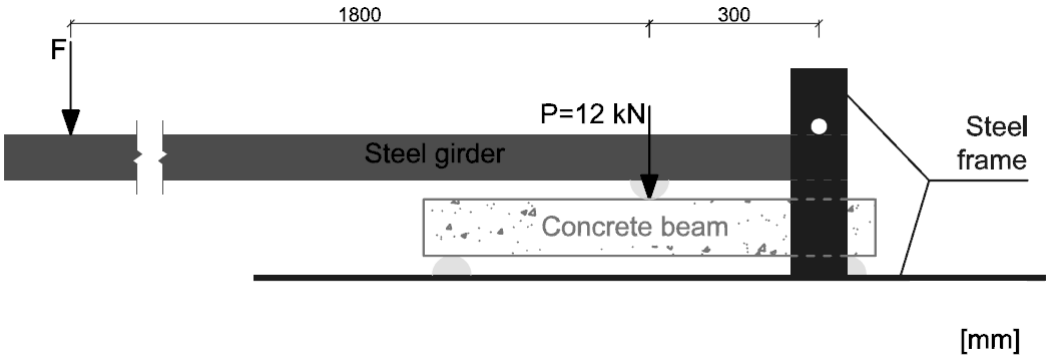

Figure 5.2 Loading system

Two of the series (L and U) were subjected to three-point bending load. One was done to examine effects of previous loading (U) on corrosion of steel reinforcement, while the other was to investigate effects of sustained loading (L). First, the load P = 12 kN was applied to the beams UF1, UF2, UW1 and UW2, which caused cracking; thereafter the load was removed. After that, beams LF1, LF2, LW1 and LW2 were loaded with P = 12 kN and this load was kept during the whole experiment.

The obtained crack widths for each beam measured by microscope are presented in Table 5.1 to Table 5.3.

Table 5.1 Crack widths and depths for beams from group L

No. of crack	LF1		LF2		LW1		LW2	
	width	depth	width	depth	width	depth	width	depth
	[mm]	[mm]	[mm]	[mm]	[mm]	[mm]	[mm]	[mm]
1	0.02	31.8	0.02	39.2	0.03	28.3	0.12	27.2
2	0.03	32.4	0.03	26.1	0.05	48.5	0.02	31.9
3	0.05	34.2	0.05	29.9	0.09	54.1	0.08	65.1
4	0.07	45.3	0.05	37.5	0.12	64.4	0.12	78.7
5	0.04	34.2	0.07	33.5	0.12	66.1	0.28	74.6
6	0.01	9.9	0.10	50.1	0.05	59.1	0.09	58.8
7	-	-	0.05	30.8	-	-	-	31.8
8	-	-	0.02	27.9	-	-	-	-
avg.	0.037		0.049		0.077		0.118	

Table 5.2 Crack widths and depths for beams from group U before unloading.

No. of crack	UF1		UF2		UW1		UW2	
	width	depth	width	depth	width	depth	width	depth
	[mm]	[mm]	[mm]	[mm]	[mm]	[mm]	[mm]	[mm]
1	0.01	13.5	0.01	44.0	0.04	62.8	0.04	46.8
2	0.04	46.2	0.06	54.5	0.05	71.6	0.12	67.3
2A	-	-	-	-	0.07	37.7	-	-
3	0.08	52.2	0.08	58.0	0.14	70.9	0.12	7.4
4	0.08	54.3	0.10	56.5	0.18	57.1	0.10	10.9
5	0.09	60.1	0.02	37.5	0.09	53.5	0.04	7.7
6	0.10	63.2	0.04	35.2	0.02	41.5	-	-
7	0.03	40.7	-	-	-	-	-	-
8	0.02	41.6	-	-	-	-	-	-
avg.	0.056		0.052		0.084		0.084	

Table 5.3 Crack widths for beams from group U after unloading.

No. of crack	UF1	UF2	UW1	UW2
	width	width	width	width
	[mm]	[mm]	[mm]	[mm]
1	0.01	-	0.01	0.01
2	0.01	0.03	0.01	0.04
2A	-	-	0.01	-
3	0.01	0.03	0.04	0.05
4	0.02	0.03	0.07	0.04
5	0.02	0.01	0.04	0.01
6	0.02	0.01	0.01	-
7	0.01	-	-	-
8	0.01	-	-	-
avg.	0.014	0.022	0.027	0.030

5.2 Exposure conditions

In this study the aim was to create a humid environment that would be more similar to real conditions outside, i.e. approximately 75 % RH. After applying the load to the beams that were subjected to sustained loading, a "tent" was built to provide such an environment; see Figure 5.3. It was made by a wooden frame covered with plastic sheets. The unloaded beams and the beams without load were placed in covered plastic containers. Inside the "tent" and the plastic containers, bowls with an oversaturated NaCl solution (i.e. non dissolved NaCl crystals present in the bottom of the containers) were placed to maintain a relative humidity around 75%. The content of these bowls were not in contact with the test specimens. Fans were installed to arrange air flow inside the closed boxes which are shown in Figure 5.4. The set-up to create the different exposure conditions are shown in Figure 5.3 and Figure 5.4.

The salinity in seawater (oceans) is normally between 3.1% and 3.8%, and this gives rise to a chloride concentration of 1.9% to 2.3% respectively: see e.g. Mehta (1990). Due to the short time of testing, the chloride concentration used in these tests was increased to 6.0 %, which corresponds to a 10% of NaCl solution in potable water. Especially prepared bowls were attached near the beam with a sponge inside. The purpose of this configuration was to transfer chlorides through the sponge to the surface of the beam which is shown in Figure 5.5. At the bottom surface of the beam the sponge were in contact over a length of 20 cm. Due to risk of evaporation of NaCl solution, the bowls were re-filled every day. The temperature inside the containers varied between 16 ºC and 19 ºC.

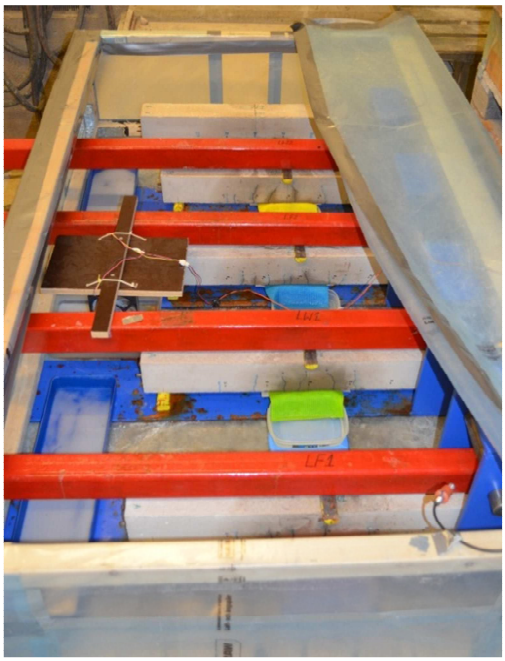

Figure 5.3 *Set up to create the exposure conditions for permanently loaded beams (group L). The containers with the oversaturated NaCl solution can be seen to the left in the figure.*

Figure 5.4 *The set up to create the exposure conditions for beams from groups U and W. The container with the oversaturated NaCl solution can be seen to the left in the figure.*

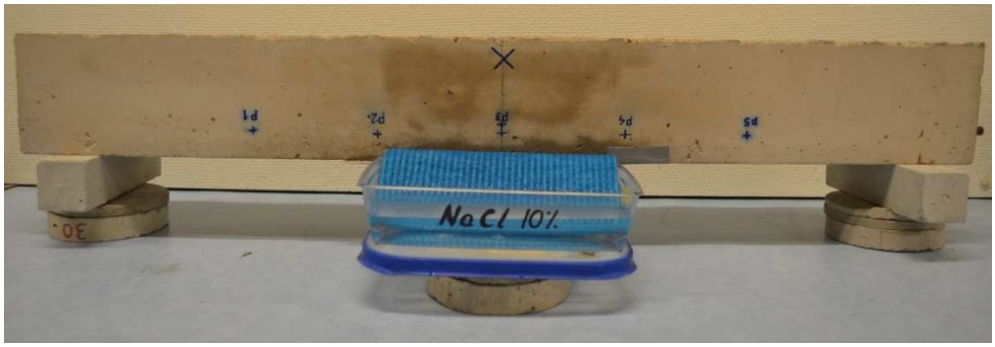

Figure 5.5 *Chloride exposure setup*

5.3 Half-cell potential measurements

The half-cell potential test method is the most commonly used method of inspecting reinforcement bars of concrete structures when it comes to estimating the corrosion state of bars. The method is well described, for example in ASTM C876 (1999) or RILEM recommendation Elsener et al. (2003). This method gives a good way of detecting areas of corrosion much earlier than they can be visible on a structure's surface. For this test, single or multiple electrode setups can be used. In this study, a single electrode was applied; whereas, multiple electrode devices can be used for assessing big structures such as bridge decks, walls or parking decks. However, half-cell potential measurements do not give sufficient information on the state of corrosion rate of the reinforcement bars. On the basis of this data decisions can be made about conducting more tests such as chloride content or carbonation depth.

Corroding and passive bars give a difference in electrical potential, hence a macrocell is generated and a current starts to flow between these areas; this is schematically

shown in Figure 5.6. This electric field can be measured by an appropriate electrode. In the tests made in this project a SCCE (Ag/AgCl electrode filled with saturated KCl solution) was used. The standard potential of a SCCE is about 0.12 V more positive than that of a CSE ($Cu/CuSO_4$ electrode), the latter is referred in the standard ASTM C 876. The measured half-cell potential can be used to estimate the probability of corrosion, see Table 5.4.

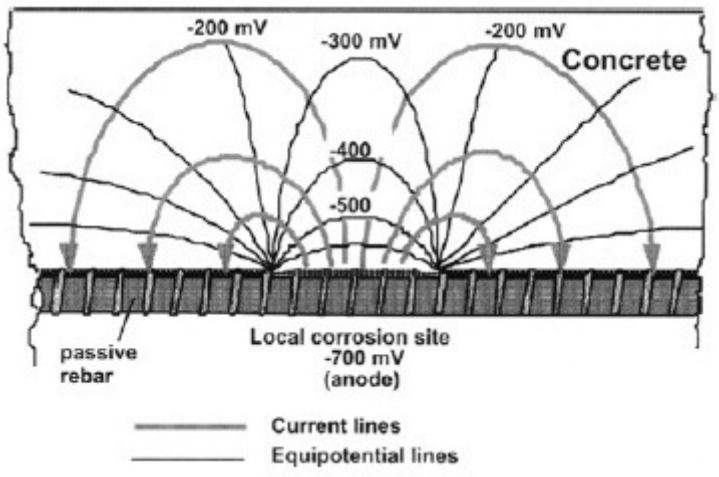

Figure 5.6 Schematic view of the electric field and current flow in an active/passive macrocell on steel in concrete, Elsener et al. (2003).

Table 5.4 Interpretation of results according to ASTM C876.

Measured potential E (CSE)	Measured potential E (SSCE)	Probability of corrosion
E > -0.20V	E > -0.08V	less than 10%
-0.20V < E < -0.35V	-0.08V < E < -0.23V	uncertain
E < -0.35V	E < -0.23V	greater than 90%

The procedure, according to ASTM C876, is this: one electrode is put on a wet sponge which is placed on the concrete surface while the second electrode is in connection with a reinforcement bar, the potential measurements are read from a voltmeter (shown in Figure 5.7 and Figure 5.8). In order to get stable results from the measurements, the sponge as well as the concrete surface needs to be wet. At the same time, the level of electrolyte in electrode should be sufficient.

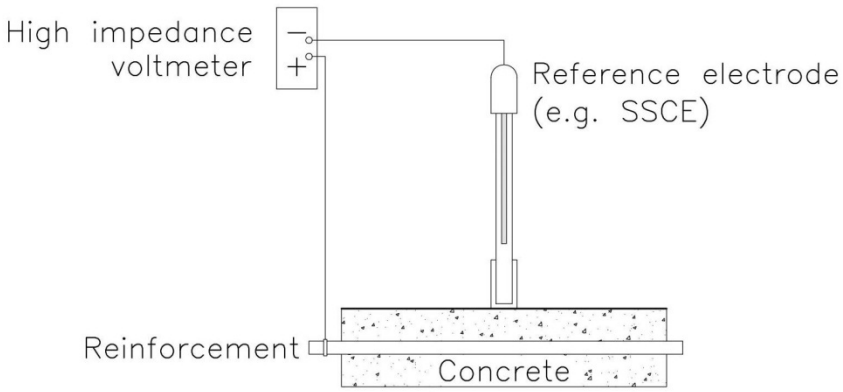

Figure 5.7 Half-cell circuitry.

Figure 5.8 Half-cell potential measurement.

In this study, the potentials were measured in 5 representative points for each beam, as in Figure 5.9.

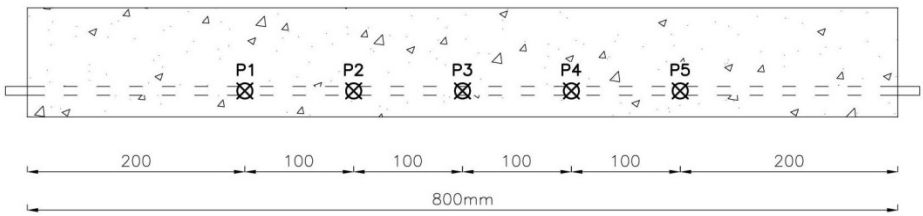

Figure 5.9 Side view of the beam with marked points for half-cell potential measurements.

The measurements were conducted around three times per week for each beam. Results for these measurements for point no. 3, which is representative with respect to the corrosion initiation, are presented in Figure 5.10 to Figure 5.12. This point was

chosen, as it was in the middle of the beams above the chloride exposure; moreover, it was in this point the highest corrosion risk was measured. The detailed results can be found in 0.

As can be seen in Table 5.5 the measured half-cell potentials can be used to evaluate the probability of corrosion of the rebars. However, in the current project, the change of potential over time was in focus. When there was a sudden drop in potential corrosion initiation of the rebars was assumed.

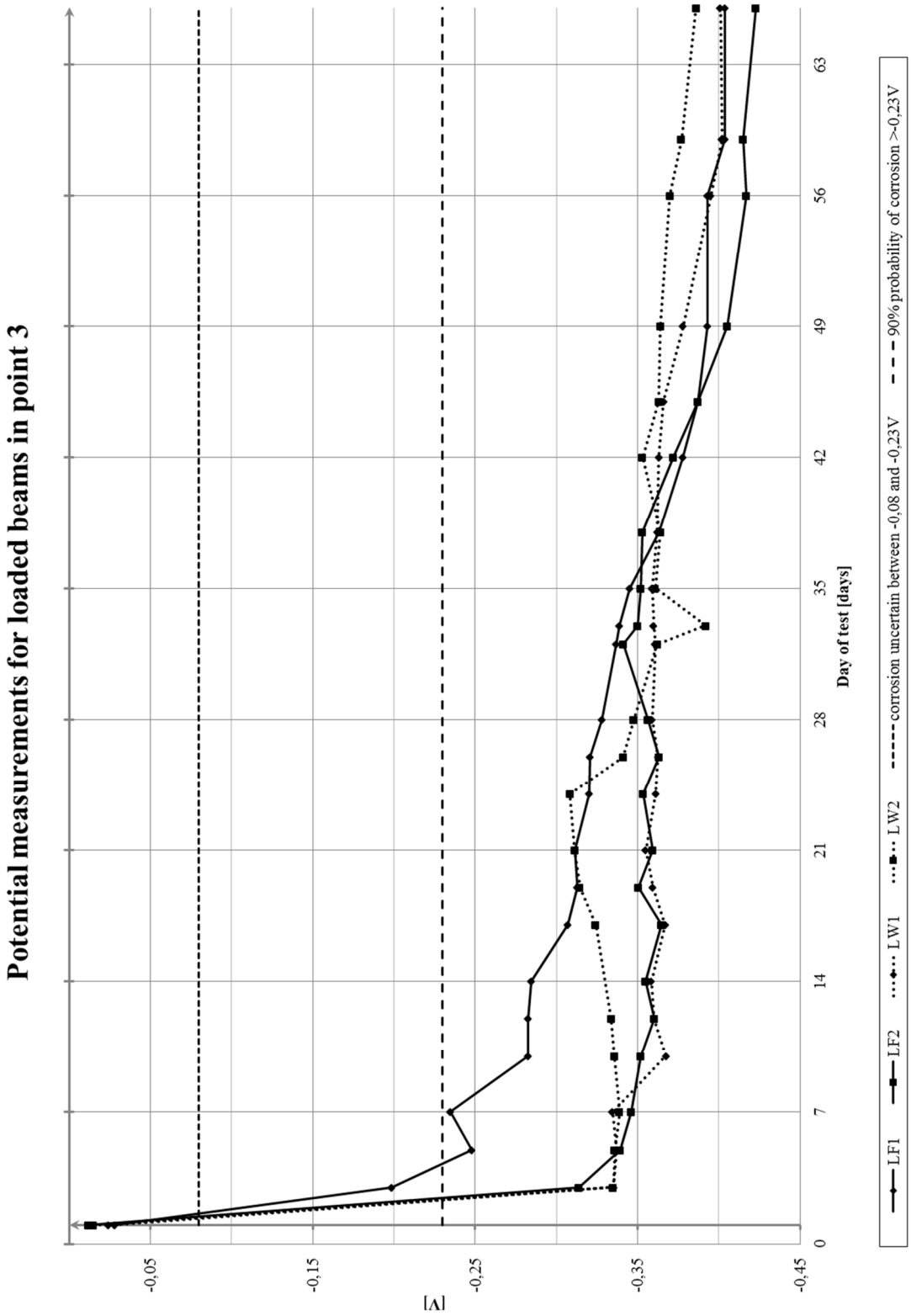

Figure 5.10 Potential measurements for permanently loaded beams in representative point no. 3.

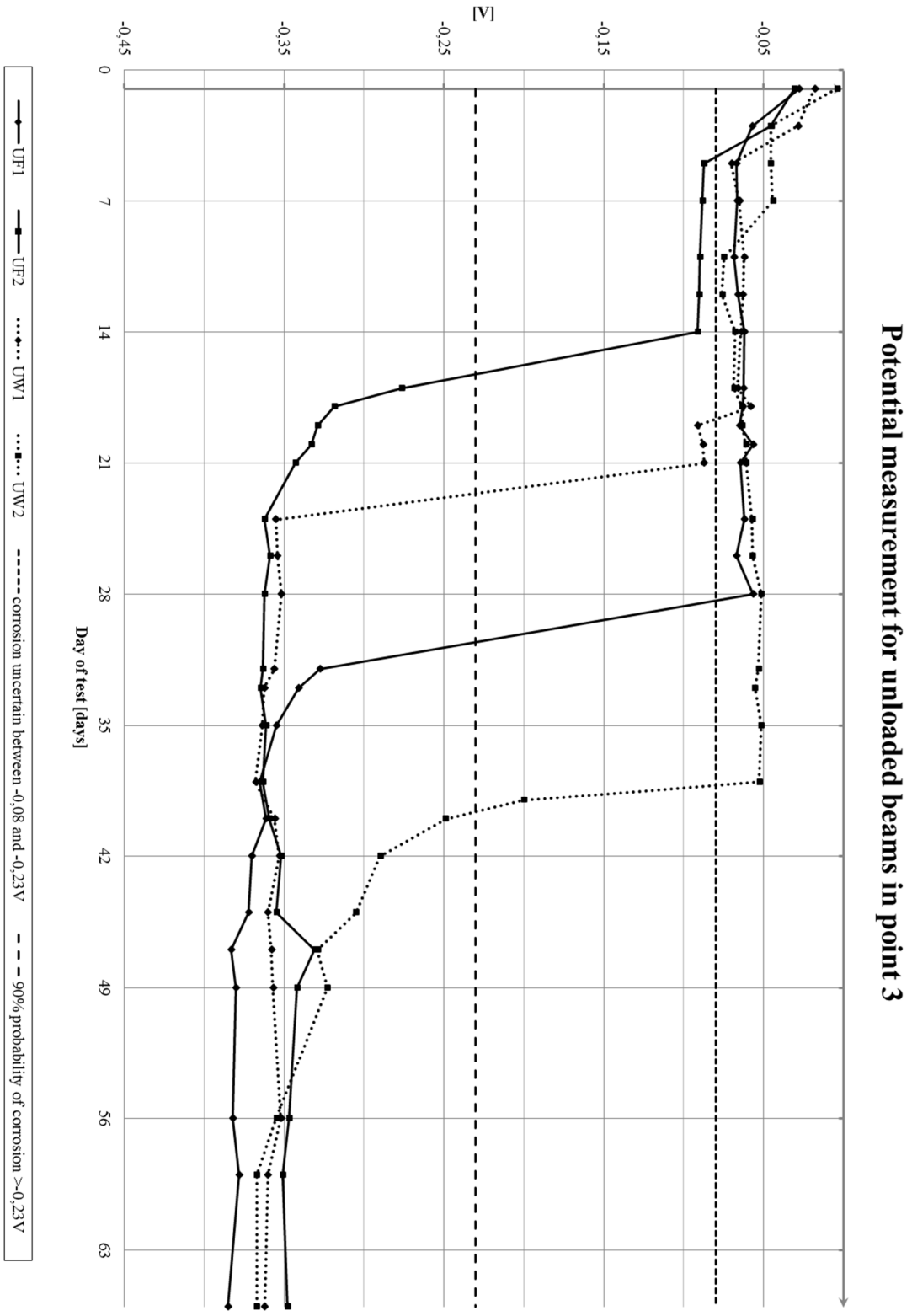

Figure 5.11 Potential measurements for loaded – unloaded beams in representative point no. 3.

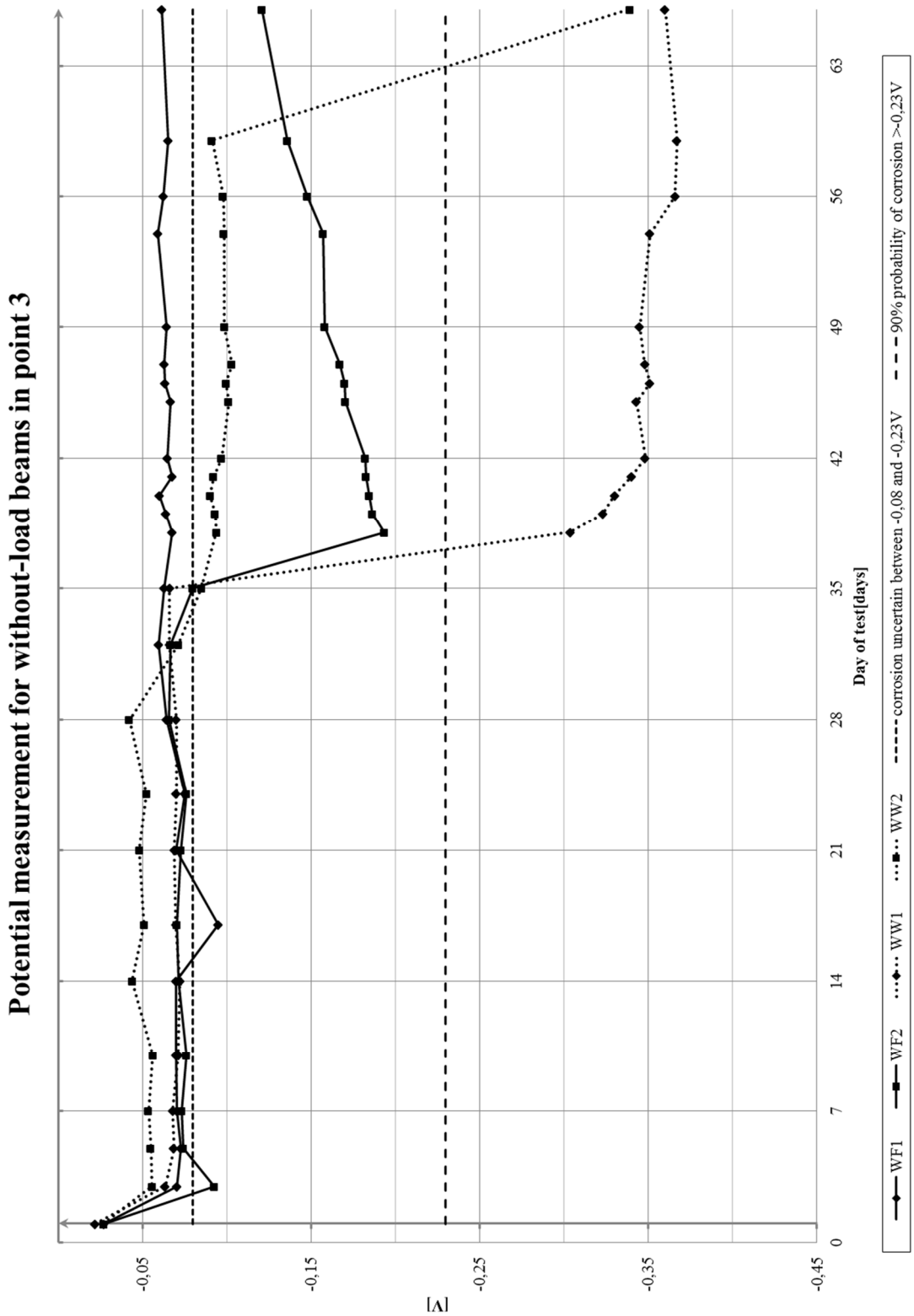

Figure 5.12 Potential measurements for without load beams in representative point no. 3.

In Figure 5.10 to Figure 5.12, the probability of corrosion is indicated (according to ASTM C (1999)), this is better described in Table 5.4. However, in the RILEM recommendation, Elsener et al. (2003), it is suggested not to use these values as an absolute criterion. This is because the results of half-cell measurements depend not only on corrosion state of the rebar but also on concrete cover, chloride content or carbonation depth and moisture content as well.

As can be noticed in Figures 5.10 to 5.12, decreasing of potentials was noted earliest for the permanently loaded beams. This is as can be expected, since the crack widths were largest in this group. In general, the wider the cracks were, the earlier was the corrosion initiation, see Figure 5.12, where the time for corrosion initiation is plotted versus the average crack width. It can be noted that all beams in group L (loaded) had at the time of the first measurement already a large negative potential indicating that corrosion was initiated. When it comes to second group – loaded/unloaded beams, the situation is a little bit different. The corrosion initiation time was longer, as the crack widths were smaller than in L group. The first beam to start corroding was one with fibres (UF2), for which drop in potential measurements was recorded earliest, even though the average crack widths was not the widest.

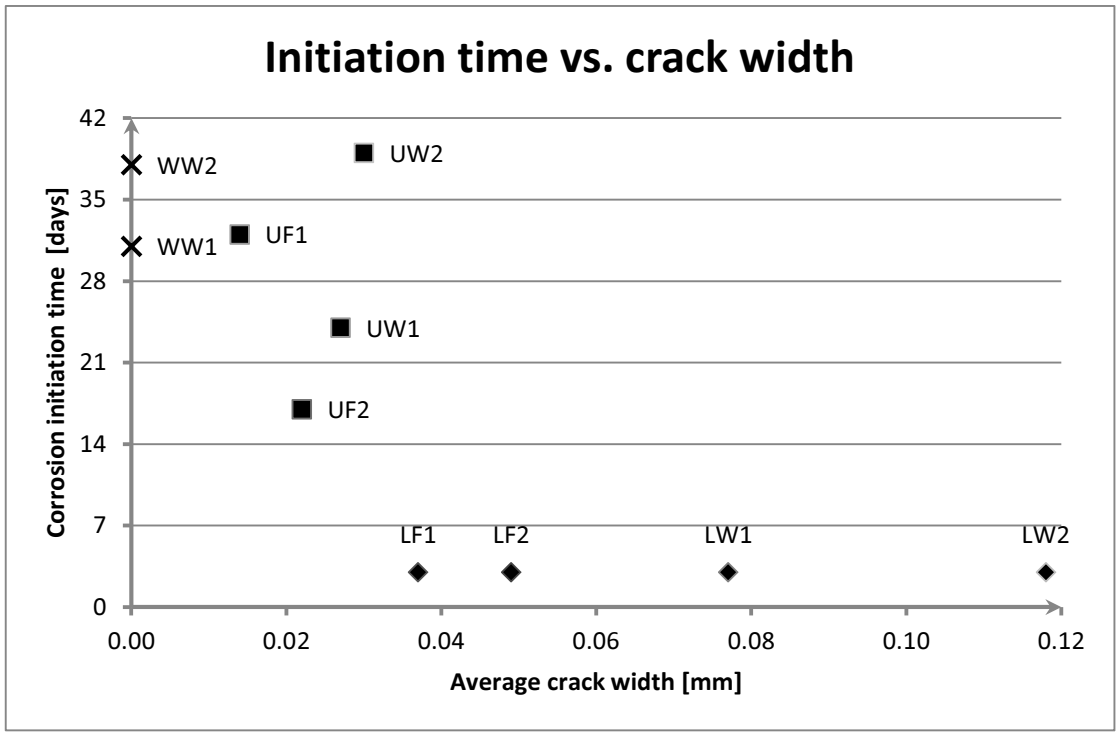

Figure 5.13 Corrosion initiation time versus average crack width. Corrosion has not started in beams WF1 and WF2.

The specimens in the loaded group started to corrode much earlier than similar ones did in the similar study conducted by Tran and Huang (2006). Their measurements showed that corrosion was initiated after around two weeks compared to after 3-7 days in this study. This can be probably explained by two main differences between these two studies. First of all is concrete curing time, in this study the beams were kept saturated in water for two weeks and then moved to conditions corresponding to relative humidity around 40 % for two following weeks. Whereas, in previous study

they were kept in water for 28 days. The second difference is exposure condition, and particularly the relative humidity during testing time. In this study specimens were subjected to 75 % ± 5 % RH. While, in the previous study the tests were conducted in dryer conditions (around 40 % RH), which resulted in more rapid chloride transport.

Apart from the initiation time for the loaded beams, there is another difference regarding to corrosion of beams without load. Two out of four un- cracked beams started to corrode as well. Of these beams all were without fibres. Again, the reason for this can be curing time and exposure conditions.

5.4 Visual observations

It was observed that chloride exposure affects also fibres and makes them corroded. As a result, fibres close to the concrete surface are causing rust stains. When it comes to using fibres for structures with visible surfaces the stains give a bad esthetical impression as shown in Figure 5.14.

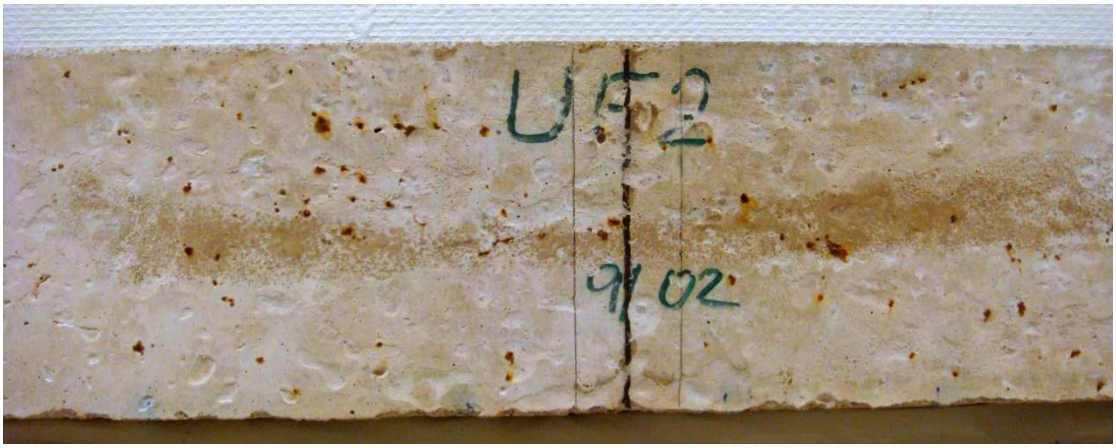

Figure 5.14 Example of corrosion of fibres close to concrete surface.

After exposure all of the specimens were destroyed in order to see how and which bars had corroded. Almost all of the rebars corroded, apart from bars from beams WF1 and WF2, which did not have any signs of corrosion. Reinforcement bars from the groups loaded (L) and not cracked (W) had a corrosion pit in the middle, where they had been exposed to chlorides. However, beams from group Loaded-Unloaded (U) did not have the corrosion pit in the middle, but around 20 cm towards one of the ends of the beam. This was outside the zone where the chlorides were directly available in the sponge, at the crack next to the one in the middle; see Figure 5.17Figure 5.18. This can be explained by the conditions in which chloride induced corrosion starts. The most probable conditions that corrosion starts are where there is around 80 % of moisture inside the concrete specimen and oxygen available. These conditions probably occurred in the side crack next to the middle one, perhaps due to lack of oxygen in the mid crack. However, it should be noted that the conditions were similar for all beams. Thus, to the authors there is no obvious explanation to why corrosion did not occur at the centre crack for the Loaded-Unloaded beams while it did for the others. The corrosion pits can be seen in Figure 5.15, Figure 5.17, Figure 5.19.

Figure 5.15 Corrosion pit on rebars from beam LW2.

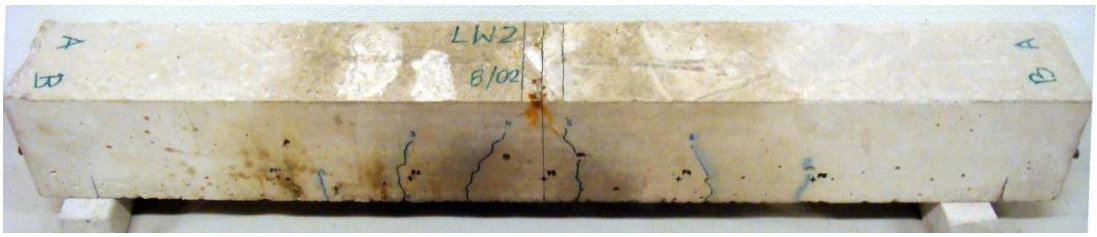

Figure 5.16 View of beam LW2 and crack patterns.

Figure 5.17 Corrosion pits on rebars from beam UF1.

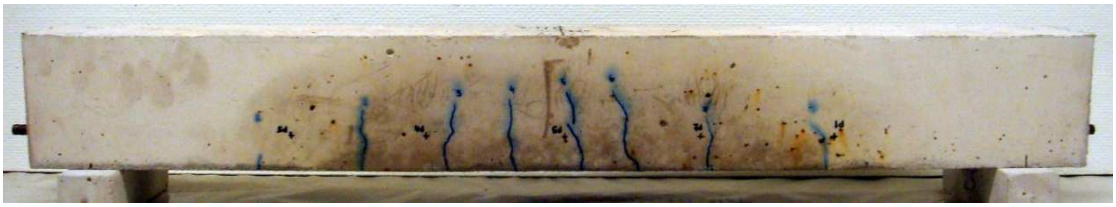

Figure 5.18 View of beam UF1 and crack patterns. First rebar is bar B.

Figure 5.19 Corrosion pits on rebars from beam WW2.

Figure 5.20 View of beam WW2.

In order to determine the amount of corrosion the next step was to clean the rebars. Mechanical cleaning of each bar was repeated several times, according to the procedure in ASTM G1-03 (2003). Before and after each cleaning cycle the bar was weighed and the mass losses for each bar are presented in Appendix F:.

6 Resistivity tests

This test was performed to determine the electrical resistance of the concrete samples. This parameter is relevant when, for example, describing resistance to chloride penetration. In general: the lower concrete resistivity, the more rapid chloride transport; see e.g. Tuutti (1982). According to Hope et al. (1985), the results are highly influenced by the following factors:

- resistivity of concrete increases with age,
- resistivity of saturated concrete increases with decreasing *w/c* ratio,
- resistivity of partially saturated concrete increases with increasing *w/c* ratio,
- resistivity of concrete increases with decreasing moisture,
- resistivity of concrete increases with decreasing temperature,
- reinforcing steel that falls within the field of influence of the resistance measuring probes will reduce the measured value of the resistance;

The experiments were conducted according to the procedure described in Tang et al. (2011). The preconditioning was conducted in the following steps: (1) the specimens were put into a vacuum container, where the pressure was reduced to the level of 10-50 mbar using a vacuum pump; (2) after three hours under vacuum, a saturated $Ca(OH)_2$ solution was added in order to immerse all of the specimens , the vacuum was kept for one more hour; (3) the pump was turned off and the samples were left in the solution for the next 18 hours.

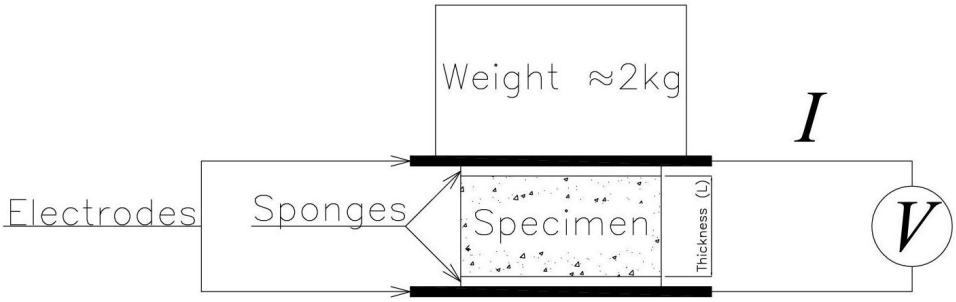

Figure 6.1 Resistivity test arrangement

After the preconditioning, the test was arranged as shown in the Figure 6.1. The resistance between two electrodes was determined by the LCR meter at a frequency of 1 kHz and recorded as R_{s+sp}. Next step was to remove the specimen (leaving the sponges and weight in the same place) and then measure the resistivity between the electrodes which was recorded as R_{sp}. The final resistivity of concrete was calculated as:

$$\rho = \frac{\pi d^2}{4000L}\left(R_{s+sp} - R_{sp}\right) \tag{6.1}$$

where:

ρ – resistivity of concrete [Ωm]

d – diameter of specimen [mm]

L – thickness of specimen [mm]

R_{s+sp} – resistance measured with the specimen and sponges [Ω]

R_{sp} – resistance measured with the sponges only [Ω]

The following charts, Figure 6.2 - Figure 6.4, are presenting results of resistivity test.

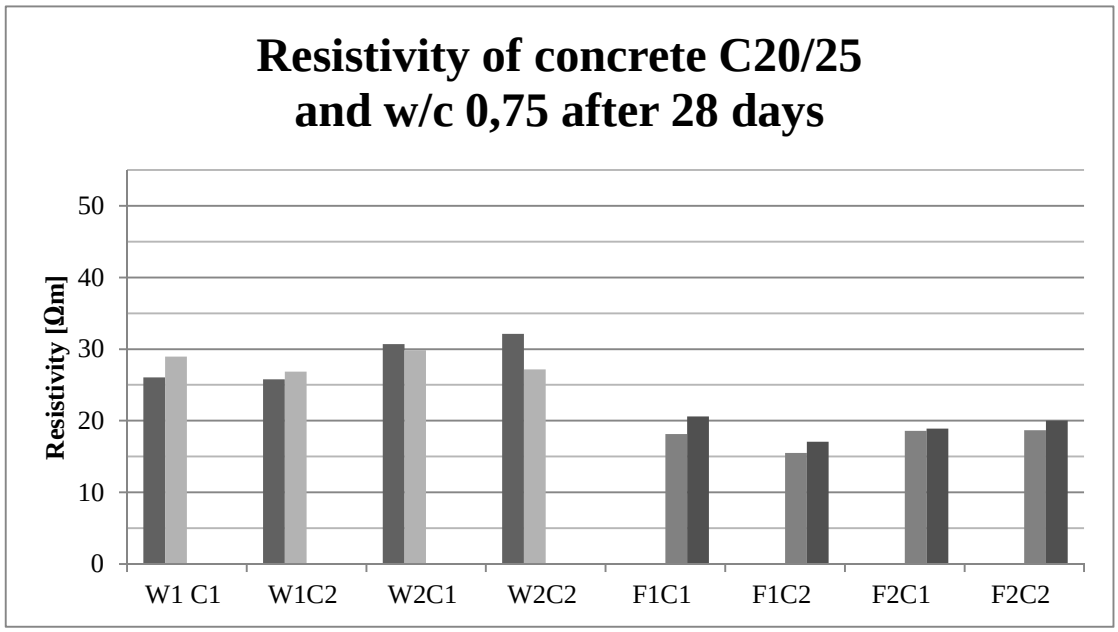

Figure 6.2 Results of resistivity tests after 28 days for concrete used for corrosion tests. W stands for specimens w/o fibres, F - w/ fibres and C – cylinder.

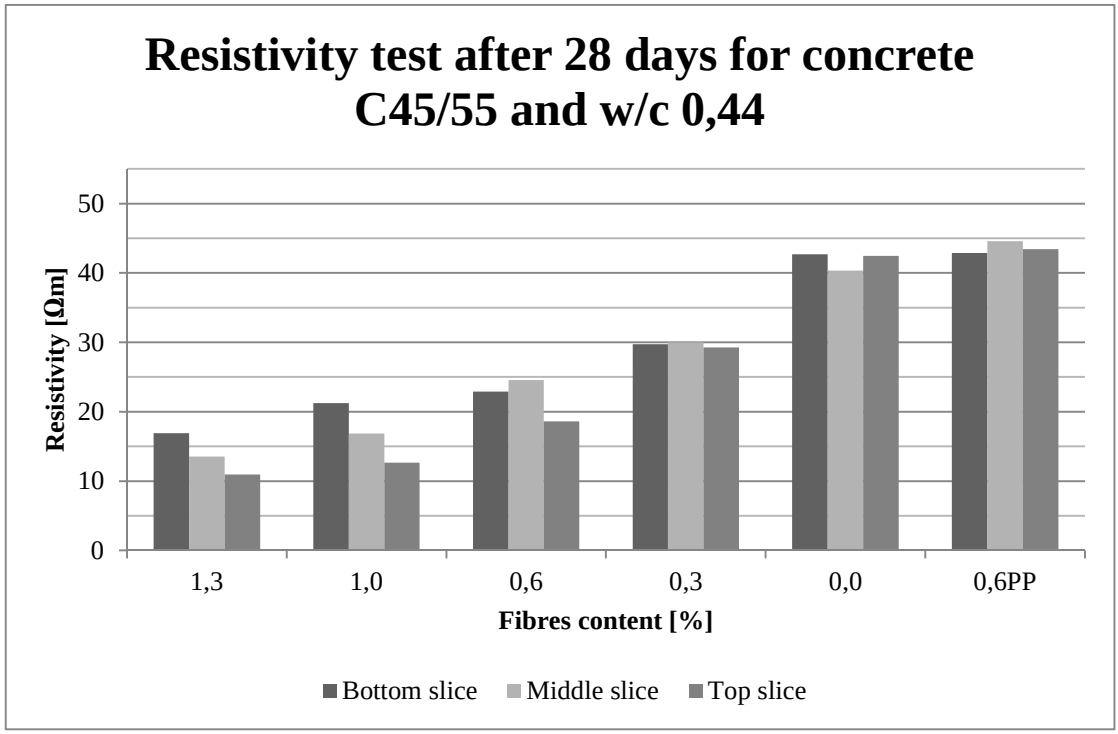

Figure 6.3 Results of resistivity test after 28 days for concrete commonly used for civil engineering structures with varying amount of fibres.

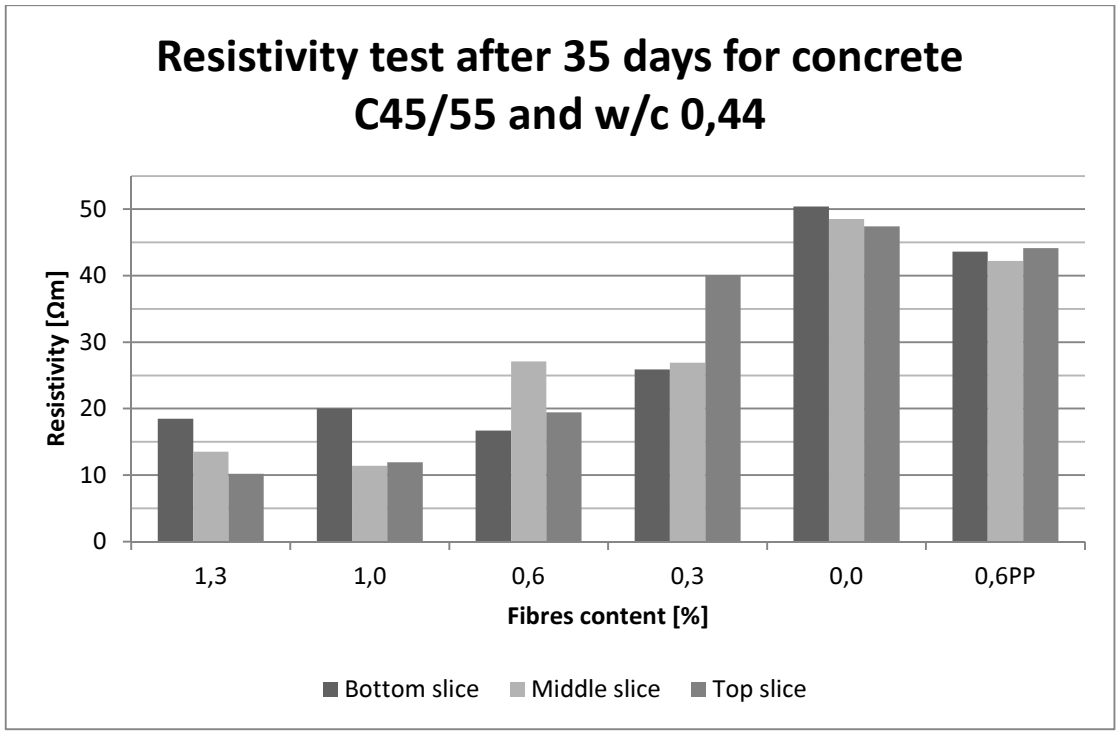

Figure 6.4 Results of resistivity test after 35 days for concrete commonly used for civil engineering structures with varying amount of fibres.

To sum up these results, it was expected that the resistivity of concrete with steel fibres is lower than without steel fibres and that the resistivity decreases with steel fibre content. Secondly, samples with plastic fibres yielded approximately the same results as samples without fibres. There is also noticeable increase of resistivity when water / cement ratio decreases – compare Figure 6.2 and 6.3.

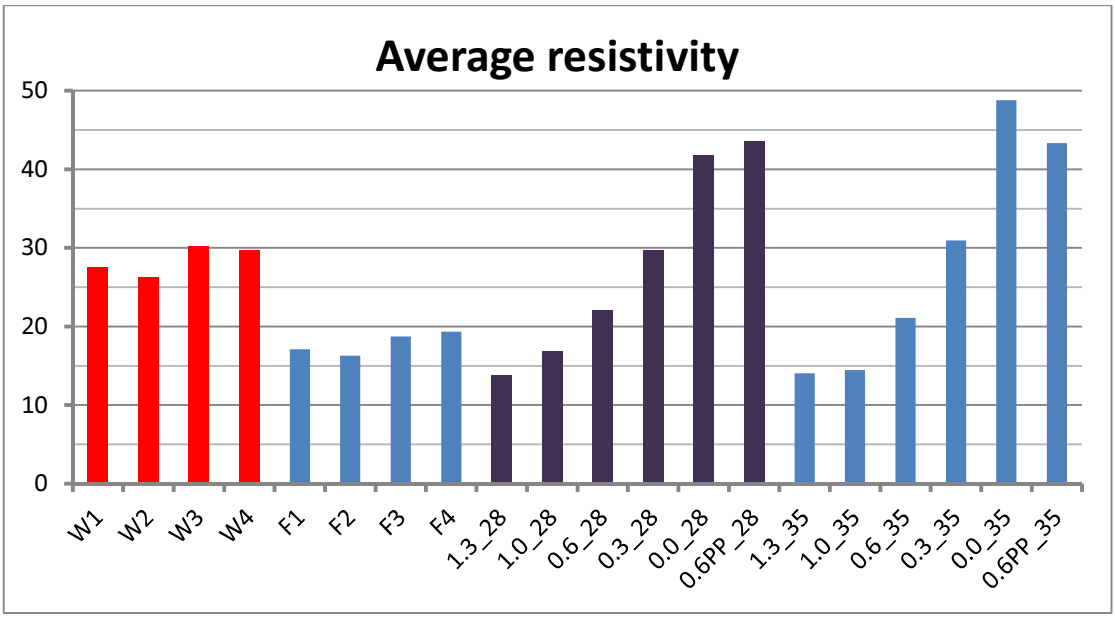

Figure 6.5 *Results of resistivity test for all of the specimens, no variation for bottom, middle and top slice – average value for 3 slices. "_28" stands for results after 28 days and "_35" after 35 days.*

7 Rapid Chloride Migration tests

Rapid Chloride Migration tests, according to NT Build 492, were conducted to determine the chloride migration coefficient. This test is a non-steady-state migration experiment, which means that flux is time dependant and diffusion seldom reaches stationary state. The specimen is situated between two solutions and is exposed to an electrical potential gradient. The main advantage of this method is that it takes only 24 hours or less to conduct the test. The testing procedure followed in this study was according to the standard NT BUILD 492, Nordtest (1992). The scheme of arrangement is shown in Figure 7.1. The used specimens and the preconditioning process, which was conducted, are the same as in Chapter 6.

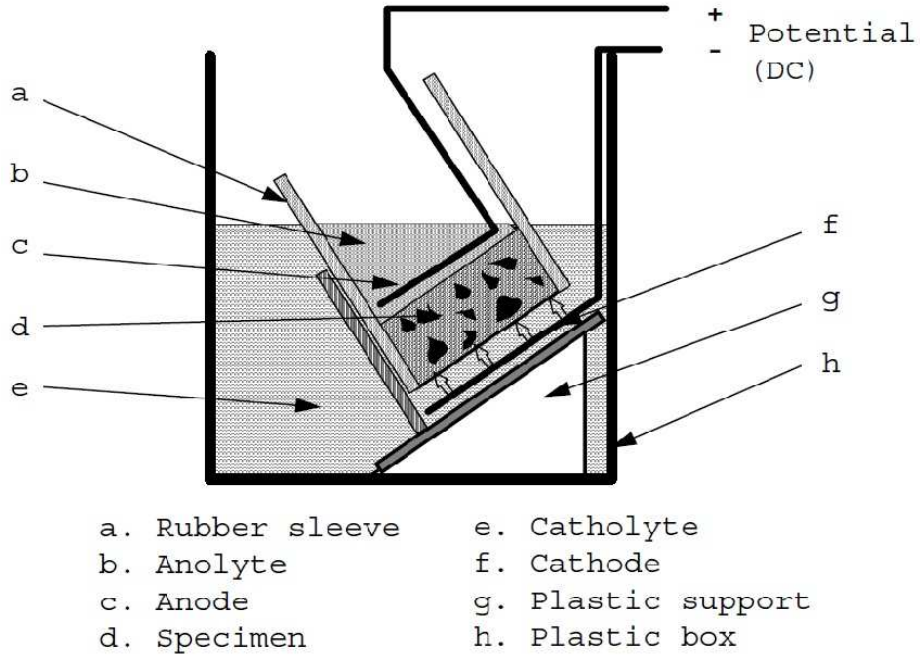

Figure 7.1 RCM experiment set-up, Tang and Nilsson (1993).

The anolyte used was a 0.3N NaOH solution and the catholyte was a solution of 10% NaCl. The samples were put in a rubber sleeve and then filled with anolyte. Next the cathode was connected to a negative pole and the anode to a positive. After turning on the power, the voltage was set to 30V and the initial current for each sample was recorded. Then the voltage was adjusted and again the initial current was read. After 24 hours the samples were taken out, cut in a half and sprayed with 0.1M silver nitrate solution. Later the penetration depth was measured at 9 points with 10mm intervals. To determine the chloride migration coefficient the non-steady-state migration coefficient equation (7.1) was used.

$$D_{nssm} = \frac{RT}{zFE} \cdot \frac{x_d - \alpha\sqrt{x_d}}{t} \quad (7.1)$$

where:

$E = \frac{U-2}{L}$ and $\alpha = 2\sqrt{\frac{RT}{zFE}} \cdot erf^{-1}\left(1 - \frac{2c_d}{c_0}\right)$

D_{nssm} – non-steady-state migration coefficient [m^2/s];

z – absolute value of ion valence, for chloride $z = 1$;

F – Faraday constant, $F = 9{,}648 \times 10^{-4}$ [J/(V·mol)];

U – absolute value of the applied voltage [V];

R – gas constant, $R = 8{,}314$ [J/(K·mol)];

T – average value of the initial and final temperatures in the anolyte solution [K];

L – thickness of the specimen [m];

x_d – average value of the penetration depths [m];

t – test duration [seconds];

erf^{-1} – inverse of error function;

c_d – chloride concentration at which the colour changes, $c_d = 0{,}07N$;

c_0 – chloride concentration in the catholyte solution, $c_0 = 2N$;

The results of the Rapid Chloride Migration test are shown in the following charts, Figure 7.2 - Figure 7.4.

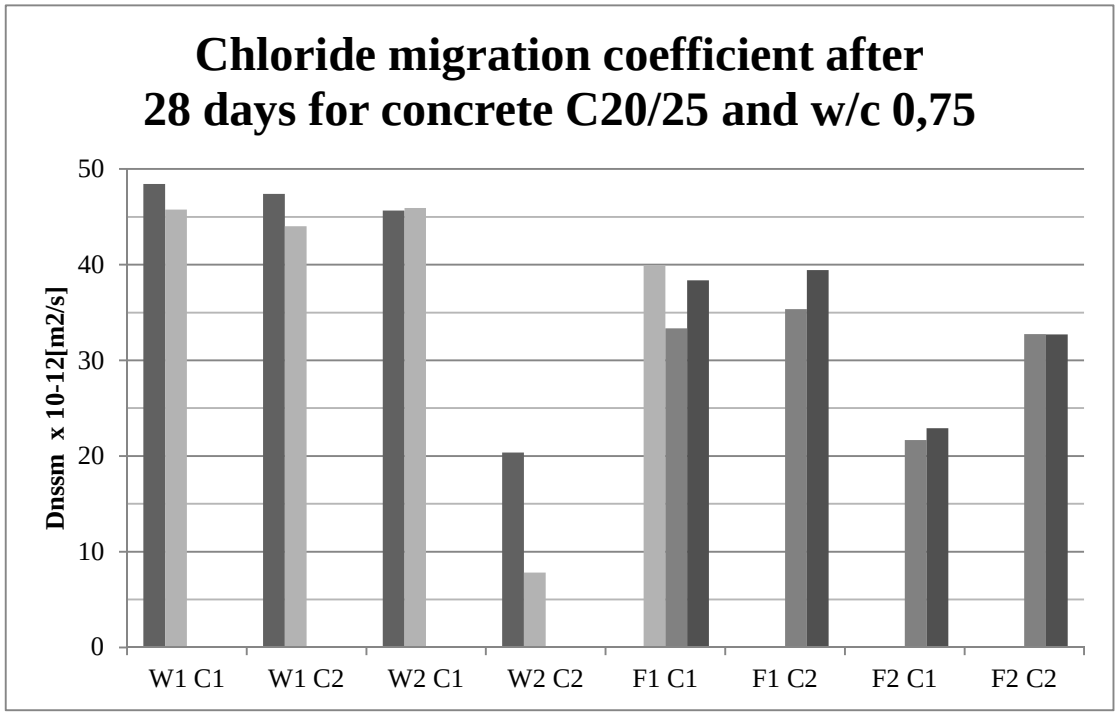

Figure 7.2 RCM test results after 28 days for concrete used for corrosion test. W stands for specimens w/o fibres, F - w/ fibres and C – cylinder.

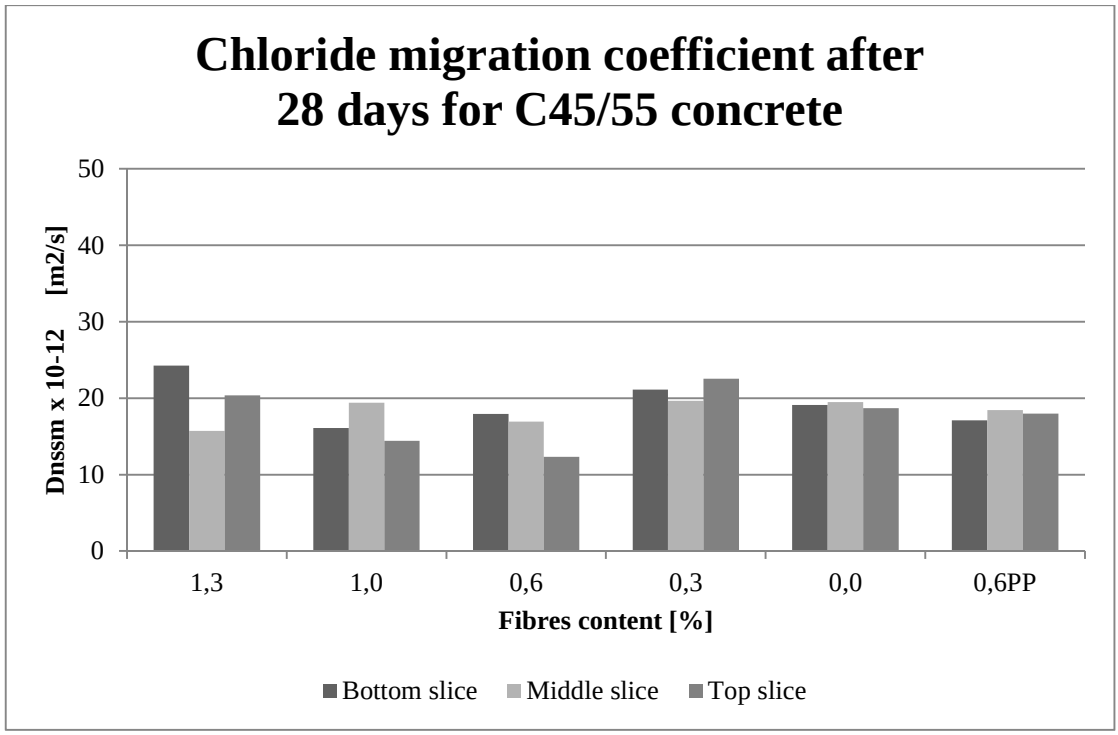

Figure 7.3 RCM test results after 28 days for concrete commonly used for civil engineering structures with different amount of fibres.

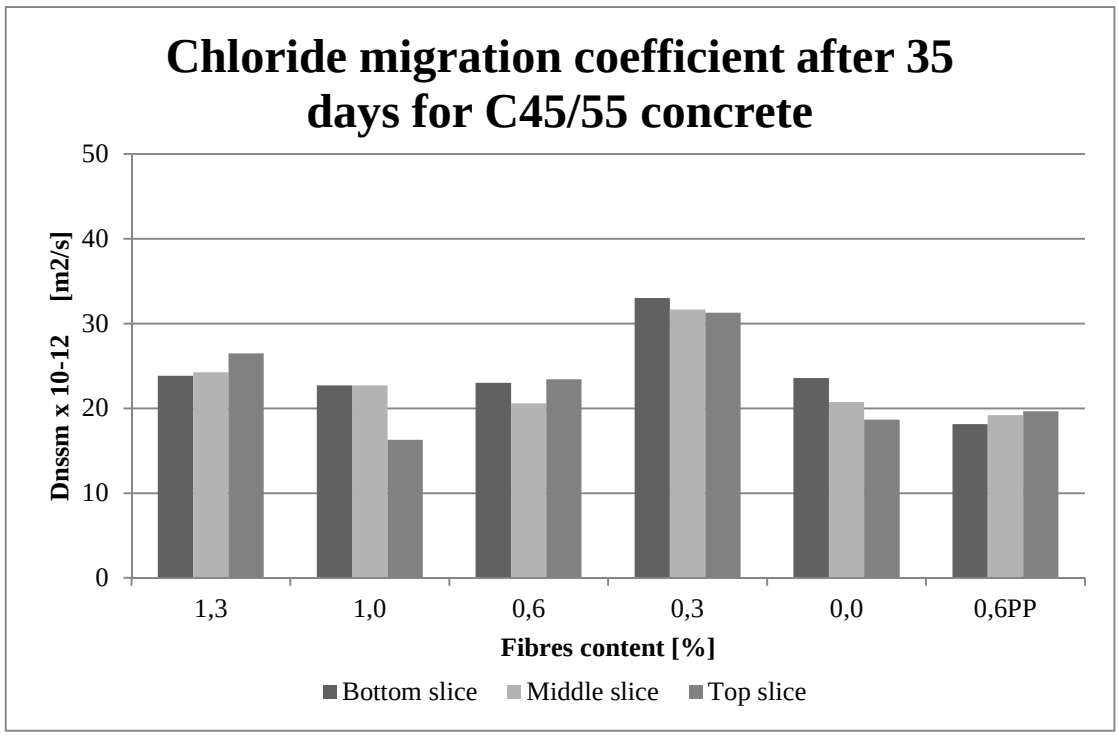

Figure 7.4 RCM test results after 35 days for concrete commonly used for civil engineering structures with different amount of fibres.

The results of the Rapid Chloride Migration test are shown in the following charts, see Figure 7.2 to Figure 7.4. Full results are presented in Appendix E:.

It can be easily observed that the water / cement ratio strongly influences the chloride migration coefficient. The samples made of C45/55 concrete were characterised by lower coefficient. It was found that the difference between specimens with fibres and without was negligible, neither steel or polymer fibres seem to influence the result. The average chloride migration coefficient from 3 slices of each specimen is shown in Figure 7.5.

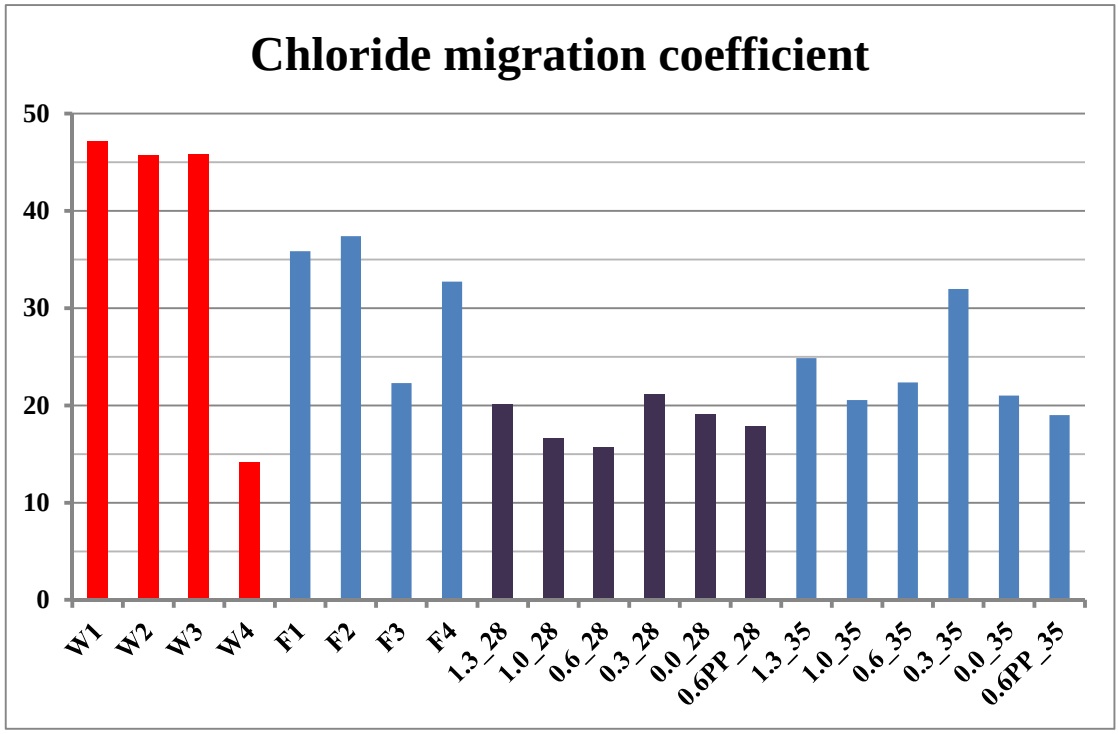

Figure 7.5 *Results of RCM test for all of the specimens, no variation for bottom, middle and top slice – average value for 3 slices. "_28" stands for results after 28 days and "_35" after 35 days.*

Some odd results for specimens W4 and 0.3 % were noticed, and these were deemed to be outliers when compared to the others. The specimen with 0.3 % amount of fibres after 35 days might be explained by wrongly situated outer sealing rings. Whereas, an explanation for the specimen W4 was not found.

8 Conclusions

In order to investigate the influence of fibres on corrosion of reinforcing steel, three types of experiments were carried out, namely: (1) corrosion test on beams to obtain time to corrosion initiation; (2) rapid chloride migration tests; and (3) resistivity tests. Due to time limitation, the corrosion tests were conducted on beams of rather porous concrete mixtures (class C20/25, *w*/*c* 0.75) exposed to a high chloride concentration.

The major conclusion that can be drawn from this study is that the chloride migration coefficient was not affected by fibres. The results for specimens with varying fibre content but same concrete class showed that the chloride migration coefficient was not affected by the fibers as the results were roughly the same for all of the specimens, regardless of the type of fibre (steel or poly-propylene). However, increasing the water/cement ratio influenced the value of the coefficient. The higher the water cement ratio, the higher the chloride migration coefficient.

Regarding electrical resistivity of concrete, a clear trend was observed. With increasing amount of steel fibres a decreasing resistivity was noticed. According to literature, the chloride migration coefficient in concrete without fibres should be related to the resistivity of concrete; for low values of resistivity, chloride migration coefficient should be high. On the other hand, this study did not show this for concrete with steel fibres. However, resistivity is influenced by the concrete porosity which then indirectly should influence the chloride migration. Hence, the fibres influenced the resistivity but they had no impact on the porosity and chloride migration. Therefore, the resistivity cannot be used as an indicator of chloride resistance of steel fibre concrete.

As for the fibres ability to supress crack width, it cannot be obviously stated that this influenced corrosion initiation time. It was noticed in the cracked and unloaded beams, that the beam with the largest crack width (UW2, without fibres) started to corrode as the last one in this group. Whereas, the first beam which started to corrode in group U was beam with fibres (UF2). The beams from the loaded group started to corrode first due to wider cracks and sustained load. These results could be affected also by galvanic corrosion; however it was hard to distinguish different types of corrosion. Hence, it is not clear what the effect of the fibres are, they help reducing the crack width but not the corrosion initiation for cracked beams.

From visual observations it was observed that steel fibres, which are close to concrete surface, corroded and gave bad esthetical effects. Moreover, areas of pitting corrosion were smaller for beams with fibres than without fibres, in the groups that were loaded; both with sustained load and those that were unloaded. When it comes to the un-cracked group, only the beams without fibres corroded, whereas rebars in beams with fibres were not corroded, probably due to the earlier surface corrosion of steel fibres which function as a sacrificed electrode and cathodically protected the rebars which may be in connection with the corroding fibres.

8.1 Further research needs

The time for this study was limited and as a result the research methods were accelerated in that sense that concrete of rather poor quality and was subjected to a rather high chloride level. After this study, some proposal for future investigation can be made.

Firstly, the corrosion tests should be developed:

- The concrete samples should be closer to concrete used in civil engineering structures, i.e. with a lower water/cement ratio.
- Moreover, the concrete cover depth should be increased according to design codes.
- Furthermore, all of the beams should be loaded, but the load can be differed for each group, as the sustained load affects corrosion initiation time.
- As for the exposure conditions, the imitation of the chloride environment might be rearranged. The chloride concentration can be decreased, corresponding to the sea water; around 2% of NaCl. Additionally, the chloride solution can be sprayed on the specimens to simulate different zones of marine and offshore structures.
- When it comes to galvanic corrosion, it would be a good idea to invent a way to distinguish galvanic corrosion and chloride-induced corrosion in steel fibre reinforced concrete.
- It could also be relevant to choose more accurate methods in order to determine corrosion rate.

It should be noted, though, that with the first four items listed here, the time for the tests will increase. It is a delicate balance between using realistic circumstances and the time available for the tests, as it is not reasonable to have test times in the range of the intended life time of real structures. Besides development of the corrosion tests, even though a large literature study research was conducted, there is still need to go deeper into the literature about these phenomena. It is also a good idea to combine different tests as in this study (simultaneously corrosion tests, RCM and resistivity tests) and develop them to have a proper point of reference.

9 References

ASTM Standard C876 - 91 (1999). Standard Test Method for Corrosion Potentials of Uncoated Reinforcing Steel in Concrete, ASTM International, West Conshohocken, PA, 1999

ASTM Standard G1-03. Standard Practise for Preparing, Cleaning and Evaluating Corrosion Test Specimens, ASTM International, West Conshohocken, PA, 2003

NT BUILD 492. Concrete, mortar and cement based repair materials: Chloride migration coefficient from non-steady state migration experiments, NORDTEST, Finland, 8, 1999

Altayyib A. H. J. and Alzahrani M. M. (1990): Corrosion of Steel Reinforcement in Polypropylene Fiber Reinforced-Concrete Structures. ACI Materials Journal, Vol. 87, No. 2, Mar-Apr, pp. 108-113.

Ballim Y., Reid J. C. and Kemp A. R. (2003): Deflection of RC beams under simultaneous load and steel corrosion. Magazine of Concrete Research, Vol. 55, No. 4, Aug, pp. 405-406.

Bentur A. and Mindess S. (2007): Fibre Reinforced Cementitious Composites. 2nd ed, Taylor & Francis. England, UK.

Bertolini L., Elsener, B., Pedeferri, P. and Polder, R.P (2004): Corrosion of steel in concrete : prevention, diagnosis, repair, Wiley-VCH, Weinheim ; Cambridge, 2004, xvii, 392 s. pp.

CEB-rilem (1983): Durability of concrete structures, International workshop, 18th – 20th may, Copenhagen, Denmark, Ed. Rostam S.

El Maaddawy T., Soudki K. and Topper T. (2005): Long-term performance of corrosion-damaged reinforced concrete beams. ACI Structural Journal, Vol. 102, No. 5, Sep-Oct, pp. 649-656.

Elsener B., Andrade C., Gulikers J., Polder R. and Raupach M. (2003): Hall-cell potential measurements—Potential mapping on reinforced concrete structures. Materials and Structures, Vol. 36, No. 7, pp. 461-471.

Féderation international du béton. (2006): Model Code for Service Life Design : model code, FIB, Lausanne, 2006, 116 s. pp.

Granju J.-L. and Ullah Balouch S. (2005): Corrosion of steel fibre reinforced concrete from the cracks. Cement and Concrete Research, Vol. 35, No. 3, pp. 572-577.

Grubb J. A., Blunt J., Ostertag C. P. and Devine T. M. (2007): Effect of steel microfibers on corrosion of steel reinforcing bars. Cement and Concrete Research, Vol. 37, No. 7, pp. 1115-1126.

Hope B. B., Ip A. K. and Manning D. G. (1985): Corrosion and electrical impedance in concrete. Cement and Concrete Research, Vol. 15, No. 3, pp. 525-534.

Löfgren I. (2005): Fibre-reinforced concrete for industrial construction : a fracture mechanics approach to material testing and structural analysis, Chalmers tekniska högskola, Göteborg, 2005, xiii, 146 s. pp.

Lundgren K. (2007): Effect of corrosion on the bond between steel and concrete: an overview. Magazine of Concrete Research, Vol. 59, No. 6, pp. 447-461.

Mangat P. and Gurusamy K. (1987): Long-term properties of steel fibre reinforced marine concrete. Materials and Structures, Vol. 20, No. 4, pp. 273-282.

Mangat P. and Gurusamy K. (1987): Permissible crack widths in steel fibre reinforced marine concrete. Materials and Structures, Vol. 20, No. 5, pp. 338-347.

Mehta P. K. (1991): Concrete in the marine environment [Elektronisk resurs], Elsevier Applied Science, London; New York, 1991, x, 214 p. pp.

Mohammed T. U., Otsuki N., Hisada M. and Shibata T. (2001): Effect of Crack Width and Bar Types on Corrosionof Steel in Concrete. Journal of Materials in Civil Engineering, Vol. 13, No. 3, pp. 194-201.

Pease B. J. G., Mette Rica; Stang, Henrik; Weiss, Jason; (2011): Influence of concrete cracking on ingress and reinforcement corrosion, 2011, pp.

Schießl P. and Raupach M. (1997): Laboratory studies and calculations on the influence of crack width on chloride-induced corrosion of steel in concrete. ACI Materials Journal, Vol. 94, No. 1, Jan-Feb, pp. 56-62.

Solgaard A. O. S., Kuter A., Edvardsen C., Stang H. and Geiker M. R. (2010): Durability aspects of steel fibre reinforced concrete in civil infrastructure, Proceedings of the 2nd International Symposium on Service Life Design for Infrastructures. 2010.

Solgaard A. O. S. and Michel A. (2009): Modelling the influence of steel fibres on the electrical resistivity of cementitious composites, 3 rd Int. PhD Workshop on Modelling the Durability of reinforced Concrete. 2009.

Tammo K. (2009): A new approach to crack control for reinforced concrete: an investigation of crack widths close to the reinforcement and the correlation to service life, Division of Structural Engineering, Lund University, Lund, 2009, ix, 81 s. pp.

Tang L. (1996): Chloride transport in concrete: measurement and prediction, Chalmers tekniska högsk., Göteborg, 1996, xvi, 88 s. pp.

Tang L., Nilsson L-O. and Basheer P. A. M. (2011): Resistance of Concrete to Chloride Ingress, CRC Press Inc, GB, 2011, pp.

Tang L. N., L.-O. (1993): Rapid Determination of the Chloride Diffusivity in Concrete by Applying an Electric Field. ACI Materials Journal, Vol. 89, No. 1, pp. 49-53.

Tang L. Nilsson., L.-O. (2002). "Prediction Of Chloride Penetration Into Concrete Exposed To Various Exposure Environments." 9th International Conference on Durability of Materials and Components, Brisbane (Australia), Vol. 3, Paper 238.

Tran The N. and Huang Q. (2006): Influence of cracks on chloride-induced corrosion in reinforced concrete structures, Chalmers tekniska högskola, Göteborg, 2006, pp.

Tuutti K. (1982): Corrosion of steel in concrete, Cement- och betonginst., Stockholm, 1982, 468 s. pp.

Yoon S. W. K. W. W. J. S. S. P. (2000): Interaction between Loading, Corrosion, and Serviceability of Reinforced Concrete. ACI Materials Journal, Vol. 97, No. 6, Nov-Dec, pp. 637-644.

Appendix A: Design calculation for load, cracking load and crack width

Calculations of mean crack width for plain concrete

Beam measurements:

$b := 100mm$

$h := 100mm$

$L := 800mm$

$c := 20mm$

$\phi := 8mm$

$d := h - \left(c + \frac{\phi}{2}\right) = 76mm$ $\quad a := c + \frac{\phi}{2} = 24mm$

C20/25 concrete:

$f_{ctm} := 2.2MPa$

$f_{ck} := 20MPa$

$E_{cm} := 30MPa$

Steel B500B:

$f_{yk} := 500MPa$

$E_s := 200GPa$

Shear capacity calculation:

$P := 12kN$

$A_s := 2 \cdot \pi \cdot \frac{\phi^2}{4} = 100.531mm^2$

$g_{Ed} := 22\frac{kN}{m^3} \cdot b \cdot h = 0.22\frac{kN}{m}$ -characteristic load

$M_{Ed} := P \cdot \frac{L - 100mm}{4} + g_{Ed} \cdot \frac{L^2}{8} = 2.118kN \cdot m$ - characteristic bending moment

$V_{Ed} := \frac{P}{2} + \frac{g_{Ed} \cdot L}{2} = 6.088kN$ - characteristic shear force

Shear capacity calculation:

$A_{ef} := b \cdot h = 0.01m^2$

$$\rho := \frac{0.08 \cdot \sqrt{\frac{f_{ck}}{1MPa}}}{\frac{f_{yk}}{1MPa}} = 7.155 \times 10^{-4}$$

$V := V_{Ed} - d \cdot g_{Ed} = 6.071kN$

$k := 1.6 - \frac{d}{1m} = 1.524$ $\quad \rho_L := \frac{A_s}{b \cdot d} = 0.013$

$V_{Rd1} := \left[0.35 \cdot k \cdot f_{ctm} \cdot \left(1.2 + 40 \cdot \rho_L\right)\right] b \cdot d = 15.421kN$

$\frac{V}{V_{Rd1}} = 39.37\%$ **no need for shear reinforcement**

Bending moment capacity:

$\xi_{eff} := \frac{A_s \cdot f_{yk}}{b \cdot d \cdot f_{ck}} = 0.331$ $\xi_{eff.lim} := 0.5$

$\mu_{eff} := 0.27$ $\zeta_{eff} := 0.83$ $\mu_{eff.lim} := 0.37$

$M_{Rd} := \mu_{eff.lim} d^2 \cdot b \cdot f_{ck} = 4.332 kN$

$\frac{M_{Ed}}{M_{Rd}} = 48.883\%$ **2 ϕ8mm sufficient**

Cracking moment:

$I_I := \frac{b \cdot h^3}{12} = 8.333 \times 10^{-6} m^4$

$M_{cr} := f_{ctm} \cdot \frac{b \cdot h^2}{6} = 0.367 kN \cdot m$

Mean crack width:

$\frac{2 \cdot b \cdot h}{2 \cdot (b + h)} = 50 mm$ $\phi_{inf.t0} := 3.7$ $\rho := \frac{A_s}{b \cdot d} = 1.323\%$

$\alpha_{et} := \frac{E_s}{E_{cm}} \cdot (1 + \phi_{inf.t0}) = 3.133 \times 10^4$

$x_{II} := d \cdot \left[\sqrt{\rho \cdot \alpha_{et} \cdot (2 + \rho \cdot \alpha_{et})} - \rho \cdot \alpha_{et} \right] = 75.909 mm$

$\sigma_s := \frac{M_{Ed}}{A_s \cdot \left(d - \frac{x_{II}}{3} \right)} = 415.49 MPa$

$\beta_1 := 1.0$ $\beta_2 := 1.0$ $k_1 := 0.5$ $k_2 := 0.5$

$A_{ct.eff} := \min \left(2.5a, \frac{h - x_{II}}{3} \right) = 8.03 mm$

$\rho_s := \frac{A_s}{A_{ct.eff}} = 12.519 mm$

$s_{rm} := 50 + \frac{1}{4} \cdot k_1 \cdot k_2 \cdot \frac{\phi}{\rho_s} = 50.04 \text{ mm}$

$w_m := s_{rm} \cdot \frac{\sigma_s}{E_s} \cdot \left[1 - \beta_1 \cdot \beta_2 \cdot \left(\frac{M_{cr}}{M_{Ed}} \right)^2 \right] = 0.101$ - mean crack width [mm]

Appendix B: Compressive strength test results

Compressive strength results for specimens used in corrosion tests.

ρ – density of specimen

f_{cm} – compressive strength of specimen

Specimens without fibres						
Dimensions of cube	Number of cube	Age of specimen	mix 1		mix 2	
			ρ	f_{cm}	ρ	f_{cm}
			[kg/m^3]	[MPa]	[kg/m^3]	[MPa]
100 x 100 x 100 mm^3	1	28	2296	34,1	2344	31,8
	2	28	2325	33,0	2333	31,6
	3	56	2319	35,0	2330	33,9
	4	56	2334	34,3	2324	33,2
	5	98	2322	35,8	2325	34,6
	6	98	2327	35,6	2323	34,7
150 x 150 x 150 mm^3	1	28	2337	28,9	2330	28,2
	2	28	2344	28,9	2327	28,6
Specimens with fibres						
100 x 100 x 100 mm^3	1	28	2291	28,6	2307	29,7
	2	28	2297	29,7	2301	29,4
	3	56	2293	31,0	2312	31,3
	4	56	2305	32,4	2305	32,0
	5	98	2303	32,9	2311	32,6
	6	98	2306	33,0	2312	32,7
150 x 150 x 150 mm^3	1	28	2315	28,2	2315	28,1
	2	28	2309	28,0	2311	28,0

Compressive strength tests results for cubes 150 x 150 x 150 mm^3 after 28 days for concrete commonly used for civil engineering structures:

	1,3 %		1,0 %		0,6 %		0,3 %		0,0 %		0,6 % PP	
	ρ	f_{cm}	ρ	f_{cm}	ρ	f_{cm}	ρ	f_{cm}	ρ	f_{cm}	ρ	f_{cm}
	[kg/m^3]	[MPa]	[kg/m^3]	[MPa]	[kg/m^3]	[MPa]	[kg/m^3]	[MPa]	[kg/m^3]	[MPa]	[kg/m^3]	[MPa]
1	2456	74,0	2424	64,8	2388	70,3	2327	72,1	2351	63,8	2362	68,6
2	2455	74,4	2433	67,1	2385	69,2	2367	71,0	2354	64,7	2363	68,4
3	2457	74,7	2423	63,3	2387	68,6	2374	70,8	2333	63,0	2371	69,3

Appendix C: Half-cell potential measurements

There are a few different types of electrodes, which can be used for these measurements. The difference between them is standard potential according to standard hydrogen electrode (SHE). Thus there are commonly used silver/silver chloride KCl saturated (Ag/AgCl - SSCE), and copper/copper sulfate saturated ($Cu/CuSO_4$ - CSE). Standard potentials of these electrodes and a few more types are shown in Table 9.1. It can be noted that CSE is mostly used for on-site work and SSCE for laboratory work.

Table 9.1 Potentials vs. SHE for reference electrodes, Elsener et al. (2003).

Electrode		Potential vs. SHE
Copper/copper sulfate sat	CSE	+0.318V SHE
Calomel (Hg/Hg_2Cl_2)	SCE	+0.241V SHE
Silver/silver chloride	SSCE	+0.199V SHE

On the next pages detailed results from half-cell potential measurements are presented.

DoT – day of test

AGE – age of specimens

Δ – potential difference between reinforcement bars

LF1 Side A	DoT	AGE	VALUES					
			1	2	3	4	5	Δ
Date	days	days	[V]	[V]	[V]	[V]	[V]	[V]
09-03-12	1	29	-0.0230	-0.0340	-0.0280	-0.0210	-0.0110	
12-03-12	3	32	-0.1326	-0.1972	-0.1985	-0.1984	-0.1450	
14-03-12	5	34	-0.1865	-0.2411	-0.2481	-0.2451	-0.1905	
16-03-12	7	36	-0.1802	-0.2299	-0.2349	-0.2350	-0.1865	
19-03-12	10	39	-0.2036	-0.2754	-0.2825	-0.2814	-0.2360	
21-03-12	12	41	-0.2094	-0.2740	-0.2826	-0.2807	-0.2365	0.0409
23-03-12	14	43	-0.2420	-0.2748	-0.2848	-0.2801	-0.2426	0.0505
26-03-12	17	46	-0.2450	-0.2974	-0.3069	-0.3055	-0.2716	0.0336
28-03-12	19	48	-0.2770	-0.3029	-0.3127	-0.3078	-0.2711	0.0307
30-03-12	21	50	-0.2710	-0.2994	-0.3114	-0.3059	-0.2761	0.0309
02-04-12	24	53	-0.2844	-0.3102	-0.3200	-0.0315	-0.2929	0.0327
04-04-12	26	55	-0.2797	-0.3098	-0.3206	-0.3151	-0.2821	0.0529
06-04-12	28	57	-0.2967	-0.3163	-0.3279	-0.3222	-0.2905	0.0508
10-04-12	32	61	-0.296	-0.327	-0.337	-0.337	-0.300	0.0519
11-04-12	33	62	-0.309	-0.325	-0.339	-0.338	-0.309	0.0511
13-04-12	35	64	-0.309	-0.335	-0.345	-0.343	-0.309	0.0412
16-04-12	38	67	-0.326	-0.348	-0.363	-0.355	-0.323	0.0341
20-04-12	42	71	-0.332	-0.362	-0.378	-0.369	-0.330	0.0221
23-04-12	45	74	-0.340	-0.370	-0.387	-0.382	-0.341	-
27-04-12	49	78	-0.347	-0.373	-0.393	-0.387	-0.341	0.0139
04-05-12	56	85	-0.358	-0.387	-0.393	-0.394	-0.353	0.0051
07-05-12	59	88	-0.360	-0.390	-0.404	-0.403	-0.363	0.0038
14-05-12	66	95	-0.360	-0.388	-0.404	-0.399	-0.360	0.0036

LF2 Side B	DoT	AGE	VALUES					
			1	2	3	4	5	Δ
Date	days	days	[V]	[V]	[V]	[V]	[V]	[V]
09-03-12	1	29	-0.0210	-0.0110	-0.0120	-0.0140	-0.0150	
12-03-12	3	32	-0.2362	-0.3414	-0.3140	-0.3008	-0.2320	
14-03-12	5	34	-0.2501	-0.3277	-0.3391	-0.3175	-0.2324	
16-03-12	7	36	-0.2624	-0.3353	-0.3462	-0.3349	-0.2405	
19-03-12	10	39	-0.2650	-0.3445	-0.3518	-0.3410	-0.2443	
21-03-12	12	41	-0.2907	-0.3518	-0.3605	-0.3517	-0.2654	0.0081
23-03-12	14	43	-0.3065	-0.3480	-0.3550	-0.3440	-0.2758	0.1001
26-03-12	17	46	-0.3083	-0.3542	-0.3647	-0.3582	-0.2824	0.0126
28-03-12	19	48	-0.3150	-0.3445	-0.3503	-0.3417	-0.2850	0.0172
30-03-12	21	50	-0.3092	-0.3490	-0.3591	-0.3514	-0.3040	0.0189
02-04-12	24	53	-0.3180	-0.3502	-0.3536	-0.3477	-0.3086	0.0212
04-04-12	26	55	-0.3191	-0.3552	-0.3631	-0.3170	-0.3118	0.0194
06-04-12	28	57	-0.3220	-0.3498	-0.3566	-0.3451	-0.3129	0.0207
10-04-12	32	61	-0.318	-0.341	-0.341	-0.337	-0.291	0.0186
11-04-12	33	62	-0.322	-0.340	-0.350	-0.342	-0.317	0.0153
13-04-12	35	64	-0.321	-0.341	-0.352	-0.336	-0.303	0.0156
16-04-12	38	67	-0.319	-0.328	-0.353	-0.345	-0.320	0.0152
20-04-12	42	71	-0.338	-0.365	-0.372	-0.358	-0.329	-0.0016
23-04-12	45	74	-0.349	-0.380	-0.387	-0.372	-0.349	-0.0040
27-04-12	49	78	-0.359	-0.393	-0.405	-0.383	-0.353	-0.0156
04-05-12	56	85	-0.372	-0.411	-0.417	-0.410	-0.372	-0.0195
07-05-12	59	88	-0.373	-0.407	-0.415	-0.407	-0.361	-0.0192
14-05-12	66	95	-0.380	-0.411	-0.423	-0.406	-0.375	-0.0207

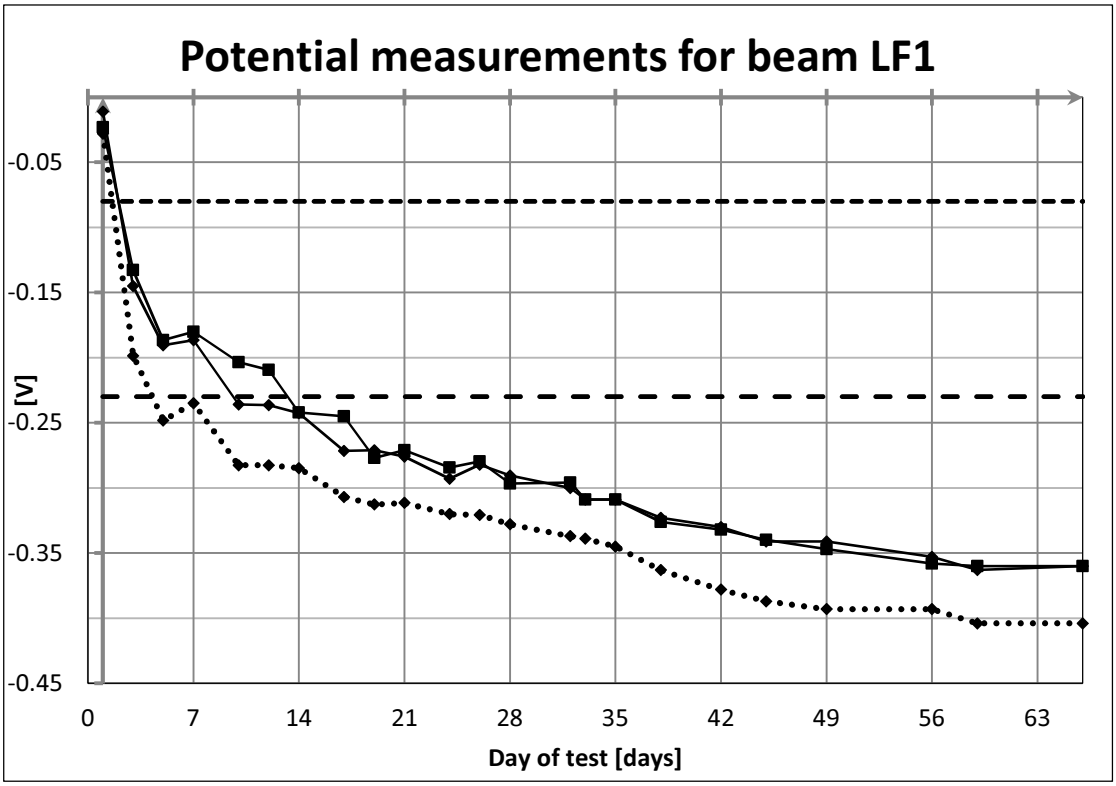
Potential measurements for beam LF1
-0.05
-0.15
-0.25
-0.35
-0.45
[V]
0
7
14
21
28
35
42
49
56
63
Day of test [days]

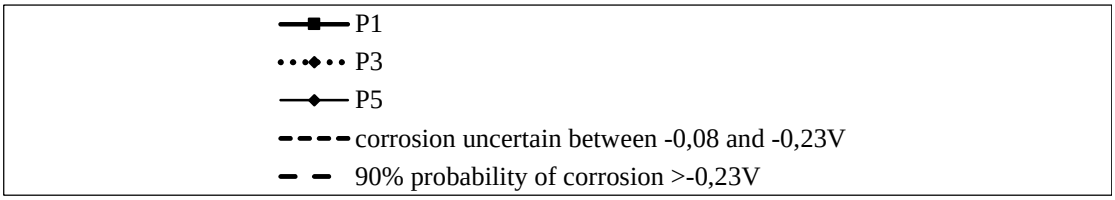
P1
P3
P5
corrosion uncertain between -0,08 and -0,23V
90% probability of corrosion >-0,23V

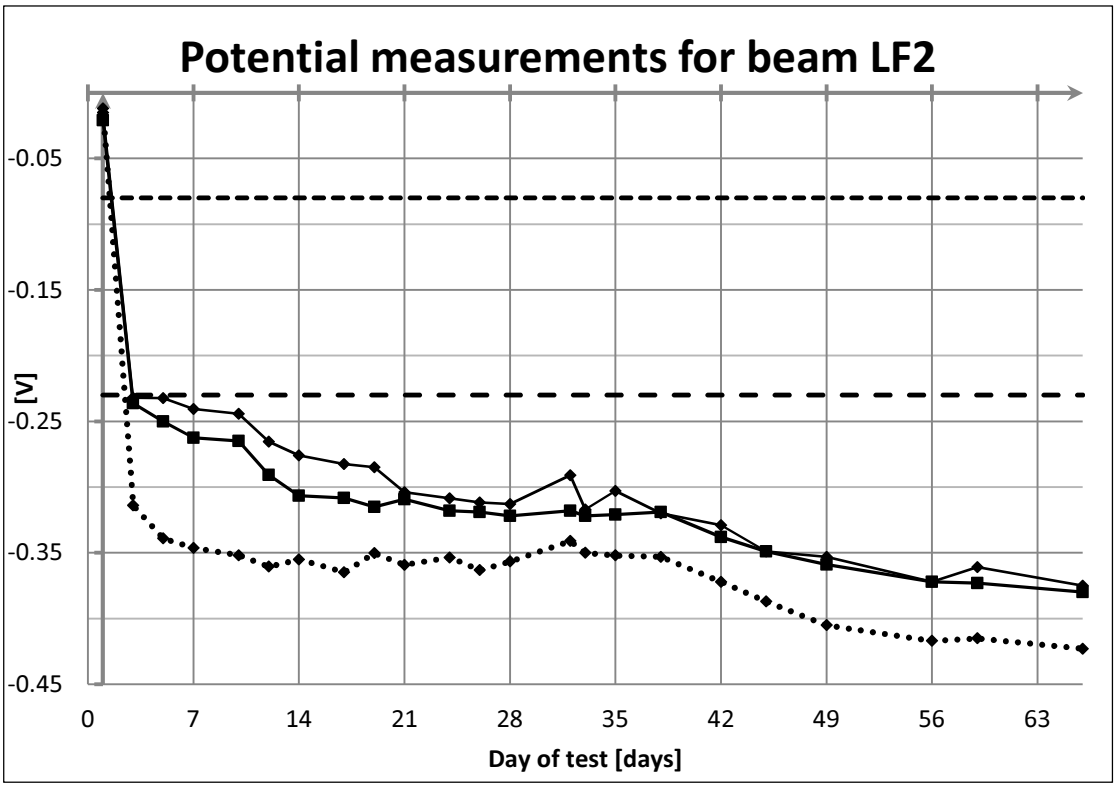
Potential measurements for beam LF2
-0.05
-0.15
-0.25
-0.35
-0.45
[V]
0
7
14
21
28
35
42
49
56
63
Day of test [days]

LW1 Side A		VALUES						
	DoT	AGE	1	2	3	4	5	Δ
Date	days	days	[V]	[V]	[V]	[V]	[V]	[V]
09-03-12	1	30	-0.0220	-0.0210	-0.0240	-0.0280	-0.0240	
12-03-12	3	33	-0.2338	-0.3296	-0.3352	-0.3195	-0.2220	
14-03-12	5	35	-0.2431	-0.3247	-0.3369	-0.3231	-0.2160	
16-03-12	7	37	-0.2412	-0.3246	-0.3345	-0.3278	-0.2228	
19-03-12	10	40	-0.2556	-0.3558	-0.3674	-0.3593	-0.2605	
21-03-12	12	42	-0.2518	-0.3535	-0.3601	-0.3514	-0.2755	-0.0109
23-03-12	14	44	-0.2792	-0.3506	-0.3585	-0.3500	-0.2716	-0.0145
26-03-12	17	47	-0.2691	-0.3544	-0.3669	-0.3570	-0.2797	-0.0134
28-03-12	19	49	-0.2845	-0.3482	-0.3594	-0.3585	-0.2799	-0.0147
30-03-12	21	51	-0.2670	-0.3448	-0.3550	-0.3509	-0.2735	-0.0175
02-04-12	24	54	-0.2913	-0.3515	-0.3612	-0.3505	-0.3030	-0.0110
04-04-12	26	56	-0.2788	-0.3502	-0.3627	-0.3525	-0.3010	-0.0100
06-04-12	28	58	-0.2866	-0.3477	-0.3589	-0.3504	-0.2969	-0.0082
10-04-12	32	62	-0.304	-0.349	-0.361	-0.351	-0.309	-0.0108
11-04-12	33	63	-0.293	-0.351	-0.360	-0.356	-0.307	-0.0137
13-04-12	35	65	-0.289	-0.344	-0.359	-0.352	-0.309	-0.0104
16-04-12	38	68	-0.305	-0.348	-0.362	-0.348	-0.305	-0.0174
20-04-12	42	72	-0.292	-0.353	-0.363	-0.351	-0.294	-0.0147
23-04-12	45	75	-0.296	-0.353	-0.366	-0.360	-0.330	-0.0213
27-04-12	49	79	-0.288	-0.362	-0.378	-0.369	-0.331	-0.0320
04-05-12	56	86	-0.330	-0.382	-0.395	-0.386	-0.342	-0.0291
07-05-12	59	89	-0.337	-0.385	-0.402	-0.387	-0.338	-0.0290
14-05-12	66	96	-0.344	-0.393	-0.401	-0.394	-0.337	-0.0326

LW2 Side B	DoT	AGE	VALUES					
			1	2	3	4	5	Δ
Date	days	days	[V]	[V]	[V]	[V]	[V]	[V]
09-03-12	1	30	-0.0220	-0.0190	-0.0150	-0.0140	-0.0130	
12-03-12	3	33	-0.1940	-0.3140	-0.3351	-0.3071	-0.3071	
14-03-12	5	35	-0.1998	-0.3124	-0.3360	-0.3260	-0.2184	
16-03-12	7	37	-0.1990	-0.3230	-0.3388	-0.3303	-0.2470	
19-03-12	10	40	-0.2022	-0.3223	-0.3357	-0.3257	-0.2510	
21-03-12	12	42	-0.2393	-0.3205	-0.3338	-0.3266	-0.2507	0.0025
26-03-12	17	47	-0.2418	-0.3087	-0.3243	-0.3180	-0.2612	0.0263
28-03-12	19	49	-0.2458	-0.2941	-0.3145	-0.3032	-0.2665	0.0356
30-03-12	21	51	-0.2490	-0.2962	-0.3112	-0.2920	-0.2405	0.0478
02-04-12	24	54	-0.2458	-0.2941	-0.3084	-0.2968	-0.2584	0.0499
04-04-12	26	56	-0.2824	-0.3172	-0.3410	-0.3250	-0.2881	0.0198
06-04-12	28	58	-0.2838	-0.3252	-0.3477	-0.3379	-0.3062	0.0073
10-04-12	32	62	-0.309	-0.341	-0.362	-0.349	-0.314	-0.0310
11-04-12	33	63	-0.339	-0.374	-0.392	-0.391	-0.349	-0.0437
13-04-12	35	65	-0.307	-0.344	-0.361	-0.348	-0.309	-0.0004
16-04-12	38	68	-0.307	-0.312	-0.364	-0.351	-0.332	-0.0038
20-04-12	42	72	-0.310	-0.341	-0.353	-0.340	-0.319	-0.0070
23-04-12	45	75	-0.312	-0.343	-0.363	-0.349	-0.329	-0.0067
27-04-12	49	79	-0.308	-0.345	-0.364	-0.352	-0.324	0.0247
04-05-12	56	86	-0.314	-0.343	-0.370	-0.349	-0.323	0.0445
07-05-12	59	89	-0.313	-0.353	-0.377	-0.354	-0.321	0.0376
14-05-12	66	96	-0.338	-0.370	-0.386	-0.360	-0.339	0.0297

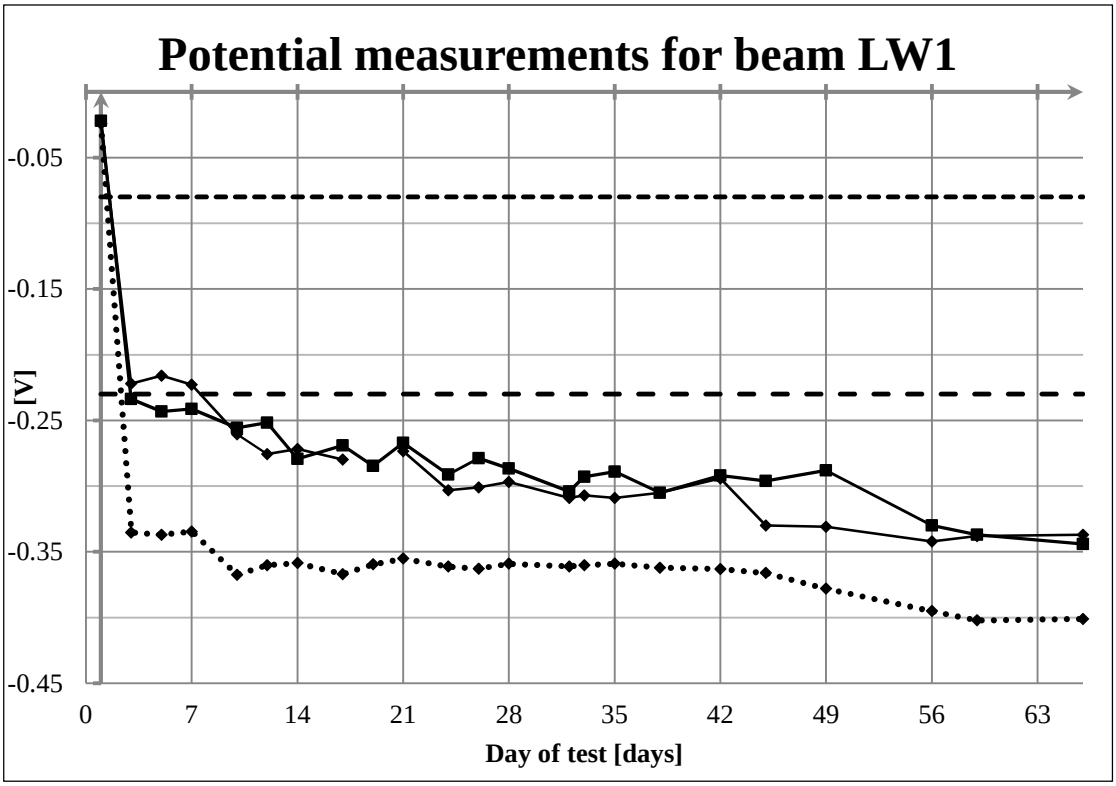
Potential measurements for beam LW1
-0.05
-0.15
-0.25
-0.35
-0.45
[V]
0
7
14
21
28
35
42
49
56
63
Day of test [days]

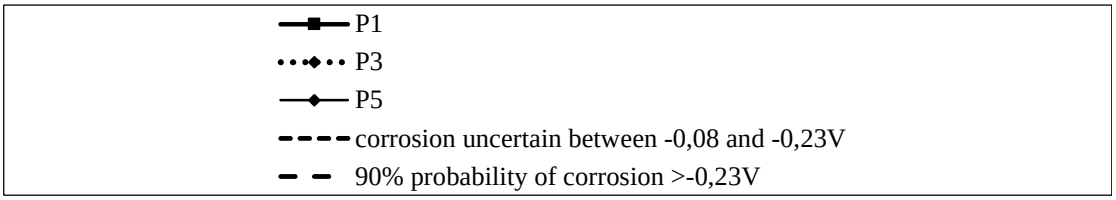
P1
P3
P5
corrosion uncertain between -0,08 and -0,23V
90% probability of corrosion >-0,23V

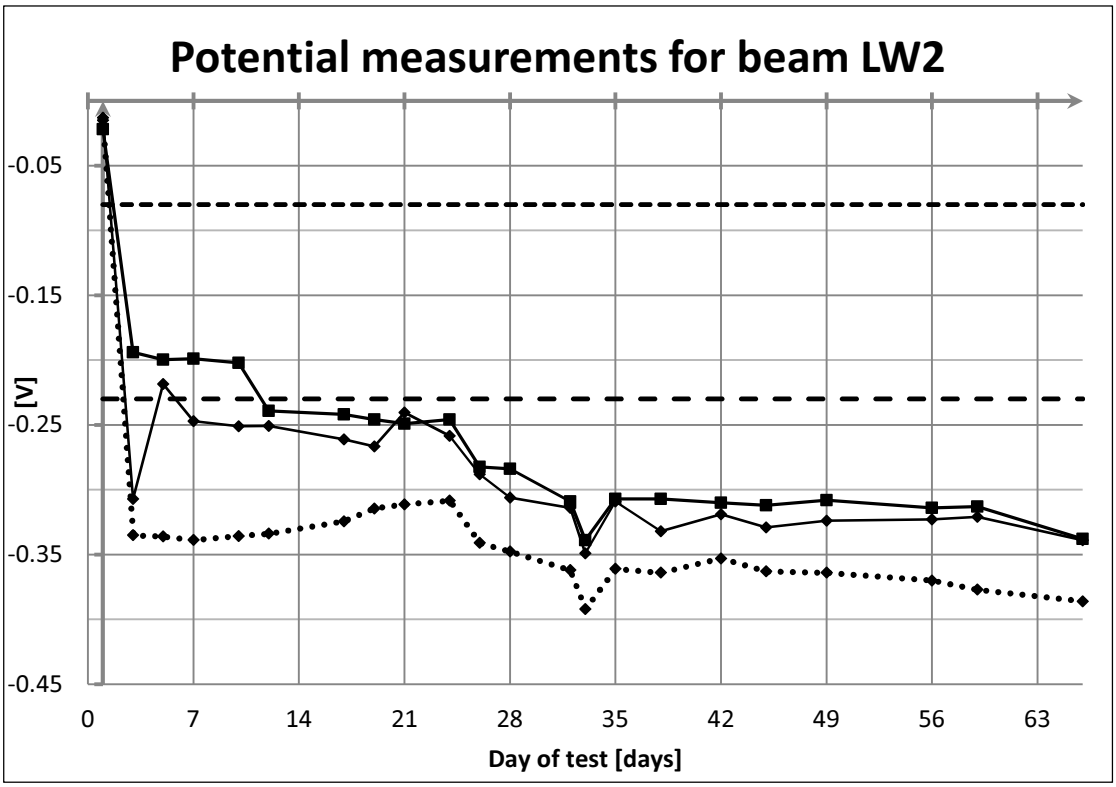
Potential measurements for beam LW2
-0.05
-0.15
-0.25
-0.35
-0.45
[V]
0
7
14
21
28
35
42
49
56
63
Day of test [days]

UF1 Side B	DoT	AGE	VALUES					
			1	2	3	4	5	Δ
Date	days	days	[V]	[V]	[V]	[V]	[V]	[V]
09-03-12	1	29	-0.0200	-0.0300	-0.0280	-0.0290	-0.0280	
12-03-12	3	32	-0.0583	-0.0621	-0.0570	-0.0663	-0.0391	
14-03-12	5	34	-0.0429	-0.0630	-0.0672	-0.0623	-0.0410	
16-03-12	7	36	-0.0461	-0.0648	-0.0665	-0.0652	-0.0411	
19-03-12	10	39	-0.0636	-0.0635	-0.0685	-0.0630	-0.0576	
21-03-12	12	41	-0.0625	-0.0654	-0.0662	-0.6160	-0.0514	0.0082
23-03-12	14	43	-0.0570	-0.0634	-0.0619	-0.0651	-0.0625	0.0077
26-03-12	17	46	-0.0605	-0.0600	-0.0626	-0.0610	-0.0526	0.0084
27-03-12	18	47	-0.0570	-0.0573	-0.0630	-0.0659	-0.0486	0.0081
28-03-12	19	48	-0.0600	-0.0616	-0.0650	-0.0650	-0.0580	0.0085
29-03-12	20	49	-0.0554	-0.0564	-0.0565	-0.0598	-0.0535	0.0079
30-03-12	21	50	-0.0633	-0.0627	-0.0645	-0.0679	-0.0551	0.0062
02-04-12	24	53	-0.0673	-0.0626	-0.0621	-0.0664	-0.0530	0.0037
04-04-12	26	55	-0.0567	-0.0648	-0.0671	-0.0692	-0.0615	0.0017
06-04-12	28	57	-0.0630	-0.0581	-0.0567	-0.0584	-0.0505	0.0045
10-04-12	32	61	-0.3268	-0.3335	-0.3275	-0.3202	-0.2848	-0.2243
11-04-12	33	62	-0.3367	-0.3459	-0.3411	-0.3341	-0.3059	-0.2295
13-04-12	35	64	-0.3476	-0.3591	-0.3549	-0.3465	-0.3089	-0.2421
16-04-12	38	67	-0.3634	-0.3685	-0.3653	-0.3521	-0.3271	-0.2495
18-04-12	40	69	-0.3629	-0.3654	-0.3613	-0.3506	-0.3190	-0.2502
20-04-12	42	71	-0.366	-0.374	-0.370	-0.358	-0.332	-0.2560
23-04-12	45	74	-0.367	-0.376	-0.372	-0.362	-0.330	-0.2561
25-04-12	47	76	-0.372	-0.392	-0.383	-0.372	-0.335	-0.2664
27-04-12	49	78	-0.379	-0.870	-0.380	-0.368	-0.341	-0.2643
04-05-12	56	85	-0.382	-0.391	-0.382	-0.362	-0.335	-0.2690
07-05-12	59	88	-0.379	-0.384	-0.378	-0.370	-0.341	-0.2712
14-05-12	66	95	-0.382	-0.392	-0.385	-0.377	-0.353	-0.2777

UF2 Side A	DoT	AGE	VALUES					
			1	2	3	4	5	Δ
Date	days	days	[V]	[V]	[V]	[V]	[V]	[V]
09-03-12	1	29	-0.0240	-0.0270	-0.0310	-0.0280	-0.0260	
12-03-12	3	32	-0.0285	-0.0253	-0.0459	-0.0275	-0.0342	
14-03-12	5	34	-0.039	-0.08	-0.087	-0.079	-0.035	
16-03-12	7	36	-0.0476	-0.0831	-0.0885	-0.0836	-0.0496	
19-03-12	10	39	-0.0617	-0.0874	-0.0900	-0.0865	-0.0564	
21-03-12	12	41	-0.0587	-0.0854	-0.0902	-0.0885	-0.0675	0.2339
23-03-12	14	43	-0.0711	-0.0894	-0.0914	-0.0863	-0.0735	0.2309
26-03-12	17	46	-0.2593	-0.2741	-0.2765	-0.2691	-0.2432	0.0587
27-03-12	18	47	-0.2981	-0.3205	-0.3184	-0.3145	-0.2926	0.0167
28-03-12	19	48	-0.3076	-0.3303	-0.3288	-0.3230	-0.3036	0.0107
29-03-12	20	49	-0.3232	-0.3470	-0.3331	-0.3294	-0.3116	-0.0068
30-03-12	21	50	-0.3194	-0.3393	-0.3430	-0.3428	-0.3223	-0.0069
02-04-12	24	53	-0.3411	-0.3636	-0.3624	-0.3553	-0.3383	-0.0183
04-04-12	26	55	-0.3397	-0.3612	-0.3589	-0.3522	-0.3322	-0.0208
06-04-12	28	57	-0.3471	-0.3645	-0.3620	-0.3526	-0.3376	-0.0148
10-04-12	32	61	-0.3462	-0.3661	-0.3632	-0.3548	-0.3421	-0.0079
11-04-12	33	62	-0.3476	-0.3683	-0.3647	-0.3806	-0.3465	-0.0062
13-04-12	35	64	-0.3446	-0.3628	-0.3610	-0.3545	-0.3400	-0.0005
16-04-12	38	67	-0.3455	-0.3666	-0.3630	-0.3578	-0.3435	-0.0014
18-04-12	40	69	-0.343	-0.363	-0.359	-0.353	-0.334	0.0006
20-04-12	42	71	-0.329	-0.355	-0.352	-0.344	-0.329	0.0039
23-04-12	45	74	-0.333	-0.357	-0.355	-0.348	-0.333	0.0041
25-04-12	47	76	-0.339	-0.354	-0.331	-0.345	-0.330	0.0049
27-04-12	49	78	-0.322	-0.342	-0.342	-0.341	-0.322	0.0039
04-05-12	56	85	-0.332	-0.351	-0.347	-0.342	-0.333	0.0105
07-05-12	59	88	-0.339	-0.352	-0.351	-0.344	-0.339	0.0107
14-05-12	66	95	-0.338	-0.350	-0.348	-0.340	-0.328	0.1340

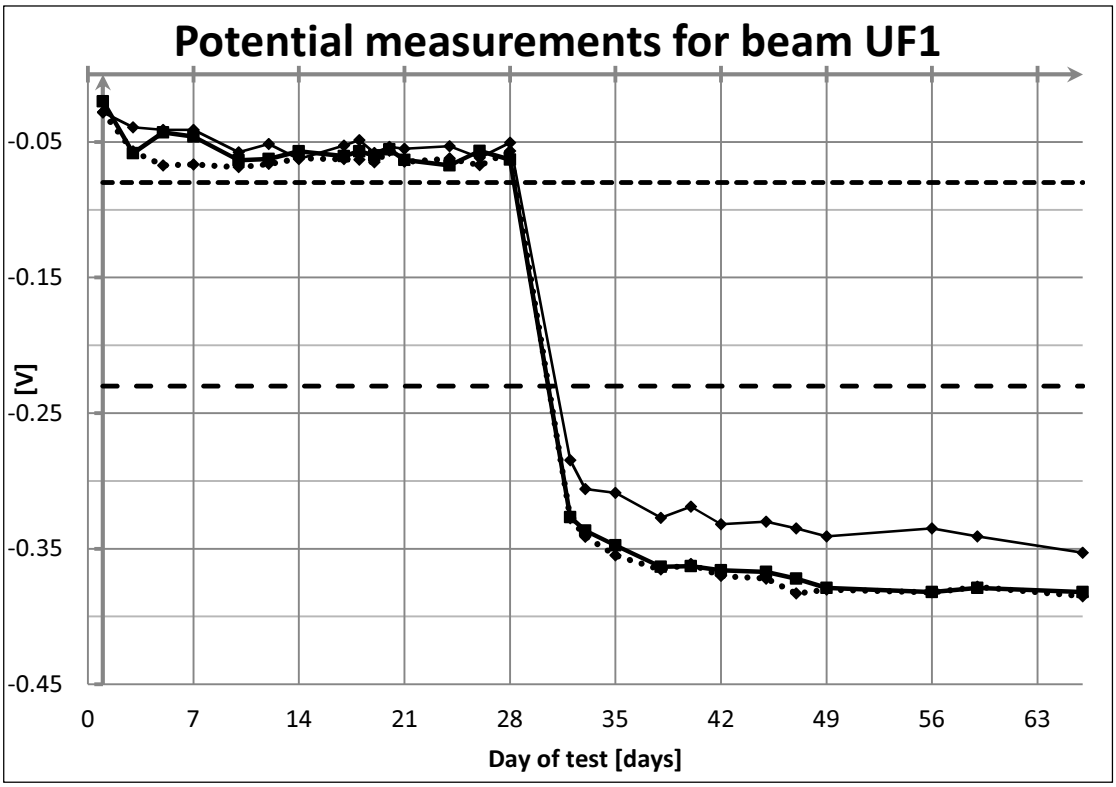
Potential measurements for beam UF1
-0.05
-0.15
-0.25
-0.35
-0.45
[V]
0
7
14
21
28
35
42
49
56
63
Day of test [days]

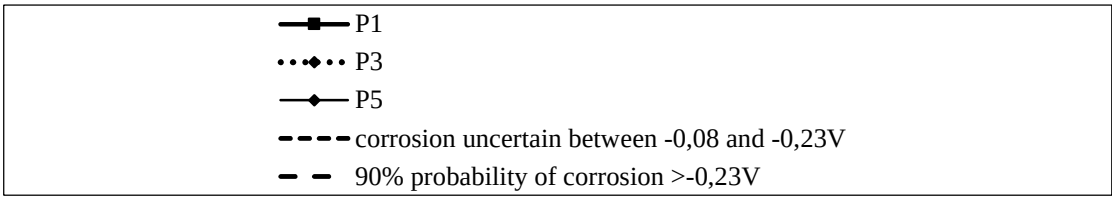
P1
P3
P5
corrosion uncertain between -0,08 and -0,23V
90% probability of corrosion >-0,23V

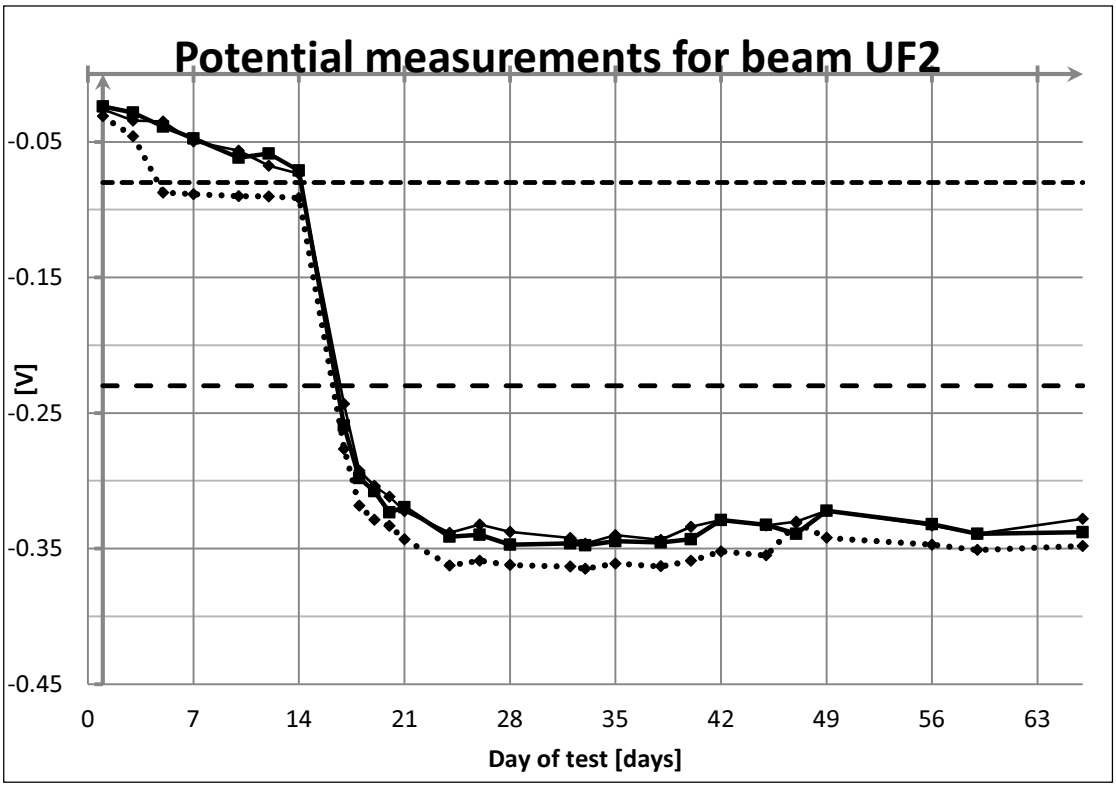
Potential measurements for beam UF2
-0.05
-0.15
-0.25
-0.35
-0.45
[V]
0
7
14
21
28
35
42
49
56
63
Day of test [days]

UW1 Side B	DoT	AGE	VALUES					
			1	2	3	4	5	Δ
Date	days	days	[V]	[V]	[V]	[V]	[V]	[V]
09-03-12	1	30	-0.0220	-0.0150	-0.0180	-0.0170	0.0240	
12-03-12	3	33	-0.0377	-0.0402	-0.0285	-0.0212	-0.0298	
14-03-12	5	35	-0.0484	-0.0645	-0.0702	-0.0650	-0.0414	
16-03-12	7	37	-0.0495	-0.0616	-0.0652	-0.0654	-0.0474	
19-03-12	10	40	-0.0573	-0.0611	-0.0621	-0.0615	-0.0530	
21-03-12	12	42	-0.0511	-0.0612	-0.0628	-0.0612	-0.0539	0.0065
23-03-12	14	44	-0.0455	-0.0627	-0.0641	-0.0620	-0.0550	0.0066
26-03-12	17	47	-0.0481	-0.0631	-0.0661	-0.0638	-0.0637	0.0065
27-03-12	18	47	-0.0565	-0.0629	-0.0580	-0.0593	-0.0560	0.0068
28-03-12	19	48	-0.0688	-0.0855	-0.0913	-0.0854	-0.0718	0.2037
29-03-12	20	49	-0.0523	-0.0764	-0.0879	-0.0825	-0.0627	0.2247
30-03-12	21	50	-0.0501	-0.0744	-0.0873	-0.0839	-0.0629	0.2289
02-04-12	24	53	-0.2966	-0.3361	-0.3551	-0.3449	-0.3005	-0.0080
04-04-12	26	55	-0.3143	-0.3424	-0.3542	-0.3412	-0.2947	-0.0097
06-04-12	28	57	-0.3105	-0.3423	-0.3517	-0.3435	-0.2998	-0.0132
10-04-12	32	61	-0.3082	-0.3435	-0.3562	-0.3435	-0.3028	-0.1090
11-04-12	33	62	-0.3263	-0.3478	-0.3624	-0.3533	-0.3068	-0.0139
13-04-12	35	64	-0.3213	-0.3516	-0.3635	-0.3541	-0.3102	-0.0153
16-04-12	38	67	-0.3245	-0.3564	-0.3677	-0.3538	-0.3169	-0.0142
18-04-12	40	69	-0.329	-0.341	-0.356	-0.346	-0.301	-0.0140
20-04-12	42	71	-0.332	-0.345	-0.353	-0.346	-0.309	-0.0149
23-04-12	45	74	-0.327	-0.347	-0.360	-0.350	-0.310	-0.0159
25-04-12	47	76	-0.337	-0.347	-0.358	-0.342	-0.321	-0.0014
27-04-12	49	78	-0.331	-0.345	-0.357	-0.346	-0.317	-0.0136
04-05-12	56	85	-0.327	-0.348	-0.352	-0.348	-0.313	-0.0085
07-05-12	59	88	-0.328	-0.342	-0.360	-0.349	-0.328	-0.0105
14-05-12	66	95	-0.331	-0.349	-0.362	-0.353	-0.327	0.0059

UW2 Side A	DoT	AGE	VALUES					
			1	2	3	4	5	Δ
Date	days	days	[V]	[V]	[V]	[V]	[V]	[V]
09-03-12	1	30	-0.0040	-0.0020	-0.0040	-0.0010	-0.0010	
12-03-12	3	33	-0.0127	-0.0331	-0.0454	-0.0254	-0.0175	
14-03-12	5	35	-0.0301	-0.0451	-0.0455	-0.0435	-0.0212	
16-03-12	7	37	-0.0286	-0.0428	-0.0442	-0.0430	-0.0316	
19-03-12	10	40	-0.0605	-0.0765	-0.0747	-0.0688	-0.0300	
21-03-12	12	42	-0.0605	-0.0767	-0.0760	-0.0687	-0.0299	0.2644
23-03-12	14	44	-0.0584	-0.0696	-0.0679	-0.0615	-0.0278	0.2731
26-03-12	17	46	-0.0574	-0.0682	-0.0685	-0.0613	-0.0314	0.2745
27-03-12	18	47	-0.0571	-0.0633	-0.0635	-0.0547	-0.0287	0.2809
28-03-12	19	48	-0.0573	-0.0661	-0.0633	-0.0564	-0.0408	0.2790
29-03-12	20	49	-0.0545	-0.0607	-0.0612	-0.0560	-0.0377	0.2810
30-03-12	21	50	-0.0557	-0.0618	-0.0610	-0.0547	-0.0312	0.2807
02-04-12	24	53	-0.0536	-0.0584	-0.0572	-0.0512	-0.0350	0.2751
04-04-12	26	55	-0.0425	-0.0527	-0.0569	-0.0519	-0.0327	0.2836
06-04-12	28	57	-0.0470	-0.0531	-0.0514	-0.0445	-0.0331	0.2957
10-04-12	32	61	-0.0407	-0.0525	-0.0531	-0.0430	-0.0296	0.2991
11-04-12	33	62	-0.0495	-0.0565	-0.0555	-0.0470	-0.0312	0.3025
13-04-12	35	64	-0.0413	-0.0513	-0.0514	-0.0429	-0.0316	0.2921
16-04-12	38	67	-0.0434	-0.0515	-0.0527	-0.0457	-0.0330	0.2905
17-04-12	39	68	-0.1978	-0.1990	-0.2000	-0.1933	-0.1787	0.1451
18-04-12	40	69	-0.255	-0.248	-0.249	-0.244	-0.224	0.0939
20-04-12	42	71	-0.302	-0.295	-0.290	-0.280	-0.262	0.0562
23-04-12	45	74	-0.313	-0.311	-0.305	-0.297	-0.270	0.0305
25-04-12	47	76	-0.333	-0.331	-0.329	-0.313	-0.295	0.0198
27-04-12	49	78	-0.332	-0.330	-0.323	-0.314	-0.293	0.0115
04-05-12	56	85	-0.373	-0.362	-0.355	-0.343	-0.329	-0.0128
07-05-12	59	88	-0.384	-0.376	-0.367	-0.360	-0.339	-0.0194
14-05-12	66	95	-0.386	-0.375	-0.367	-0.352	-0.355	-0.0220

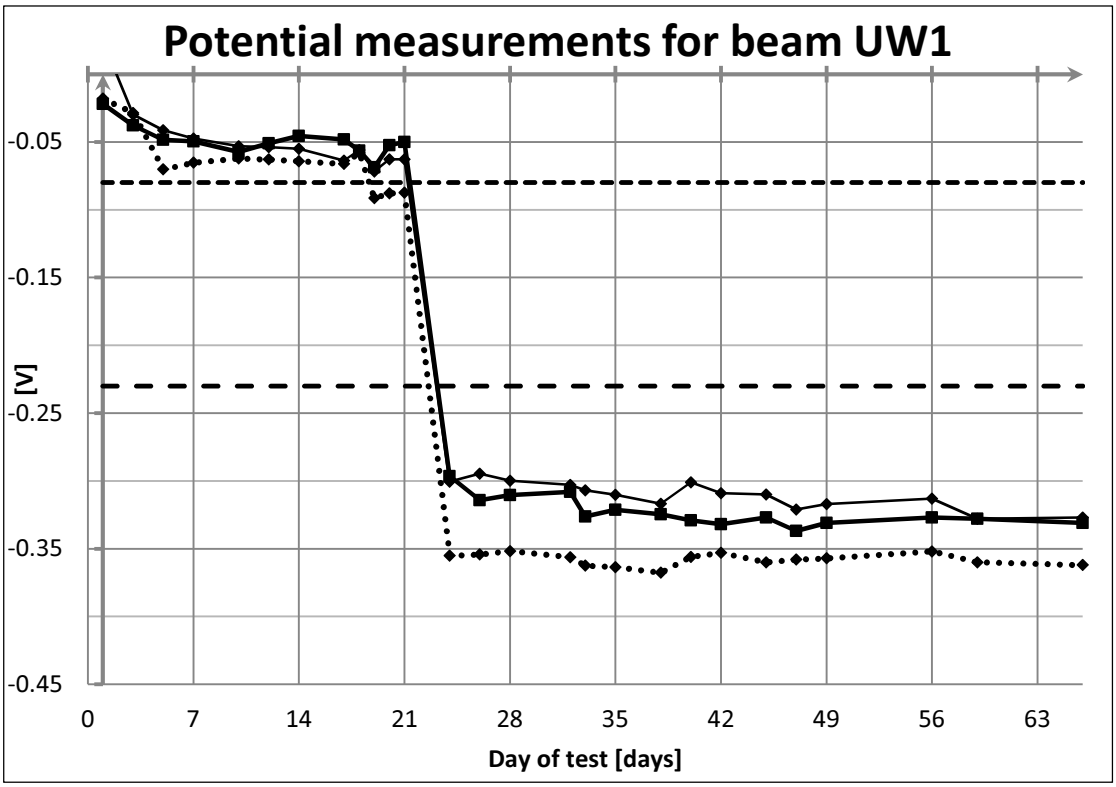
Potential measurements for beam UW1
-0.05
-0.15
-0.25
-0.35
-0.45
[V]
0
7
14
21
28
35
42
49
56
63
Day of test [days]

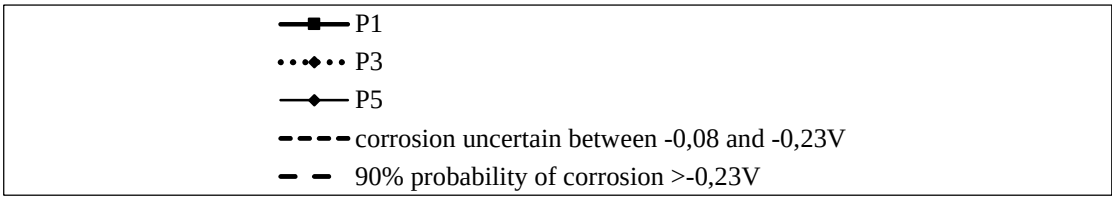
P1
P3
P5
corrosion uncertain between -0,08 and -0,23V
90% probability of corrosion >-0,23V

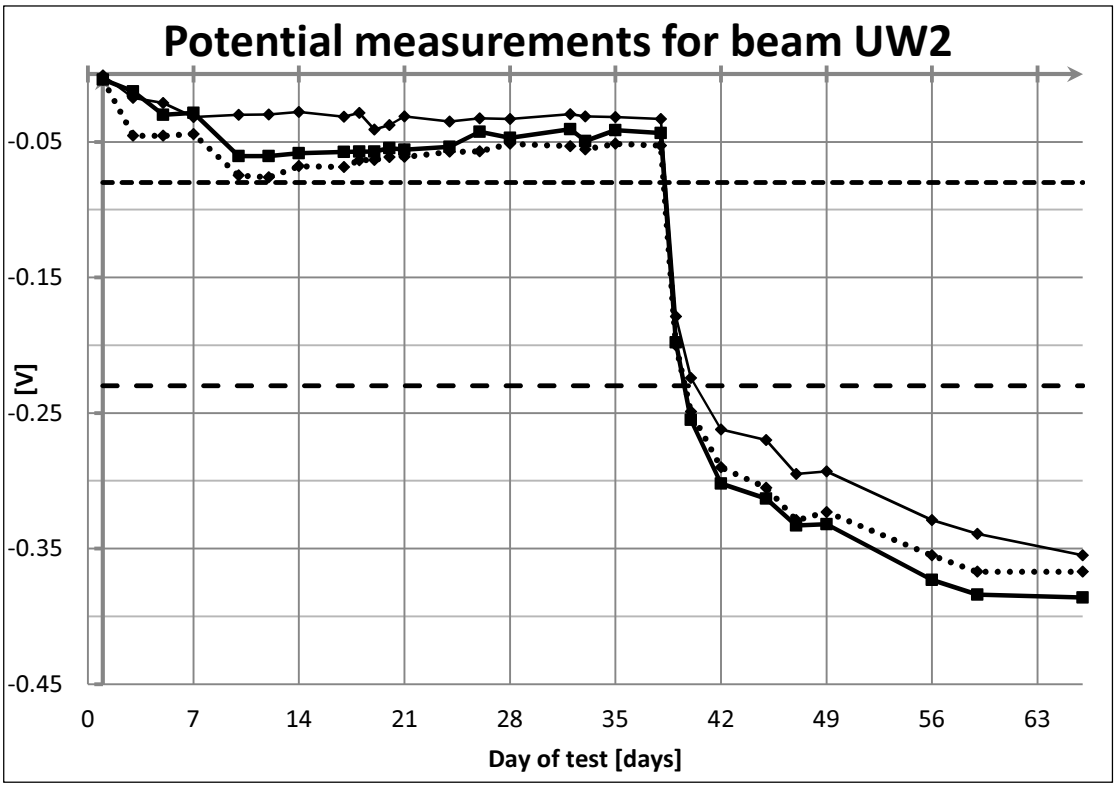
Potential measurements for beam UW2
-0.05
-0.15
-0.25
-0.35
-0.45
[V]
0
7
14
21
28
35
42
49
56
63
Day of test [days]

WF1 Side A	DoT	AGE	VALUES					
			1	2	3	4	5	Δ
Date	days	days	[V]	[V]	[V]	[V]	[V]	[V]
09-03-12	1	29	-0.0260	-0.0290	-0.0270	-0.0250	-0.0180	-0.2380
12-03-12	3	32	-0.0405	-0.0662	-0.0705	-0.0658	-0.0418	
14-03-12	5	34	-0.0342	-0.0695	-0.0728	-0.0688	-0.0428	
16-03-12	7	36	-0.0336	-0.0661	-0.0705	-0.0728	-0.0472	
19-03-12	10	39	-0.0546	-0.0661	-0.0702	-0.0721	-0.0473	
23-03-12	14	43	-0.0471	-0.0705	-0.0701	-0.0723	-0.0385	-0.0007
26-03-12	17	46	-0.0748	-0.0911	-0.0951	-0.0948	-0.0635	-0.0012
30-03-12	21	50	-0.0487	-0.0723	-0.0701	-0.0728	-0.0415	-0.0016
02-04-12	24	53	-0.0574	-0.0765	-0.0751	-0.0749	-0.0571	-0.0012
06-04-12	28	57	-0.0611	-0.0695	-0.0644	-0.0651	-0.0582	-0.0013
10-04-12	32	61	-0.0582	-0.0650	-0.0597	-0.0639	-0.0501	-0.0005
13-04-12	35	64	-0.0431	-0.0612	-0.0627	-0.0616	-0.0482	-0.0007
16-04-12	38	67	-0.0476	-0.0667	-0.0678	-0.0670	-0.0518	-0.0008
17-04-12	39	68	-0.0537	-0.6430	-0.0640	-0.0639	-0.0516	-0.0009
18-04-12	40	69	-0.0684	-0.0600	-0.0600	-0.0626	-0.0537	-0.0009
19-04-12	41	70	-0.0572	-0.0696	-0.0675	-0.0660	-0.0514	-0.0007
20-04-12	42	71	-0.0565	-0.6520	-0.0650	-0.6590	-0.0460	-0.0009
23-04-12	45	74	-0.0660	-0.0666	-0.0665	-0.0659	-0.0588	-0.0013
24-04-12	46	75	-0.0620	-0.0624	-0.0633	-0.0637	-0.0560	-0.0012
25-04-12	47	76	-0.0525	-0.0675	-0.0628	-0.0619	-0.0522	-0.0007
27-04-12	49	78	-0.0523	-0.0696	-0.0643	-0.0642	-0.0527	-0.0009
02-05-12	54	83	-0.0628	-0.0652	-0.0592	-0.0618	-0.0472	0.0020
04-05-12	56	85	-0.0612	-0.0638	-0.0625	-0.0626	-0.0529	-0.0001
07-05-12	59	88	-0.0603	-0.0636	-0.0653	-0.0631	-0.0623	0.0004
14-05-12	66	95	-0.0662	-0.0616	-0.0616	-0.0614	-0.0550	0.0005

WF2 Side A	DoT	AGE	VALUES					
			1	2	3	4	5	Δ
Date	days	days	[V]	[V]	[V]	[V]	[V]	[V]
09-03-12	1	29	-0.0260	-0.0290	-0.0270	-0.0250	-0.0180	-0.2380
12-03-12	3	32	-0.0490	-0.0687	-0.0927	-0.0683	-0.0487	
14-03-12	5	34	-0.0464	-0.0708	-0.0742	-0.0722	-0.0584	
16-03-12	7	36	-0.0453	-0.0720	-0.0732	-0.0704	-0.0457	
19-03-12	10	39	-0.0563	-0.0754	-0.0759	-0.0705	-0.0469	
23-03-12	14	43	-0.0482	-0.0758	-0.0712	-0.0710	-0.0468	-0.0130
26-03-12	17	46	-0.0569	-0.0700	-0.0704	-0.0702	-0.0459	-0.0122
30-03-12	21	50	-0.0662	-0.0717	-0.0726	-0.0719	-0.0442	-0.0116
02-04-12	24	53	-0.0737	-0.0754	-0.0762	-0.0767	-0.0585	-0.0112
06-04-12	28	57	-0.0694	-0.0670	-0.0659	-0.0654	-0.0617	-0.0107
10-04-12	32	61	-0.0680	-0.0662	-0.0669	-0.0664	-0.0697	-0.0110
13-04-12	35	64	-0.0732	-0.0775	-0.0800	-0.0825	-0.0660	-0.0107
16-04-12	38	67	-0.1940	-0.1925	-0.1935	-0.1934	-0.1883	-0.1485
17-04-12	39	68	-0.1907	-0.1851	-0.1863	-0.1890	-0.1884	-0.1412
18-04-12	40	69	-0.1907	-0.1847	-0.1845	-0.1887	-0.1852	-0.1388
19-04-12	41	70	-0.1858	-0.1852	-0.1826	-0.1847	-0.1814	-0.1349
20-04-12	42	71	-0.1851	-0.1812	-0.1820	-0.1830	-0.1812	-0.1349
23-04-12	45	74	-0.1767	-0.1702	-0.1706	-0.1692	-0.1708	-0.1200
24-04-12	46	75	-0.175	-0.170	-0.170	-0.170	-0.173	-0.1182
25-04-12	47	76	-0.169	-0.165	-0.167	-0.164	-0.162	-0.1153
27-04-12	49	78	-0.164	-0.156	-0.158	-0.160	-0.152	-0.1091
02-05-12	54	83	-0.157	-0.155	-0.157	-0.157	-0.152	-0.1007
04-05-12	56	85	-0.150	-0.149	-0.148	-0.147	-0.148	-0.0937
07-05-12	59	88	-0.147	-0.137	-0.136	-0.137	-0.140	-0.0857
14-05-12	66	95	-0.133	-0.123	-0.121	-0.123	-0.124	-0.0741

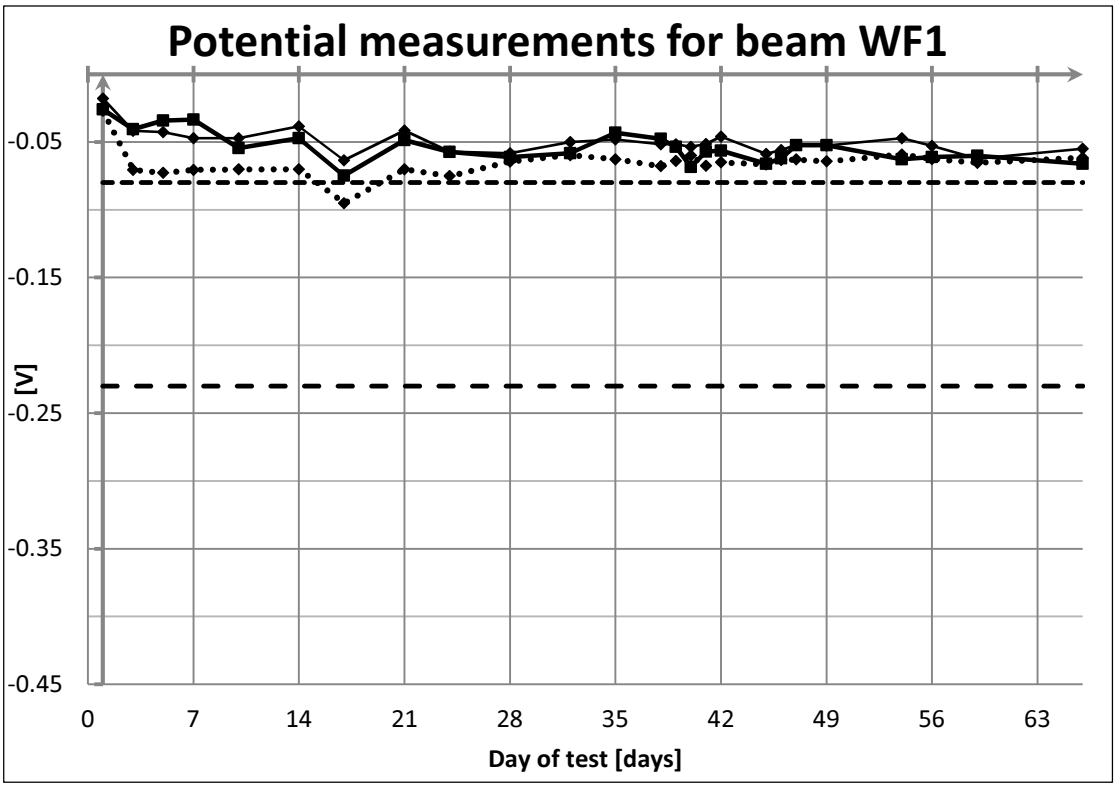
Potential measurements for beam WF1
-0.05
-0.15
-0.25
-0.35
-0.45
[V]
0
7
14
21
28
35
42
49
56
63
Day of test [days]

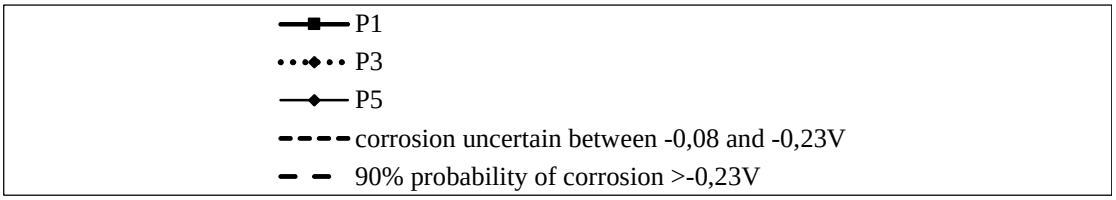
P1
P3
P5
corrosion uncertain between -0,08 and -0,23V
90% probability of corrosion >-0,23V

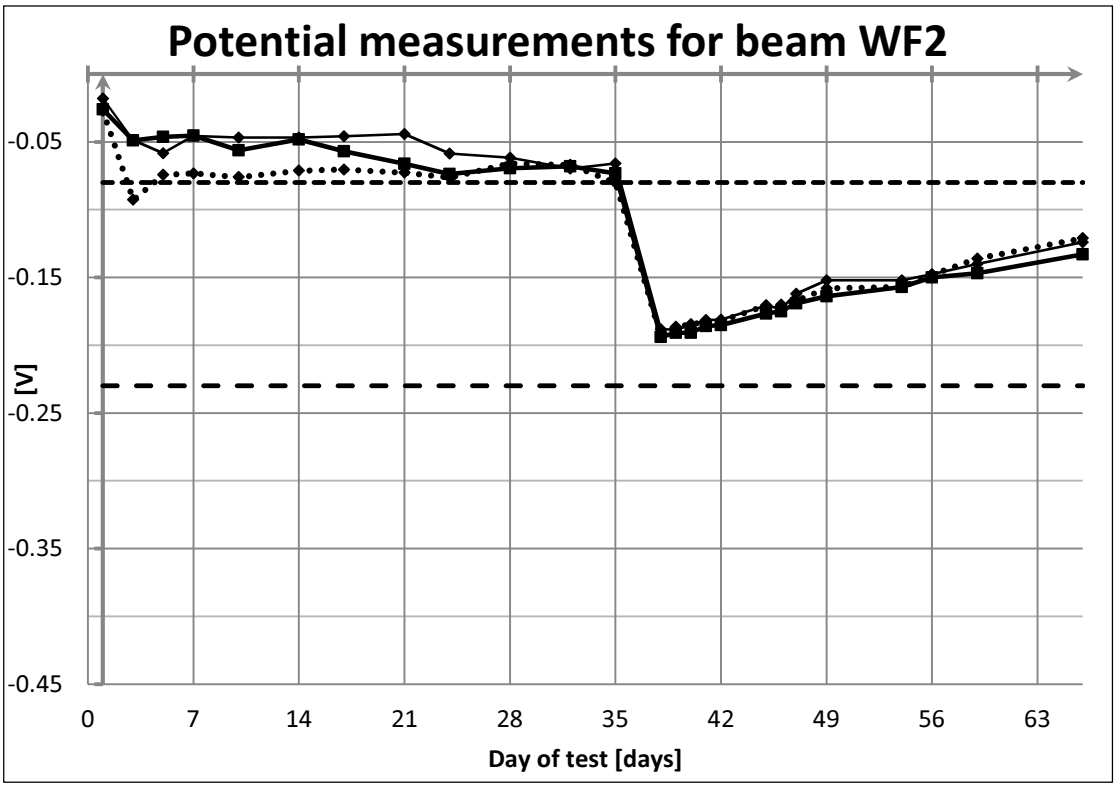
Potential measurements for beam WF2
-0.05
-0.15
-0.25
-0.35
-0.45
[V]
0
7
14
21
28
35
42
49
56
63
Day of test [days]

WW1 Side B	DoT	AGE	VALUES					
			1	2	3	4	5	Δ
Date	days	days	[V]	[V]	[V]	[V]	[V]	[V]
09-03-12	1	30	-0.0280	-0.0220	-0.0220	-0.0230	-0.0220	-0.2070
12-03-12	3	33	-0.0351	-0.0574	-0.0636	-0.0383	-0.0284	
14-03-12	5	35	-0.0374	-0.0649	-0.0688	-0.0626	-0.0341	
16-03-12	7	37	-0.0452	-0.0661	-0.0680	-0.0634	-0.0411	
19-03-12	10	40	-0.0388	-0.0674	-0.0712	-0.0675	-0.0443	
23-03-12	14	44	-0.0451	-0.0687	-0.0722	-0.0693	-0.0425	0.0024
26-03-12	17	47	-0.0422	-0.0715	-0.0699	-0.0683	-0.0497	0.0010
30-03-12	21	51	-0.0388	-0.0650	-0.0689	-0.0662	-0.0418	0.0023
02-04-12	24	54	-0.0461	-0.0706	-0.0700	-0.0725	-0.0611	0.0022
06-04-12	28	58	-0.0545	-0.0653	-0.0700	-0.0693	-0.0627	-0.0026
10-04-12	32	62	-0.0449	-0.0655	-0.0661	-0.0666	-0.0681	-0.0018
13-04-12	35	65	-0.0574	-0.0630	-0.0661	-0.0631	-0.0645	-0.0014
16-04-12	38	68	-0.2349	-0.2932	-0.3038	-0.3034	-0.2804	0.0032
17-04-12	39	68	-0.2596	-0.3095	-0.3230	-0.3224	-0.2988	0.1300
18-04-12	40	70	-0.2611	-0.3209	-0.3302	-0.3325	-0.3040	0.0206
19-04-12	41	70	-0.2717	-0.3292	-0.3400	-0.3425	-0.3095	0.0253
20-04-12	42	72	-0.2722	-0.3344	-0.3482	-0.3460	-0.3131	0.0331
23-04-12	45	75	-0.283	-0.342	-0.343	-0.347	-0.327	0.0317
24-04-12	46	75	-0.274	-0.338	-0.351	-0.351	-0.319	0.0354
25-04-12	47	77	-0.268	-0.339	-0.348	-0.339	-0.327	0.0405
27-04-12	49	79	-0.285	-0.340	-0.345	-0.343	-0.321	0.0435
02-05-12	54	84	-0.263	-0.353	-0.351	-0.362	-0.325	0.0512
04-05-12	56	86	-0.286	-0.353	-0.366	-0.364	-0.333	0.0504
07-05-12	59	89	-0.317	-0.350	-0.367	-0.365	-0.337	0.0570
14-05-12	66	96	-0.309	-0.341	-0.360	-0.361	-0.338	0.0659

WW2 Side B	DoT	AGE	VALUES					
			1	2	3	4	5	Δ
Date	days	days	[V]	[V]	[V]	[V]	[V]	[V]
09-03-12	1	30	-0.0260	-0.0290	-0.0270	-0.0250	-0.0180	-0.2380
12-03-12	3	33	-0.0278	-0.0498	-0.0556	-0.0528	-0.0273	
14-03-12	5	35	-0.0279	-0.0529	-0.0551	-0.0527	-0.0221	
16-03-12	7	37	-0.0248	-0.0564	-0.0535	-0.0545	-0.0273	
19-03-12	10	40	-0.0225	-0.0579	-0.0563	-0.0544	-0.0308	
23-03-12	14	44	-0.0256	-0.0500	-0.0440	-0.0523	-0.0316	0.0040
26-03-12	17	47	-0.0257	-0.0479	-0.0510	-0.0520	-0.0497	0.0040
30-03-12	21	51	-0.0400	-0.0475	-0.0481	-0.0485	-0.0355	0.0038
02-04-12	24	54	-0.0408	-0.0533	-0.0525	-0.0528	-0.0402	0.0057
06-04-12	28	58	-0.0507	-0.0463	-0.0422	-0.0453	-0.0392	0.0038
10-04-12	32	62	-0.0505	-0.0660	-0.0712	-0.0680	-0.0580	0.1990
13-04-12	35	65	-0.0445	-0.0740	-0.0849	-0.0744	-0.0450	0.2513
16-04-12	38	68	-0.0508	-0.0836	-0.0940	-0.0850	-0.0430	0.2806
17-04-12	39	68	-0.0513	-0.0830	-0.0931	-0.0874	-0.0545	0.2871
18-04-12	40	70	-0.0522	-0.0759	-0.0901	-0.0832	-0.0519	0.2906
19-04-12	41	70	-0.0517	-0.0830	-0.0923	-0.0835	-0.0480	0.2986
20-04-12	42	72	-0.0505	-0.0849	-0.0969	-0.0875	-0.0560	0.3070
23-04-12	45	75	-0.0506	-0.0891	-0.1011	-0.0907	-0.0533	0.3207
24-04-12	46	75	-0.0523	-0.0875	-0.0996	-0.0905	-0.0549	0.3261
25-04-12	47	77	-0.0584	-0.0848	-0.1031	-0.0900	-0.0493	0.3272
27-04-12	49	79	-0.0505	-0.0864	-0.0987	-0.0849	-0.0516	0.3318
02-05-12	54	84	-0.0538	-0.0903	-0.0984	-0.0928	-0.0498	0.3387
04-05-12	56	86	-0.0557	-0.0824	-0.0980	-0.0908	-0.0556	0.3385
07-05-12	59	89	-0.0506	-0.0805	-0.0914	-0.0805	-0.0479	0.3430
14-05-12	66	96	-0.274	-0.319	-0.339	-0.324	-0.273	0.1107

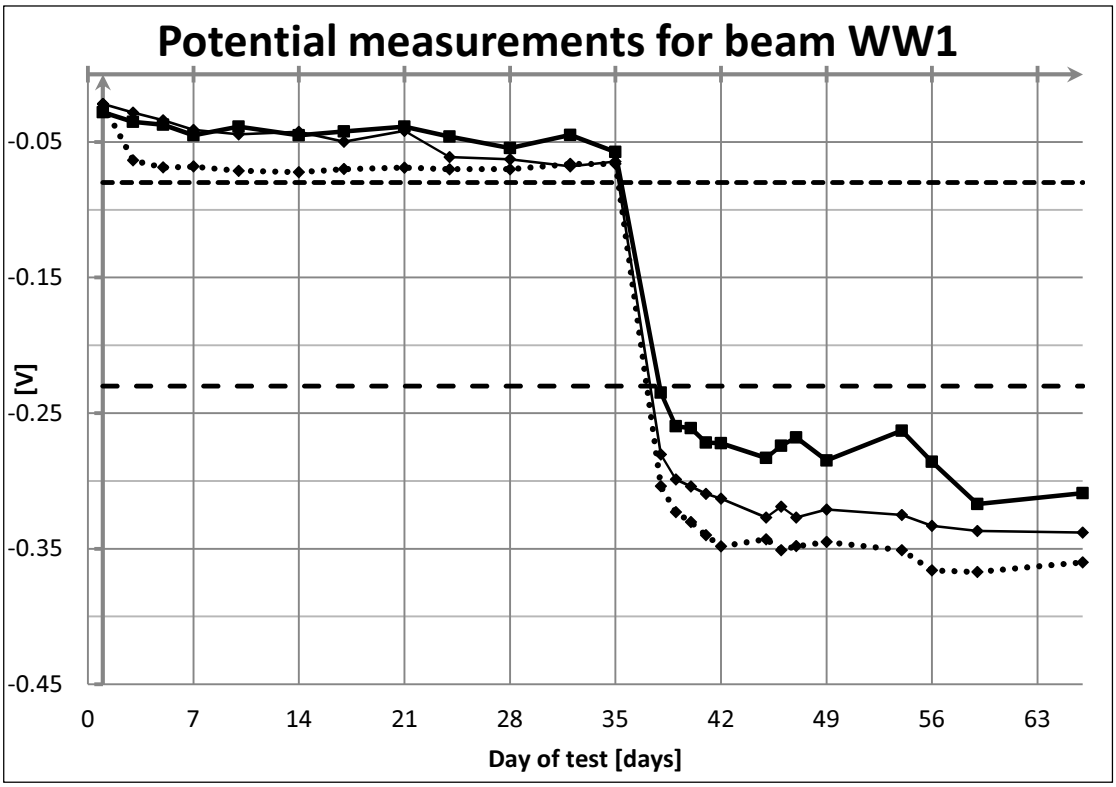
Potential measurements for beam WW1
-0.05
-0.15
-0.25
-0.35
-0.45
[V]
0
7
14
21
28
35
42
49
56
63
Day of test [days]

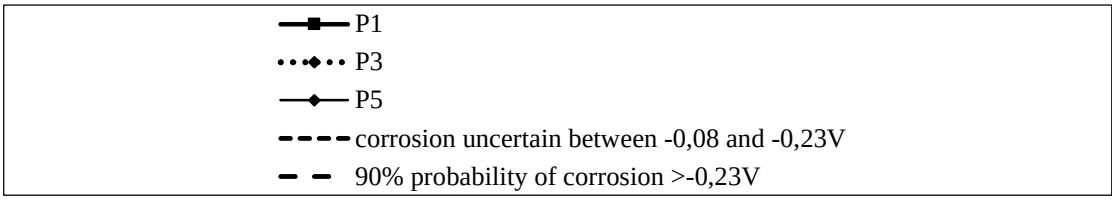
P1
P3
P5
corrosion uncertain between -0,08 and -0,23V
90% probability of corrosion >-0,23V

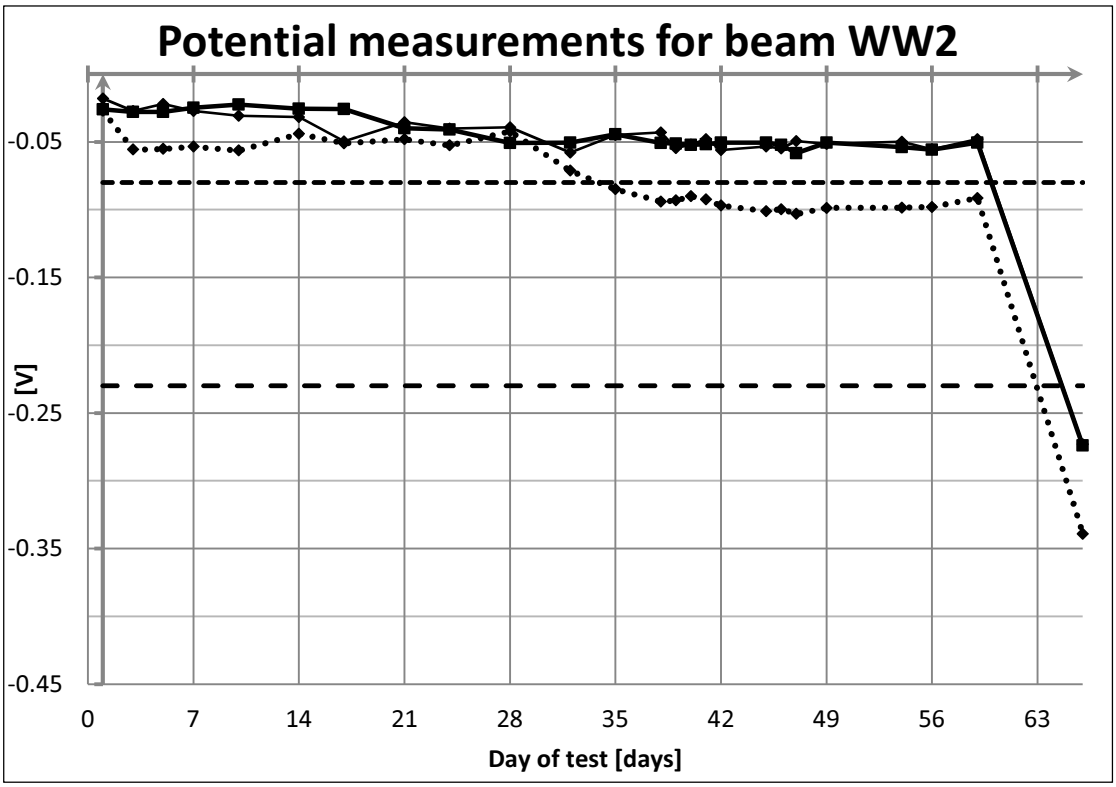
Potential measurements for beam WW2
-0.05
-0.15
-0.25
-0.35
-0.45
[V]
0
7
14
21
28
35
42
49
56
63
Day of test [days]

Appendix D: Resistivity test results

Test laboratory: CTH

Mixture ID: without fibres – C20/25

Casting date: 8 February 2012

Date of testing: 7 March 2012

Age [days]: 28

Name		d	L_1	L_2	L_3	L_{avg}	R_{s+sp}	R_{sp}	ρ
		[mm]	[mm]	[mm]	[mm]	[mm]	[Ω]	[Ω]	[Ωm]
Mix 1	2	100	51,8	52,1	51,7	51,9	200,40	28,40	26,029
	3	100	51,8	51,7	51,8	51,8	242,20	51,10	28,975
	2	100	51,5	51,0	51,0	51,2	189,90	21,77	25,791
	3	100	51,3	50,5	51,2	51,0	198,30	23,98	26,845
Mix 2	1	100	51,9	51,3	50,7	51,3	246,00	45,48	30,699
	2	100	52,9	51,6	51,3	51,9	226,40	29,29	29,828
	1	100	49,5	49,5	49,8	49,6	236,00	33,18	32,116
	2	100	50,5	51,4	50,5	50,8	218,00	42,30	27,164

Test laboratory: CTH

Mixture ID: with fibres – C20/25

Casting date: 9 February 2012

Date of testing: 8 March 2012

Age [days]: 28

Name		d	L_1	L_2	L_3	L_{avg}	R_{s+sp}	R_{sp}	ρ
		[mm]	[mm]	[mm]	[mm]	[mm]	[Ω]	[Ω]	[Ωm]
Mix 1	1	100	50,2	50,5	51,0	50,6	143,50	62,83	12,521
	2	100	50,2	49,8	49,9	50,0	128,89	13,29	18,158
	3	100	50,9	52,0	50,9	51,3	146,66	12,03	20,612
	2	100	50,7	51,4	51,0	51,0	114,30	13,63	15,503
	3	100	51,2	51,8	51,5	51,5	126,78	14,91	17,061
Mix 2	2	100	49,5	48,8	49,3	49,2	130,35	14,02	18,570
	3	100	52,8	51,8	51,9	52,2	142,55	16,94	18,899
	2	100	49,5	49,8	49,8	49,7	130,29	12,22	18,658
	3	100	50,5	51,2	50,2	50,6	143,16	14,34	19,995

Test laboratory: CTH

Mixture ID: C45/55

Casting date: 22 March 2012

Date of testing: 19 April 2012

Age [days]: 28

Name		d	L_1	L_2	L_3	L_{avg}	R_{s+sp}	R_{sp}	ρ
		[mm]	[mm]	[mm]	[mm]	[mm]	[Ω]	[Ω]	[Ωm]
1,3	1	100	51,4	51,4	52,1	51,6	130,67	19,65	16,898
	2	100	51,1	51,4	51,7	51,4	103,29	14,83	13,517
	3	100	50,5	49,7	50,2	50,1	85,43	15,42	10,975
1,0	1	100	51,0	52,3	51,7	51,7	156,06	16,36	21,222
	2	100	51,1	50,4	51,6	51,0	114,68	5,22	16,856
	3	100	50,7	51,2	51,3	51,1	102,25	19,88	12,660
0,6	1	100	51,3	52,4	51,2	51,6	167,80	17,26	22,914
	2	100	52,0	51,4	51,4	51,6	178,90	17,63	24,547
	3	100	51,5	52,9	51,8	52,1	168,90	45,40	18,617

Test laboratory: CTH

Mixture ID: C45/55

Casting date: 22 March 2012

Date of testing: 26 April 2012

Age [days]: 35

Name		d	L_1	L_2	L_3	L_{avg}	R_{s+sp}	R_{sp}	ρ
		[mm]	[mm]	[mm]	[mm]	[mm]	[Ω]	[Ω]	[Ωm]
1,3	1	100	49,1	49,6	49,1	49,3	140,65	24,75	18,464
	2	100	48,7	49,7	48,8	49,1	106,82	22,22	13,533
	3	100	49,6	49,1	49,3	49,3	82,22	18,26	10,189
1,0	1	100	48,3	48,5	48,3	48,4	137,26	13,84	20,028
	2	100	49,4	50,5	49,2	49,7	84,24	12,15	11,393
	3	100	50,0	50,2	51,1	50,4	89,13	12,49	11,943
0,6	1	100	49,3	49,3	49,2	49,3	116,26	11,33	16,717
	2	100	50,3	50,3	50,8	50,5	187,80	13,62	27,090
	3	100	48,5	48,5	48,6	48,5	134,04	14,05	19,431

Test laboratory: CTH

Mixture ID: C45/55

Casting date: 23 March 2012

Date of testing: 20 April 2012

Age [days]: 28

Name		d	L_1	L_2	L_3	L_{avg}	R_{s+sp}	R_{sp}	ρ
		[mm]	[mm]	[mm]	[mm]	[mm]	[Ω]	[Ω]	[Ωm]
0,3	1	100	51,2	52,0	53,0	52,1	215,30	18,11	29,726
	2	100	50,2	49,8	50,0	50,0	205,50	14,61	29,985
	3	100	52,0	51,9	52,1	52,0	208,30	14,65	29,249
0,0	1	100	51,5	51,5	53,0	52,0	299,70	17,20	42,668
	2	100	51,2	51,4	51,5	51,4	279,30	15,23	40,350
	3	100	51,2	50,9	51,0	51,0	292,10	16,35	42,465
0,6PP	1	100	51,9	52,8	51,9	52,2	301,20	16,17	42,885
	2	100	51,9	52,0	52,0	52,0	315,10	20,01	44,570
	3	100	51,3	50,2	50,6	50,7	302,90	22,60	43,422

Test laboratory: CTH

Mixture ID: C45/55

Casting date: 23 March 2012

Date of testing: 27 April 2012

Age [days]: 35

Name		d	L_1	L_2	L_3	L_{avg}	R_{s+sp}	R_{sp}	ρ
		[mm]	[mm]	[mm]	[mm]	[mm]	[Ω]	[Ω]	[Ωm]
0,3	1	100	49,0	49,5	49,0	49,2	183,2	21,07	25,881
	2	100	49,4	49,7	49,3	49,5	190,6	21,09	26,896
	3	100	50,6	50,0	50,7	50,4	280,5	23,15	40,104
0,0	1	100	49,1	49,5	49,6	49,4	345,8	28,89	50,385
	2	100	49,2	49,0	49,3	49,2	330,7	26,76	48,519
	3	100	50,2	50,3	49,9	50,1	326,9	24,49	47,408
0,6PP	1	100	49,2	49,3	49,7	49,4	294,4	20,20	43,594
	2	100	49,8	49,6	50,0	49,8	287,7	19,89	42,236
	3	100	50,1	50,7	50,2	50,3	306,5	23,66	44,163

Appendix E: RCM tests results

Test laboratory: CTH

Mixture ID: C45/55

Casting date: 22 March 2012

Date of testing: 19 April 2012

Age [days]: 28

NaCl: 10%

NaOH: 0.3N

	Fibre content		1,3			1,0		
	Slice		1	2	3	1	2	3
Sample diameter	D	[mm]	100	100	100	100	100	100
Sample length	L	[mm]	51,6	51,4	50,1	51,7	51,0	51,1
Chloride concentration	c_0	-	10	10	10	10	10	10
Initial temp.	T_i	[^oC]	18,0	18,0	18,0	18,5	18,5	18,5
Initial current at 30V	I_i	[mA]	255,0	350,0	620,0	168,0	289,0	440,0
Applied Voltage	U	[V]	10	10	10	10	10	10
Adj. initial current	I_a	[mA]	48,0	63,8	98,0	37,7	55,0	76,2
Duration of test	t	[h]	23	23	23	23	23	23
Final current	I_f	[mA]	38,2	44,0	55,0	32,5	44,3	51,4
Final temp.	T_f	[^oC]	19,0	19,0	19,0	20,0	20,0	20,0
Average depth	X_d	[mm]	16,6	11,6	14,6	11,7	13,8	10,8
Migration coefficient	D_{nssm}	x 10^{-12} [m^2/s]	24,246	15,736	20,350	16,082	19,388	14,418

			penetration depth											
		1	19,1	14,9	11,8	10,2	14,8	14,8	11,9	12,6	11,9	12,2	10,8	10,8
		2	17,5	15,3	12,5	10,1	13,2	15,9	11,8	11,2	14,4	15,3	9,9	10,8
		3	19,7	14,2	10,7	10,3	12,9	14,9	10,7	11,2	14,2	16,4	10,7	12,7
		4	18,4	14,5	12,6	9,9	14,6	15,8	10,0	10,8	15,8	14,9	10,3	11,0
		5	21,8	14,6	11,4	10,5	12,6	14,5	9,7	11,1	15,2	15,8	9,6	10,0
		6	15,5	12,3	13,8	10,7	16,6	18,4	9,9	9,5	14,9	15,8	9,9	10,3
		7	24,2	14,5	12,2	12,5	11,9	13,8	12,5	14,0	13,5	13,2	9,7	10,7
		8	13,8	-	15,4	-	14,6	17,6	13,1	13,8	11,7	10,7	13,1	12,8
		9	-	14,7	12,3	12,3	-	12,3	14,3	13,8	10,7	10,1	12,7	11,1

Test laboratory:	CTH	CTH
Mixture ID:	C45/55	C45/55
Casting date:	22 March 2012	23 March 2012
Date of testing:	19 April 2012	20 April 2012
Age [days]:	28	28
NaCl:	10%	10%
NaOH:	0.3N	0.3N

	Fibre content		**0,6**			**0,3**		
	Slice		**1**	**2**	**3**	**1**	**2**	**3**
Sample diameter	**D**	**[mm]**	100	100	100	100	100	100
Sample length	**L**	**[mm]**	51,6	51,6	52,1	52,1	50,0	52,0
Chloride concentration	c_0	-	10	10	10	10	10	10
Initial temp.	T_i	[°C]	18,0	18,0	18,0	19,0	19,0	19,0
Initial current at 30V	I_i	**[mA]**	175,3	168,9	340,0	134,0	142,6	137,9
Applied Voltage	**U**	**[V]**	10	10	10	10	10	10
Adj. initial current	I_a	**[mA]**	37,5	36,2	61,7	33,4	35,7	33,0
Duration of test	**t**	**[h]**	23	23	23	23	23	23
Final current	I_f	**[mA]**	32,6	32,6	45,7	30,5	31,2	30,0
Final temp.	T_f	[°C]	19,0	19,0	19,0	20,0	20,0	20,0
Average depth	X_d	**[mm]**	12,9	12,3	9,4	14,7	14,2	15,5
Migration coefficient	D_{nssm}	**x 10^{-12} [m^2/s]**	17,926	16,928	12,322	21,133	19,645	22,532

			penetration depth											
		1	13,4	13,9	-	-	14,1	15,8	15,4	14,3	13,3	12,5	16,9	14,9
		2	12,7	11,7	15,4	12,3	13,5	12,9	14,3	14,9	18,1	11,7	18,2	18,4
		3	12,9	11,5	12,9	11,9	9,4	9,7	14,9	13,9	16,0	14,2	17,8	16,8
		4	11,0	12,1	16,0	13,5	7,5	7,8	15,5	15,0	16,4	12,9	12,3	16,8
		5	13,2	11,3	14,4	14,6	7,1	7,9	13,2	14,8	17,0	10,4	14,9	17,5
		6	13,6	12,3	11,7	11,2	8,1	7,6	16,0	15,6	17,3	11,5	11,5	18,0
		7	12,9	13,0	9,9	9,1	7,6	7,0	12,6	12,5	14,6	12,5	13,8	15,0
		8	14,4	12,7	10,3	9,9	7,1	8,0	16,2	18,4	16,9	12,8	12,4	16,4
		9	14,5	15,4	13,0	10,9	10,5	12,1	14,9	11,7	12,7	13,2	13,4	13,5

Test laboratory: CTH

Mixture ID: C45/55

Casting date: 23 March 2012

Date of testing: 20 April 2012

Age [days]: 28

NaCl: 10%

NaOH: 0.3N

	Fibre content		0,0			0,6PP		
	Slice		1	2	3	1	2	3
Sample diameter	D	[mm]	100	100	100	100	100	100
Sample length	L	[mm]	52,0	51,4	51,0	52,2	52,0	50,7
Chloride concentration	c_0	-	10	10	10	10	10	10
Initial temp.	T_i	[°C]	19,5	19,5	19,5	18,5	18,5	18,5
Initial current at 30V	I_i	[mA]	101,0	109,0	103,5	101,0	102,5	106,0
Applied Voltage	U	[V]	20	20	20	20	20	20
Adj. initial current	I_a	[mA]	65,0	70,1	66,4	65,0	66,0	68,2
Duration of test	t	[h]	23	23	23	23	23	23
Final current	I_f	[mA]	59,6	63,6	61,1	57,6	59,0	51,0
Final temp.	T_f	[°C]	21,0	21,0	21,0	19,0	19,0	19,0
Average depth	X_d	[mm]	25,2	25,9	25,1	22,8	24,5	24,4
Migration coefficient	D_{nssm}	x 10^{-12} [m^2/s]	19,100	19,502	18,703	17,123	18,441	17,971

			penetration depth											
		1	24,8	24,0	25,1	25,6	25,3	24,7	22,7	22,6	25,4	21,0	23,3	23,8
		2	26,0	25,6	25,4	25,7	25,6	24,8	23,2	23,6	23,3	23,2	23,9	24,2
		3	24,8	24,9	25,9	25,6	25,2	24,8	19,4	21,0	24,0	22,9	23,4	24,3
		4	25,3	25,5	25,0	25,1	25,2	25,1	22,0	23,6	22,1	26,1	25,1	25,3
		5	24,2	25,6	27,1	28,0	24,6	24,6	22,2	22,5	25,1	24,3	23,9	24,6
		6	25,4	25,6	23,6	23,9	24,9	25,7	21,7	23,4	27,8	27,5	25,0	25,3
		7	26,6	27,1	28,0	26,8	25,4	25,1	21,5	21,8	23,4	24,7	24,1	24,2
		8	24,5	24,7	26,0	25,9	28,1	26,5	26,6	24,7	26,7	28,9	25,4	25,0
		9	25,5	24,2	26,5	27,2	22,6	25,0	23,9	24,4	23,5	22,8	23,9	25,1

Test laboratory: CTH

Mixture ID: C45/55

Casting date: 22 March 2012

Date of testing: 26 April 2012

Age [days]: 35

NaCl: 10%

NaOH: 0.3N

	Fibre content		1,3			1,0		
	Slice		1	2	3	1	2	3
Sample diameter	D	[mm]	100	100	100	100	100	100
Sample length	L	[mm]	49,3	49,1	49,3	48,4	49,7	50,4
Chloride concentration	c_0	-	10	10	10	10	10	10
Initial temp.	T_i	[^oC]	20,0	20,0	20,0	19,5	19,5	19,5
Initial current at 30V	I_i	[mA]	270,0	410,0	670,0	198,0	500,0	530,0
Applied Voltage	U	[V]	10	10	10	10	10	10
Adj. initial current	I_a	[mA]	50,4	66,0	97,2	37,6	77,8	82,0
Duration of test	t	[h]	24	24	24	24	24	24
Final current	I_f	[mA]	39,0	49,0	59,0	32,4	56,0	56,4
Final temp.	T_f	[^oC]	20,0	20,0	20,0	20,0	20,0	20,0
Average depth	X_d	[mm]	17,5	17,8	19,2	17,0	16,7	12,5
Migration coefficient	D_{nssm}	x 10^{-12} [m^2/s]	23,820	24,264	26,486	22,683	22,689	16,296

			penetration depth											
		1	15,3	13,5	14,1	15,5	15,0	14,1	14,2	14,4	14,8	21,3	11,9	11,3
		2	17,2	13,3	19,4	20,1	19,5	17,2	14,2	15,7	16,7	18,1	11,8	12,9
		3	18,3	14,3	17,6	18,3	23,6	21,0	18,4	18,6	15,7	20,5	12,6	13,7
		4	18,7	16,9	16,8	17,5	17,6	19,2	17,4	20,0	15,2	20,4	11,5	15,9
		5	20,0	16,9	18,0	16,5	15,9	18,2	17,2	19,2	11,3	16,0	9,1	12,4
		6	20,7	15,2	18,4	16,7	19,9	18,1	16,5	20,5	17,4	21,2	12,0	14,8
		7	20,8	15,6	16,3	16,5	25,0	25,3	17,2	18,0	11,0	12,7	10,3	10,5
		8	21,0	16,2	20,1	17,9	22,9	19,6	14,2	17,8	-	20,2	14,0	14,4
		9	21,7	16,2	22,9	18,5	17,4	19,2	17,0	20,3	10,4	9,5	10,8	15,0

Test laboratory:	CTH	CTH
Mixture ID:	C45/55	C45/55
Casting date:	22 March 2012	23 March 2012
Date of testing:	26 April 2012	27 April 2012
Age [days]:	35	35
NaCl:	10%	10%
NaOH:	0.3N	0.3N

	Fibre content		**0,6**			**0,3**		
	Slice		**1**	**2**	**3**	**1**	**2**	**3**
Sample diameter	**D**	**[mm]**	100	100	100	100	100	100
Sample length	**L**	**[mm]**	49,3	50,5	48,5	49,2	49,5	50,4
Chloride concentration	c_0	-	10	10	10	10	10	10
Initial temp.	T_i	[°C]	19,0	19,0	19,0	20,5	20,5	20,5
Initial current at 30V	I_i	**[mA]**	340,0	173,0	274,0	201,0	198,0	170,0
Applied Voltage	**U**	**[V]**	10	10	10	10	10	10
Adj. initial current	I_a	**[mA]**	68,5	37,5	49,4	44,0	45,6	36,3
Duration of test	**t**	**[h]**	24	24	24	24	24	24
Final current	I_f	**[mA]**	41,5	30,1	40,0	35,0	34,0	31,0
Final temp.	T_f	[°C]	19,5	19,5	19,5	20,0	20,0	20,0
Average depth	X_d	**[mm]**	17,0	15,2	17,5	23,2	22,3	21,8
Migration coefficient	D_{nssm}	$\times 10^{-12}$ [m^2/s]	23,014	20,587	23,428	32,988	31,644	31,279
			penetration depth					
		1	16,2	18,5	18,9	19,2	16,5	17,3	25,7	29,3	23,5	27,1	22,5	27,1
		2	18,9	24,0	17,1	16,8	15,3	18,4	21,1	29,4	20,0	21,2	22,5	22,7
		3	17,8	16,4	19,6	15,0	17,4	17,0	20,4	22,7	18,9	26,9	23,7	24,2
		4	18,6	19,2	16,1	15,2	16,8	18,2	16,4	26,2	18,6	25,5	19,4	24,1
		5	16,0	15,8	16,7	12,3	18,4	19,8	21,3	18,7	17,1	26,3	20,2	22,4
		6	17,7	17,7	15,8	12,8	17,6	-	19,1	24,6	17,0	23,1	18,2	24,3
		7	14,7	11,9	14,8	12,2	-	15,8	22,5	25,2	19,5	29,0	17,5	23,3
		8	20,5	17,9	15,5	13,5	18,7	19,9	-	-	-	-	14,9	18,4
		9	13,7	12,5	13,9	12,3	16,2	16,1	-	-	-	-	19,6	-

Test laboratory: CTH

Mixture ID: C45/55

Casting date: 23 March 2012

Date of testing: 27 April 2012

Age [days]: 35

NaCl: 10%

NaOH: 0.3N

	Fibre content		0,0			0,6PP		
	Slice		1	2	3	1	2	3
Sample diameter	D	[mm]	100	100	100	100	100	100
Sample length	L	[mm]	49,4	49,2	50,1	49,4	49,8	50,3
Chloride concentration	c_0	-	10	10	10	10	10	10
Initial temp.	T_i	[°C]	20,5	20,5	20,5	20,0	20,0	20,0
Initial current at 30V	I_i	[mA]	99,0	101,0	103,0	102,0	105,0	102,0
Applied Voltage	U	[V]	20	20	20	20	20	20
Adj. initial current	I_a	[mA]	64,0	65,2	66,3	66,5	68,1	66,5
Duration of test	t	[h]	24	24	24	24	24	24
Final current	I_f	[mA]	56,5	57,3	58,8	57,8	58,7	57,2
Final temp.	T_f	[°C]	21,0	21,0	21,0	21,0	21,0	21,0
Average depth	X_d	[mm]	33,2	29,6	26,4	26,0	27,3	27,6
Migration coefficient	D_{nssm}	x 10^{-12} [m^2/s]	23,550	20,750	18,678	18,127	19,191	19,641

			penetration depth											
		1	35,6	32,5	35,0	28,6	26,5	26,4	22,8	26,7	25,9	26,9	28,7	28,6
		2	34,4	32,4	31,9	29,5	25,3	27,8	23,3	30,0	27,5	26,6	28,6	30,2
		3	33,6	31,3	29,8	29,0	27,3	27,6	24,1	26,8	26,0	28,3	30,5	25,7
		4	36,8	30,0	31,4	29,1	24,0	27,2	23,2	29,9	29,7	26,6	27,7	28,4
		5	36,5	29,5	28,0	28,3	25,9	27,1	25,7	24,5	26,6	27,3	25,6	27,0
		6	35,7	30,1	29,6	28,3	24,9	26,5	25,1	31,6	27,3	28,8	26,4	28,2
		7	36,9	28,9	27,9	29,2	25,6	27,9	25,5	25,8	30,0	25,2	27,0	25,3
		8	-	-	-	-	-	-	-	-	-	-	-	-
		9	-	-	-	-	-	-	-	-	-	-	-	-

Appendix F: Mass losses

Cleaning cycle	LF1				LF2			
	A		B		A		B	
	mass	loss	mass	loss	mass	loss	mass	loss
0	320.02	-	320.08	-	322.40	-	321.21	-
1	320.09	-	320.04	-	322.39	-	321.22	-
2	319.52	0.20%	319.11	0.29%	321.51	0.29%	320.28	0.31%
3	319.19	0.30%	318.82	0.38%	321.29	0.36%	320.01	0.40%
4	319.01	0.36%	318.53	0.47%	321.10	0.42%	319.81	0.46%
5	318.92	0.39%	318.42	0.51%	320.91	0.48%	319.64	0.51%
6	318.84	0.41%	318.38	0.52%	320.79	0.52%	319.49	0.56%
7					320.69	0.55%	319.35	0.60%
8					320.60	0.58%	319.24	0.63%

0 – weight before casting

1 – weight after destroying beams

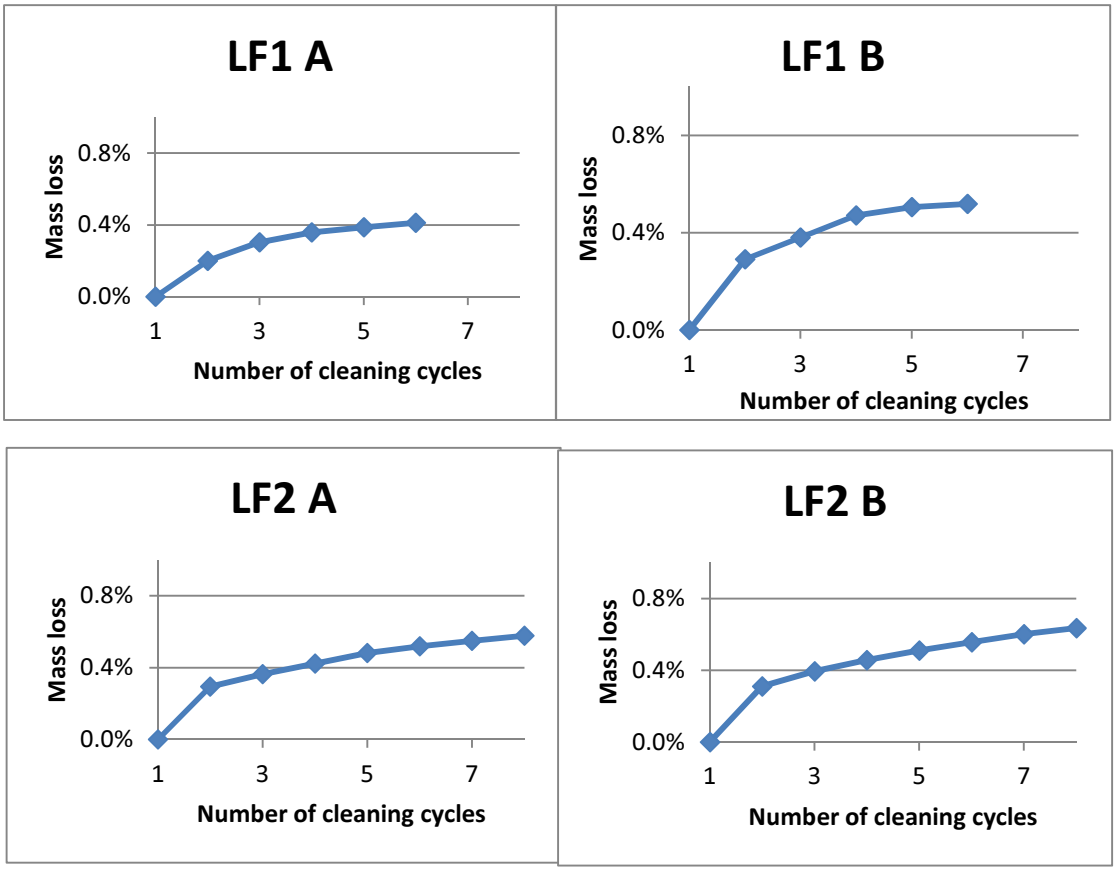

Cleaning cycle	LW1				LW2			
	A		B		A		B	
	mass	loss	mass	loss	mass	loss	mass	loss
0	323.09	-	322.42	-	322.41	-	320.85	-
1	322.76	-	322.00	-	322.07	-	320.59	-
2	321.84	0.30%	320.70	0.42%	320.99	0.35%	319.38	0.40%
3	321.36	0.45%	320.35	0.53%	320.56	0.48%	318.87	0.56%
4	321.16	0.51%	320.06	0.62%	320.37	0.54%	318.58	0.65%
5	321.03	0.55%	319.94	0.66%	320.19	0.60%	318.39	0.71%
6	320.94	0.58%	319.87	0.68%	320.07	0.63%	318.22	0.76%
7	320.85	0.61%	319.80	0.70%	320.04	0.64%	318.04	0.82%
8	320.80	0.63%	319.75	0.71%			317.99	0.83%

0 – weight before casting

1 – weight after destroying beams

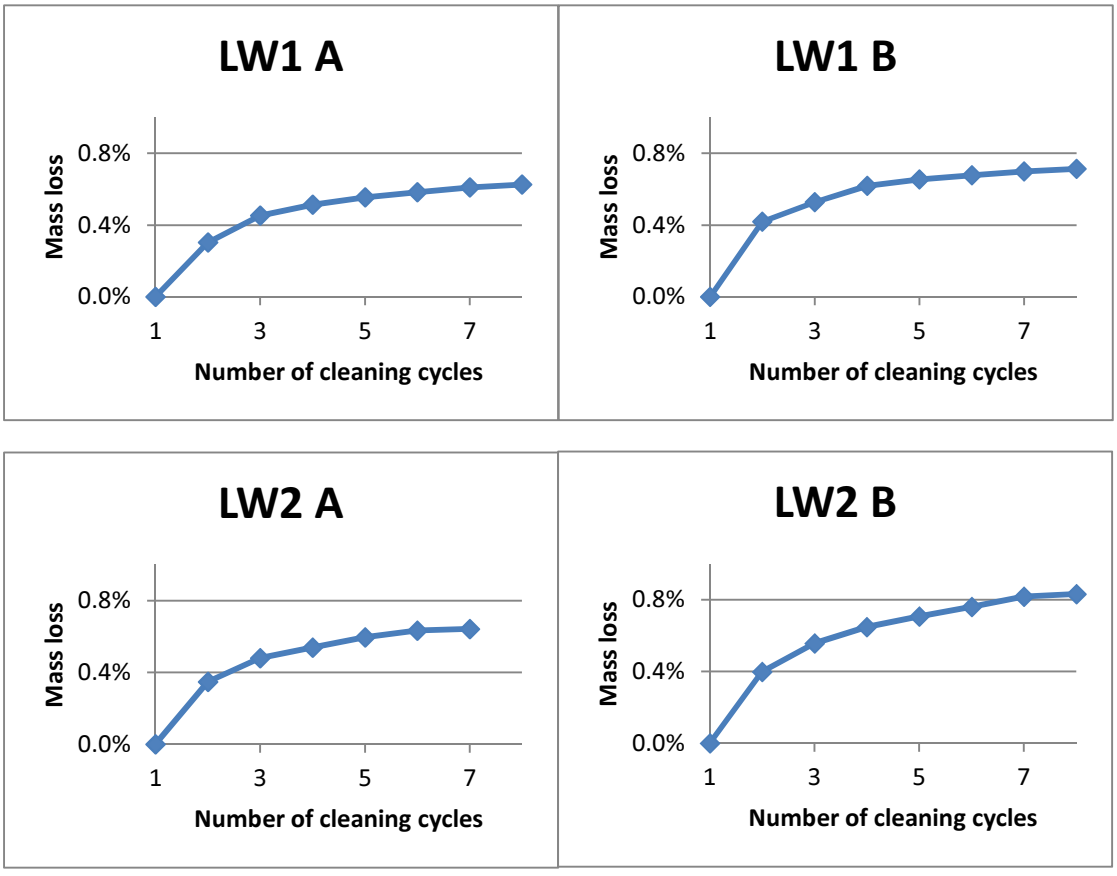

Cleaning cycle	UF1				UF2			
	A		B		A		B	
	mass	loss	mass	loss	mass	loss	mass	loss
0	321.62	-	320.82	-	323.56	-	322.25	-
1	321.71	-	320.80	-	322.53	-	321.55	-
2	321.40	0.10%	320.39	0.13%	321.96	0.18%	320.81	0.23%
3	321.20	0.16%	320.08	0.22%	321.53	0.31%	320.38	0.36%
4	320.98	0.23%	319.83	0.30%	321.24	0.40%	320.13	0.44%
5	320.77	0.29%	319.65	0.36%	321.05	0.46%	320.00	0.48%
6	320.64	0.33%	319.45	0.42%	320.83	0.53%	319.86	0.53%
7	320.54	0.36%	319.25	0.48%	320.79	0.54%	319.81	0.54%
8	320.47	0.39%	319.13	0.52%	320.69	0.57%	319.75	0.56%

0 – weight before casting

1 – weight after destroying beams

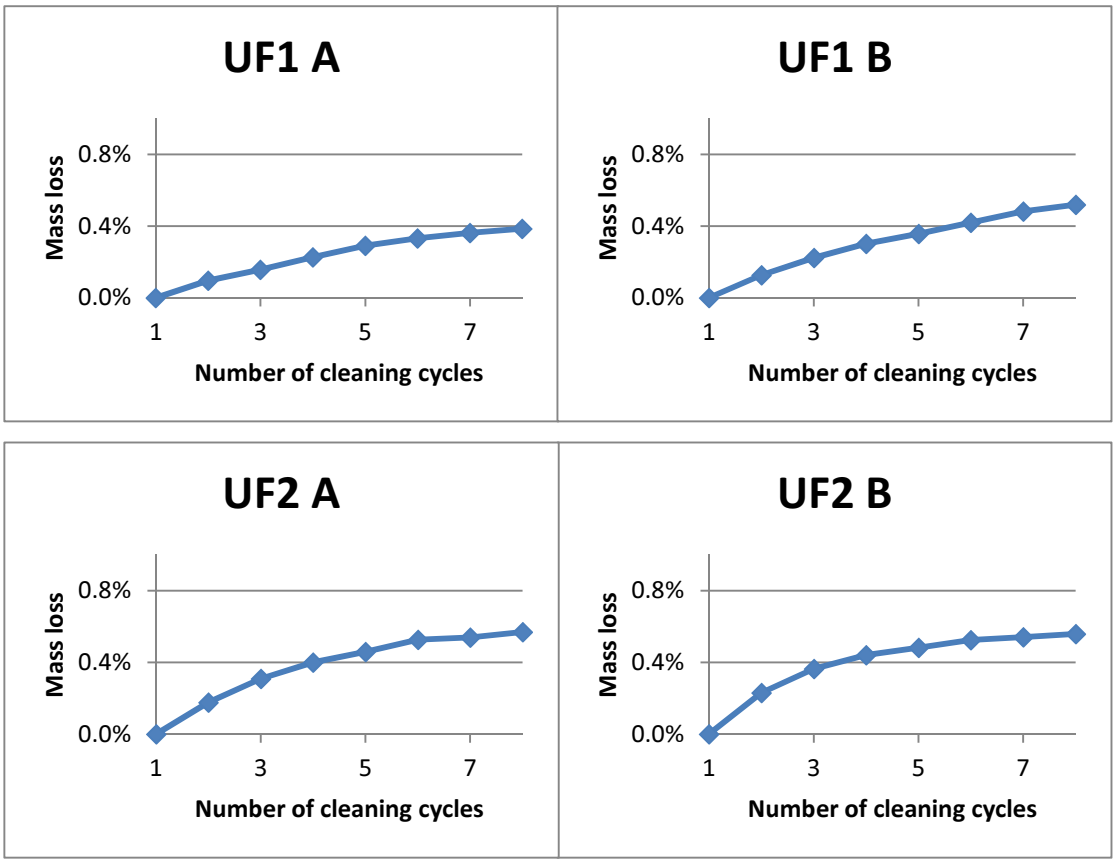

Cleaning cycle	UW1			
	A		B	
	mass	loss	mass	loss
0	321.51	-	323.56	
1	321.45	-	322.87	-
2	320.65	0.25%	322.01	0.27%
3	320.18	0.40%	321.58	0.40%
4	319.92	0.48%	321.22	0.51%
5	319.72	0.54%	321.04	0.57%
6	319.64	0.56%	320.85	0.63%
7	319.58	0.58%	320.77	0.65%

0 – weight before casting

1 – weight after destroying beams

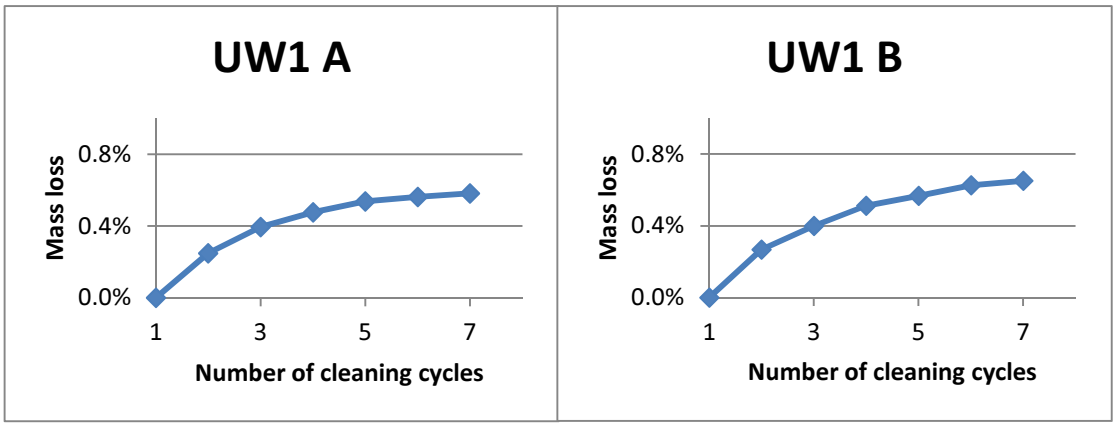

Cleaning cycle	WF1				WF2			
	A		B		A		B	
	mass	loss	mass	loss	mass	loss	mass	loss
0	321.48	-	323.00	-	321.58	-	319.76	-
1	321.30	-	321.33	-	321.59	-	319.51	-
2	320.52	0.24%	320.57	0.24%	320.79	0.25%	318.09	0.44%
3	320.09	0.38%	320.35	0.30%	320.48	0.35%	317.73	0.56%
4	319.78	0.47%	320.10	0.38%	320.25	0.42%	317.53	0.62%
5	319.52	0.55%	319.91	0.44%	320.04	0.48%	317.34	0.68%
6	319.41	0.59%	319.84	0.46%	319.89	0.53%	317.25	0.71%
7	319.33	0.61%	319.79	0.48%	319.77	0.57%	317.16	0.74%
8	319.27	0.63%			319.72	0.58%		

0 – weight before casting

1 – weight after destroying beams

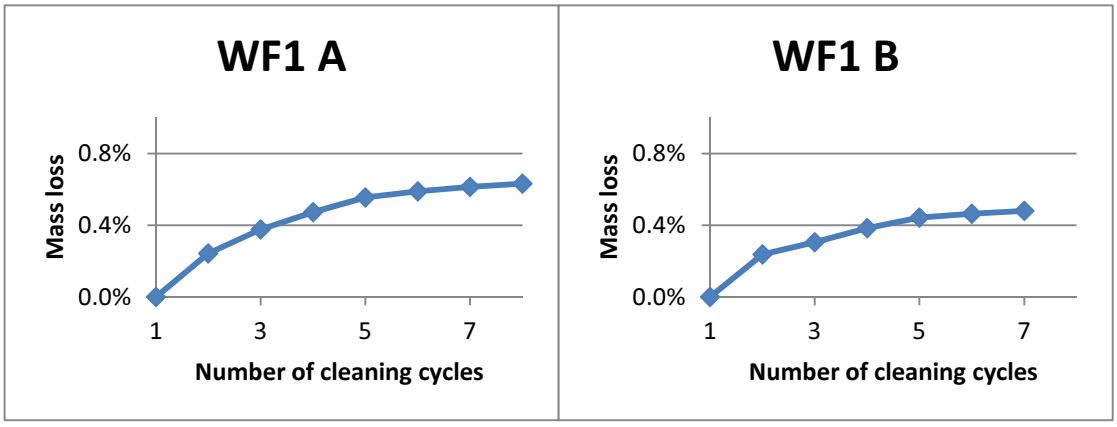

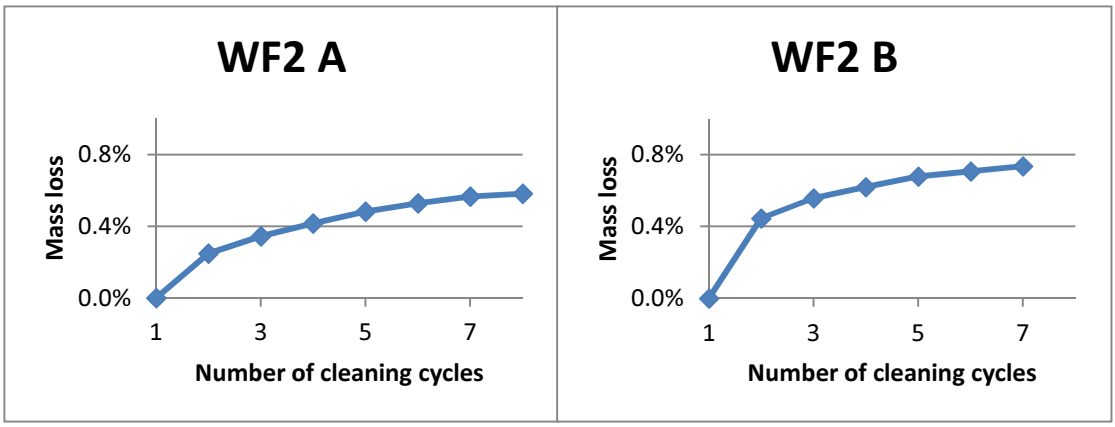

Cleaning cycle	WW1				WW2			
	A		B		A		B	
	mass	loss	mass	loss	mass	loss	mass	loss
0	321.09	-	321.13		321.84	-	319.30	-
1	321.35	-	322.95	-	321.34	-	319.76	-
2	320.46	0.28%	322.14	0.25%	320.27	0.33%	318.74	0.32%
3	320.09	0.39%	321.79	0.36%	319.86	0.46%	318.31	0.45%
4	319.85	0.47%	321.56	0.43%	319.68	0.52%	318.09	0.52%
5	319.65	0.53%	321.35	0.50%	319.49	0.58%	317.97	0.56%
6	319.51	0.57%	321.19	0.54%	319.36	0.62%	317.89	0.58%
7	319.39	0.61%	321.07	0.58%	319.24	0.65%	317.80	0.61%
8	319.27	0.65%	320.97	0.61%	319.16	0.68%		

0 – weight before casting

1 – weight after destroying beams